Understanding Odd−Even Effects in Organic Self-Assembled Monolayers

Feng Tao and Steven L. Bernasek*

Department of Chemistry, Princeton University, Princeton, New Jersey, 08544

Received March 13, 2006

Contents

1. Introduction

Odd−even effects on structure and property is a widely observed phenomenon in chemistry, physics, biology, and materials sciences. In general, it describes an alternative alteration of materials structures and/or properties depending on the odd or even number of structural units in a molecule. The structural unit could be one CH_2 group, one metal atom, or another more complicated unit. It exists in macroscale materials such as in the boiling points of liquid *n*-alcohols.[1] It was also revealed in microscale materials such as in the odd−even difference in properties of nanoclusters which are made of an odd or even number of atoms.[2−8] In addition, it is widely observed at various organic/solid surfaces and interfaces.

Surface and interfacial interactions are a central issue for the growth of heterogeneous materials, such as heterogeneous catalysts and various functional organic thin films, and for the design of nanodevices and biosensors. Interactions at the surface and interface can be categorized as weak noncovalent interactions and strong chemical-bond interactions. Recent systematic studies have shown that organic thin films can be formed through these two distinctly different interfacial interactions at the organic/solid interface.[9−11]

10.1021/cr050258d CCC: $65.00 © 2007 American Chemical Society
Published on Web 04/18/2007

Feng Tao received his Master's degree from Sichuan University and carried out research following his degree at the Beijing Institute of Physics of the Chinese Academy of Science. He then spent about 3 years as a research scientist studying organic modification and functionalization of semiconductor surfaces with Professor Xu Guo-Qin at the National University of Singapore. In 2002, he moved to Princeton University and joined Professor Steven L. Bernasek's group as a Ph.D. candidate. There he studied molecular self-assembly on solid surfaces using STM and silicon surface chemistry using UHV HREELS. He received his Ph.D. degree from Princeton University in Chemistry in 2006. He is an author of about 40 publications in international journals and one book chapter. He received the American Vacuum Society National Graduate Research Award, the Materials Research Society Graduate Research Silver Award, the Schering-Plough Presentation award, the Hugh Stott Taylor Merit Prize, and the Harold W. Dodds Honorific Fellowship during his studies at Princeton. Currently he is a postdoctoral fellow working at the Lawrence Berkeley Laboratory with the group of Gabor Somorjai, on the catalysis and surface science of nanostructural materials.

Steven L. Bernasek was born in 1949 in Holton, KS. He graduated from Kansas State University with a B.S. degree in Chemistry in 1971. He received his Ph.D. degree in Physical Chemistry from the University of California, Berkeley in 1975, where he was an NSF Graduate Fellow working in the laboratory of Professor Gabor A. Somorjai. His thesis work examined hydrogen–deuterium exchange at stepped platinum surfaces using molecular beam scattering methods. After receiving his Ph.D. in January 1975, he was a postdoctoral fellow at the Lawrence Berkeley Laboratory for 6 months. In July 1975 he moved to Princeton, where he is currently Professor of Chemistry. At Princeton he is an Associated Faculty Member of the Princeton Research Institute for the Science and Technology of Materials and the Princeton Environmental Institute and a member of the Executive Committee for the Program in Plasma Science and Technology. The application of gas-phase molecular reaction dynamics tools to the study of heterogeneous reactions has been the major focus of Dr. Bernasek's research. He has contributed to the study of transition-metal compound surfaces, the dynamics of small molecule surface reactions on iron, molybdenum, and platinum, the structure and reactivity of organic monolayers, and investigation of energy transfer in surface reactions. He has published over 175 papers, co-edited three books, and authored the monograph *Heterogeneous Reaction Dynamics*. He has advised over 36 Ph.D. students and 20 postdoctoral associates in his laboratory at Princeton. He was elected a Fellow of the AAAS in 1994 and a Fellow of the AVS in 2001. In 1981, he was awarded the Exxon Faculty Fellowship in Solid State Chemistry by the Division of Inorganic Chemistry of the American Chemical Society. He received the ACS Arthur W. Adamson Award for Distinguished Service in the Advancement of Surface Chemistry in 2006.

Organic thin film techniques have been developed as the basis for a wide spectrum of advanced applications including molecule-based devices and sensing techniques, lubricating systems, and corrosion inhibitors. The advantage of organic thin films is their ability to functionalize a surface and the flexibility of tuning physical and chemical properties of a surface by tailoring molecular structures and functional groups. With increasing studies devoted to organic thin films, a number of self-assembled monolayers of organic molecules and biospecies on solid surfaces have been developed, and their growth mechanisms, monolayer structures, and interfacial and surface properties have been systematically investigated.[9,11−17] A classic example of the organic thin films formed via weak noncovalent interactions is the self-assembled monolayer on highly oriented pyrolyic graphite (HOPG) formed via weak van der Waals forces. For organic thin films formed on solid surfaces via chemical bonds, one representative example is the self-assembled alkanethiolate monolayer on Au(111) formed via strong chemical bonds.

In the studies of these self-assembled thin films, a great number of new odd−even chain-length effects have been observed. They originate from various complex interactions between the self-assembled molecules and the substrate, interactions among the packed molecules in the monolayer, or both. More importantly, these structural odd−even effects induce odd−even alterations of chemical, physical, and surface and interfacial properties such as chemical reactivity, electronic property, friction behavior, and electrochemical property. Understanding the odd−even effects of various structures and properties based on organic/solid interfacial interactions is an important part of mechanistic studies of the growth and function of various organic thin films on solid surfaces.

This review will focus on the structure and property odd−even effects of various organic monolayers self-assembled on solid surfaces. It is organized by the class of solid substrate on which organic self-assembled monolayers were formed and includes HOPG, molybdenum disulfide (MoS_2), metal substrates including Au(111), Ag(111), Cu, Al, and Hg, and inorganic compound substrates Al_2O_3 and SiO_x/Si. For each substrate, the presentation is categorized by the different series of organic molecules. The odd−even effects seen for the different categories of organic molecules on the same substrate are compared when they are described. Following the description of structural effects, the induced odd−even differences in various properties and functions of these thin films are rationalized. Finally, the origin and features of odd−even effects on different substrates are contrasted and discussed. Table 1 briefly lists various odd−even effects of organic self-assembled thin films on different solid substrates formed through weak noncovalent interactions and strong chemical-bond formation.

For the preparation of organic self-assembled monolayers on HOPG, a HOPG surface is prepared by peeling off layers to expose a mirror-like smooth fresh layer. This substrate has a high affinity for numerous categories of organic

Table 1. Brief Summary of Odd−Even Effects in Molecular Self-Assembled Monolayers on Different Substrates Formed through Weak Noncovalent Interactions and/or Chemical Bonds

substrate	self-assembled monolayers	structural and property odd−even effect	main refs	section in review
HOPG	$CH_3(CH_2)_{n-2}COOH$	molecular packing, chirality	41, 45−49	2.1
	cis-$CH_3(CH_2)_{p-1}HC{=}CH(CH_2)_{m-1}COOH$ ($p \neq m$)	molecular packing, chirality	51	2.1
	cis-$CH_3(CH_2)_{m-1}HC{=}CH(CH_2)_{m-1}COOH$	molecular packing, chirality	51	2.1
	$Br(CH_2)_{n-1}COOH$	molecular packing, chirality	52	2.2
	$CH_3(CH_2)_{n-2}COOH$ coadsorption with $CH_3(CH_2)_{13}CHBrCOOH$	molecular packing, chiral separation	53−55	2.3
	$CH_3-(CH_2)_7-NH-COO-(CH_2)_n-OOC-NH-(CH_2)_7CH_3$	molecular conformation, hydrogen-bond network	65, 66	2.4
	$CH_3(CH_2)_{n-1}-R-(CH_2)_{n-1}CH_3$ (R ≠ all-trans alkyl chain)	molecular packing, chirality	67	2.5
	$N{\equiv}C-(C_6H_4)_2-O-(CH_2)_{n-1}CH_3$	molecular packing	72, 73	2.6
	$N{\equiv}C-(C_6H_4)_2-(CH_2)_{n-1}CH_3$	molecular packing	72, 73	2.6
	$HO(CH_2)_{n-1}COOH$	molecular packing, hydrogen-bond network	75, 76	2.7
	$HO(CH_2)_{n-1}CH_3$	molecular packing, melting point	78	2.8
M_0S_2	$N{\equiv}C-(C_6H_4)_2-O-(CH_2)_{n-1}-CH_3$	molecular packing	72, 73	2.6
	$N{\equiv}C-(C_6H_4)_2-(CH_2)_{n-1}CH_3$	molecular packing	72, 73	2.6
Au(111)	$CH_3(CH_2)_nSH$	monolayer structure, wettability, tribological property, chemical reactivity	12, 79, 94−99, 186−190	3.2.1, 3.5.5, 3.6.1
	$CH_3(CH_2)_nCS_2H$	monolayer structure, wettability	101, 102	3.2.2
	$C_6H_5(CH_2)_nSH$	monolayer structure, wettability	79	3.2.3
	$C_6H_5-(C_6H_4)_2-(CH_2)_n-SH$	monolayer structure, wettability	105−112	3.2.4
	$CH_3-(C_6H_4)_2-(CH_2)_n-SH$	monolayer structure, wettability, molecular exchange kinetics, chemical reactivity	63, 113−116, 173, 174	3.2.5, 3.5.4, 3.5.7
	4-$CH_3(CH_2)_mOC_6H_4C_6H_4-4-CH_2SH$	monolayer structure, wettability, chemical reactivity	100	3.2.6, 3.6.1
	6-$CH_3(CH_2)_mOC_{10}H_6-2-CH_2SH$	monolayer structure, wettability	100	3.2.6
	4-$CH_3(CH_2)_mOC_6H_4C_6H_4-4-SH$	monolayer structure, wettability	100, 190	3.2.6, 3.6.1
	$CF_3(CH_2)_nSH$	monolayer structure, surface work function, chemical reactivity	96, 103, 124, 170	3.2.7, 3.5.2, 3.6.1
	diamidothiols	molecular structure, electron transfer	129	3.2.8, 3.5.6
	$HO(CH_2)_nSH$	adhesion, friction	171	3.5.3
	$HOOC(CH_2)_nSH$	adhesion, friction	171, 181	3.5.3, 3.5.5
	$CH_3(CH_2)_{15}-C{\equiv}C-CC-(CH_2)_n-SH$	polymerization, phase formation	228	3.6.3
Ag(111)	$CH_3(CH_2)_nSH$	monolayer structure	100, 149	3.3.1
	$C_6H_5-(C_6H_4)_2-(CH_2)_n-SH$	monolayer structure	106	3.3.2
	$CH_3-(C_6H_4)_2-(CH_2)_n-SH$	monolayer structure	113, 115	3.3.3
	4-$CH_3(CH_2)_mOC_6H_4C_6H_4-4-CH_2SH$	monolayer structure, wettability	100	3.3.4
	6-$CH_3(CH_2)_mOC_{10}H_6-2-CH_2SH$	monolayer structure, wettability	100	3.3.4
	4-$CH_3(CH_2)_mOC_6H_4C_6H_4-4-SH$	monolayer structure, wettability	100	3.3.4
	$CH_3(CH_2)_nCOOH$	monolayer structure, wettability	30	3.3.5

molecules. A droplet of solution of the molecule of interest in a suitable solvent is very gently added onto a freshly cleaved HOPG surface, allowing homogeneous spreading on the surface. A few minutes or longer is needed for a complete spreading and two-dimensional (2D) crystallization of the molecule on the surface.

Metal surfaces such as Au and Ag supported on mica, silicon wafer, or glass are prepared by various methods including physical vapor deposition (PVD),[18,19] electrodeposition,[20] or electroless deposition.[21−24] The deposited Au and Ag thin films have a dominant (111) surface structure. There is a tremendous amount literature about the preparation of Au(111) thin film and functionalization of this substrate with inorganic, organic, and biomolecules[9,25−28] The self-assembled monolayers of organic molecules on metal substrates such as Au(111) or Ag(111) films were generally prepared from organic solution. A metal substrate is immersed into an organic solution of the target organic molecules for some time, and then the sample is carefully rinsed with solvent such as chloroform or pure ethanol. Several factors including solvents, solution concentration, substrate temperature, immersion time, cleanliness of substrate, purity of solution, and even oxygen content of the solution can influence the quality of these self-assembled monolayers.[9] Notably, although each research group may use slightly different procedures to grow self-assembled monolayers, this slight difference in preparation procedure does not result in an identifiable differences in structures and properties of the self-assembled monolayers. Preparation of other substrates such as Cu, Al, and Hg and inorganic compound substrates such as Al_2O_3 and SiO_x/Si and self-assembled monolayers on them have been described in detail elsewhere.[29−36]

The surface structures of all the self-assembled monolayers on graphite and MoS_2 discussed here were studied by scanning tunneling microscopy (STM) and X-ray diffraction (XRD). For the self-assembled monolayers on metal surfaces, STM, atomic force microscopy (AFM), and XRD were used for investigation of the surface structures. Conventional X-ray photoelectron spectroscopy (XPS) and synchrotron-based high-resolution XPS were employed to study chemical binding between the head groups of organic molecules and the atoms of the substrate. A number of techniques including high-resolution electron energy loss spectroscopy (HREELS), infrared reflection absorption spectroscopy (IRAS), Raman spectroscopy, near-edge X-ray absorption fine structure (NEXAFS), and ellipsometric measurement of film thickness were used to investigate molecular packing, the geometry of the alkyl chain, and the orientation of the terminal group. Ultraviolet photoelectron spectroscopy (UPS), contact angle measurement, and theoretical simulation have also been used to study the surface and interfacial properties of the self-assembled monolayers. Low-energy ion/surface collision and

electron irradiation techniques have been employed to study the reactivity of the self-assembled monolayers.

2. Odd–Even Effect of Organic Self-Assembled Monolayers on HOPG

HOPG is widely used as a model substrate for exploring molecular self-assembly at a solid−liquid interface.[37−39] It has a layered structure as do mica and MoS_2. In each layer, the carbon atoms adopt sp^2 hybridization. The remaining p orbitals are perpendicular to the plane and parallel to each other. Thus, all atoms in one layer form an infinite super-conjugated π-bond network at the macroscopic scale of the sample size (Figure 1a). This provides a good substrate for investigating how the molecule−substrate interaction influences formation of the self-assembled structures of various molecules. Two adjacent layers with a large separation of 3.35 Å are weakly linked by van der Waals forces, which make it easy to prepare a fresh surface by simply peeling off the outer layers. As shown in Figure 1b, the lattice of two adjacent layers (*A* and *B*) is offset from each other. Each atomic layer of graphite packs in an *ABABAB*··· pattern. Thus, the upper layer has one-half of the atoms overlapping with its adjacent lower layer. This overlap makes one-half of the atoms of the upper layer identifiable in a STM image.

The graphite surface has three-fold symmetry, and the carbon atoms along the direction of any C_3 axis display the same zigzag extension as the zigzag skeleton of the carbon backbone of an all-trans alkyl chain (Figure 1c). The distance 2.46 Å between two interval carbon atoms along any C_3 axis is very close to the separation of two interval carbon atoms of the all-trans alkyl chain, 2.52 Å. This coincidence makes the all-trans alkyl chain match very well with the underlying zigzag lattice of the graphite surface when it self-assembles on graphite, maximizing the molecule−substrate interaction. This lattice match for self-assembly of all-trans long-chain organic molecules on HOPG has been confirmed widely.[39−44]

2.1. Odd–Even Effect on Packing Structure and Chirality of *n*-Carboxylic Acids

Those achiral organic molecules which may be induced to have 2D chirality upon self-assembly on an achiral surface mainly include carboxylic acids, anhydrides, esters, and amides due to the asymmetry of the carboxyl groups in these molecules. Recent investigations[45−49] of self-assembled monolayers of myristic, palmitic, stearic, arachidic, behenic, heptadecanoic, and nonadecanoic acids on HOPG demonstrated an odd−even effect in the molecular packing and induced chirality of these *n*-carboxylic acids. Fatty acids with an even number of carbon atoms in the alkyl chain spontaneously separate into two categories of enantiomer domains with opposite chirality during self-assembly. In contrast, acids with an odd number of carbon atoms form racemic structures on HOPG.

To understand the formation of distinctly different self-assembled structures and the accompanying chirality from saturated *n*-carboxylic acids with an even and odd number of carbon atoms, Figure 2 illustrates two possibilities for each of the two classes of acids. $CH_3(CH_2)_{10}COOH$ and $CH_3(CH_2)_9$-COOH are used as the examples for them, respectively.[41] In the simulated racemic structure formed from an acid with an even number of carbon atoms, the H atoms of one-half of the COOH groups are much closer to the H atoms of the adjacent CH_3 groups marked with green solid circles in

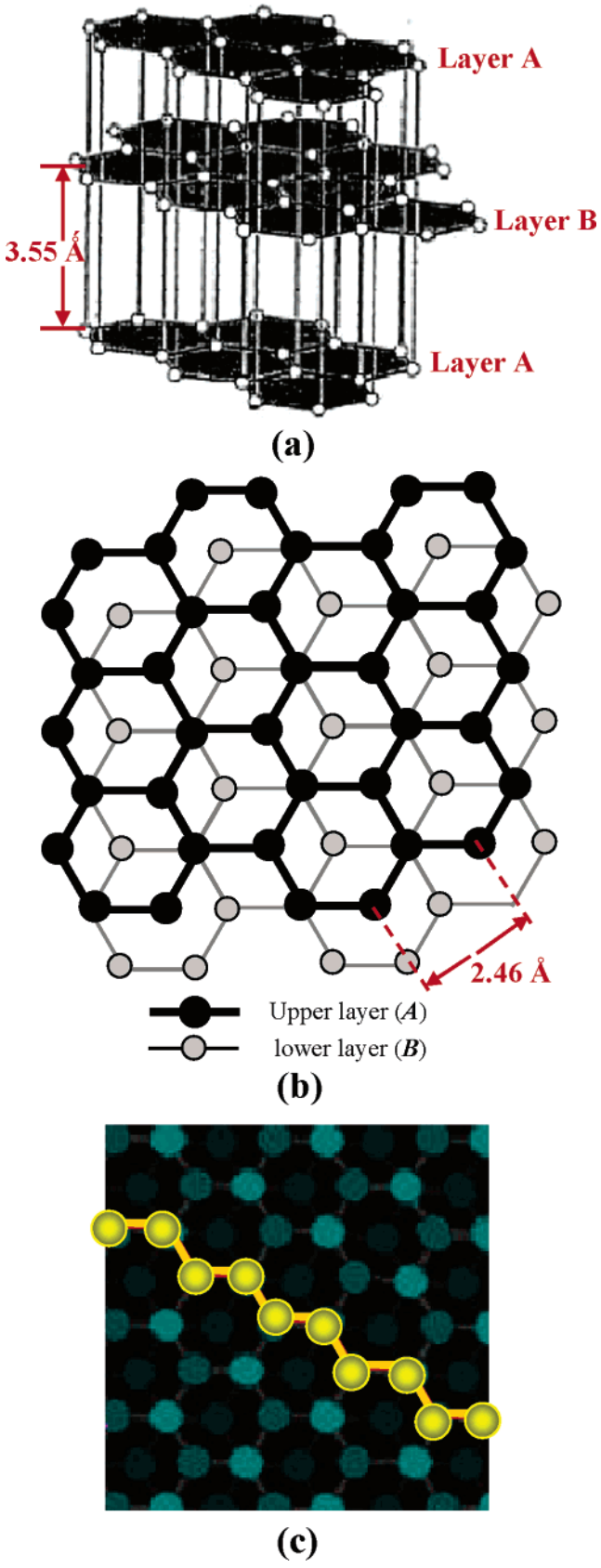

Figure 1. (a) Positional relationship between two adjacent graphite layers *A* and *B*. (b) Graphite structure can be described as an alternate succession of these planes ···*ABABAB*···. (c) Structural match between the carbon skeleton of all-trans long-chain organic molecules and the zigzag lattice of the graphite surface. The superimposed zigzag chain represents the carbon skeleton of an all-trans alkyl chain.

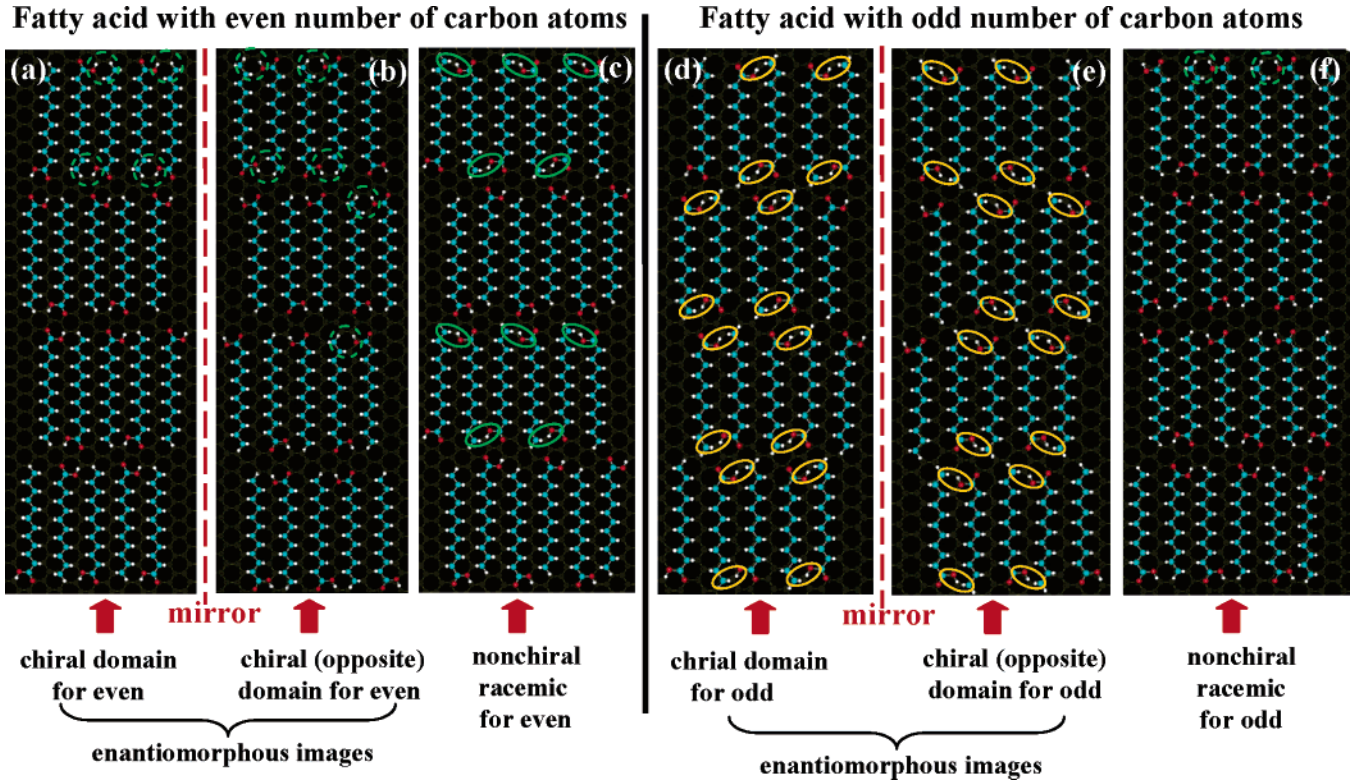

Figure 2. Possible molecular arrangement of carboxylic acid molecule with even number of carbon atoms such as $CH_3(CH_2)_{10}COOH$ and carboxylic acid molecule with odd number of carbon atoms such as $CH_3(CH_2)_9COOH$. (a−c) Acid with even number of carbon-atom series. (a and b) Two enantiomers with opposite chirality. (c) Racemic mixture. (d−f) Acid with an odd number of carbon atoms. (d and e) Two enantiomers with opposite chirality. (f) Racemic mixture. (Red dashed line) Mirror plane between two 2D enantiopure images. All circles mark the interactions between the H atom of the COOH group and one H atom of the terminal CH_3 group of one adjacent molecule.

Figure 2c than those in the enantiomer domains marked with green dashed circles in Figure 2a,b. Apparently, this large steric repulsion makes the racemic structure of $CH_3(CH_2)_{10}$-COOH unstable. The steric repulsion between two adjacent molecules in a lamella is weakened in the enantiomer structures (Figure 2a,b) due to the reduced steric repulsion between the end methyl groups of one molecule and the hydroxyl group of its adjacent molecule in a lamella. Thus, structural analysis suggests that thermodynamic factors determine the preferred formation of the two categories of 2D enantiomer domains with opposite chirality for an acid with an even number of carbon atoms. For the acid with an odd number of carbon atoms, however, two adjacent molecules in the enantiomer domains (Figure 2d,e) have larger steric repulsion than in the racemic mixture (Figure 2f). This suggests that the racemic structure is thermodynamically preferred over chiral domains for the acid with an odd number of carbon atoms. The energetically favorable 2D molecular arrangement and the induced chirality as shown in Figure 2a,b,f are consistent with the experimental observations[45−47] in which only domains of the racemic structure were seen for $CH_3(CH_2)_{n-2}COOH$ (n = odd) and only the enantiomorphous structures for $CH_3(CH_2)_{n-2}COOH$ (n = even).

This odd−even effect of structure and chirality of saturated all-trans fatty acids demonstrates that a subtle structural variation of the individual molecule can result in a significant difference in the molecular arrangement and chirality upon self-assembly, showing the complexity of the molecular packing and introduction of chirality for the achiral molecules on an achiral surface. Notably, whether the odd−even effect seen for the saturated all-trans acids can be applied to the unsaturated acids with one or more *trans*-C═C bonds is not clear, though the trans conformation of the C═C bond does not alter the zigzag extension of the carbon skeleton for the all-trans alkyl chain. This kind of unsaturated acid may not adopt the head-to-tail packing of saturated acids in a lamella. For example, brassidic acid self-assembles on HOPG via a head-to-head arrangement,[50] allowing the off-center C═C bonds to pack adjacent to one another in the structure.

For unsaturated acids with a cis conformation at the C═C bond, the extension of the carbon skeleton is changed abruptly at the *cis*-C═C bond. Experimental investigation combined with simulation of molecular packing and analysis of structural models suggests different odd−even effects in two categories of *cis*-unsaturated carboxylic acid.[51] The first class is *cis*-$CH_3(CH_2)_{p-1}HC{=}CH(CH_2)_{m-1}COOH$ ($p \neq m$, $m = 2n$ or $2n - 1$). For a *cis*-$CH_3(CH_2)_{p-1}HC{=}CH(CH_2)_{2n-1}$-COOH ($p \neq m$, $m = 2n$) acid such as *cis*-15-tetracosenoic acid, it is possible to form two enantiomers with opposite 2D chirality (Figure 3a,b). For *cis*-$CH_3(CH_2)_{p-1}HC{=}CH$-$(CH_2)_{2n-2}COOH$ ($p \neq m$, $m = 2n - 1$), however, there is a large steric repulsion (marked with a pink ring in Figure 3d) between the −OH and the α-CH_2 of two adjacent molecules in a lamella, though the packing possibly forms a hydrogen-bond network between two adjacent lamellae, indicating that *cis*-$CH_3(CH_2)_{p-1}HC{=}CH(CH_2)_{2n-2}COOH$ ($p \neq 2n - 1$) possibly cannot form a stable self-assembled monolayer. This prediction for $CH_3(CH_2)_{p-1}HC{=}CH(CH_2)_{2n-2}COOH$ is supported by the absence of any observable self-assembled domain of *cis*-$CH_3(CH_2)_7CH{=}CH(CH_2)_8COOH$.[51] Therefore, the *cis*-unsaturated acids having two alkyl chains with different chain-length *cis*-$CH_3(CH_2)_{p-1}HC{=}CH(CH_2)_{m-1}$-COOH ($p \neq m$, $m = 2n$ or $2n - 1$) exhibit an odd−even effect which is somewhat different from that of the saturated acids.

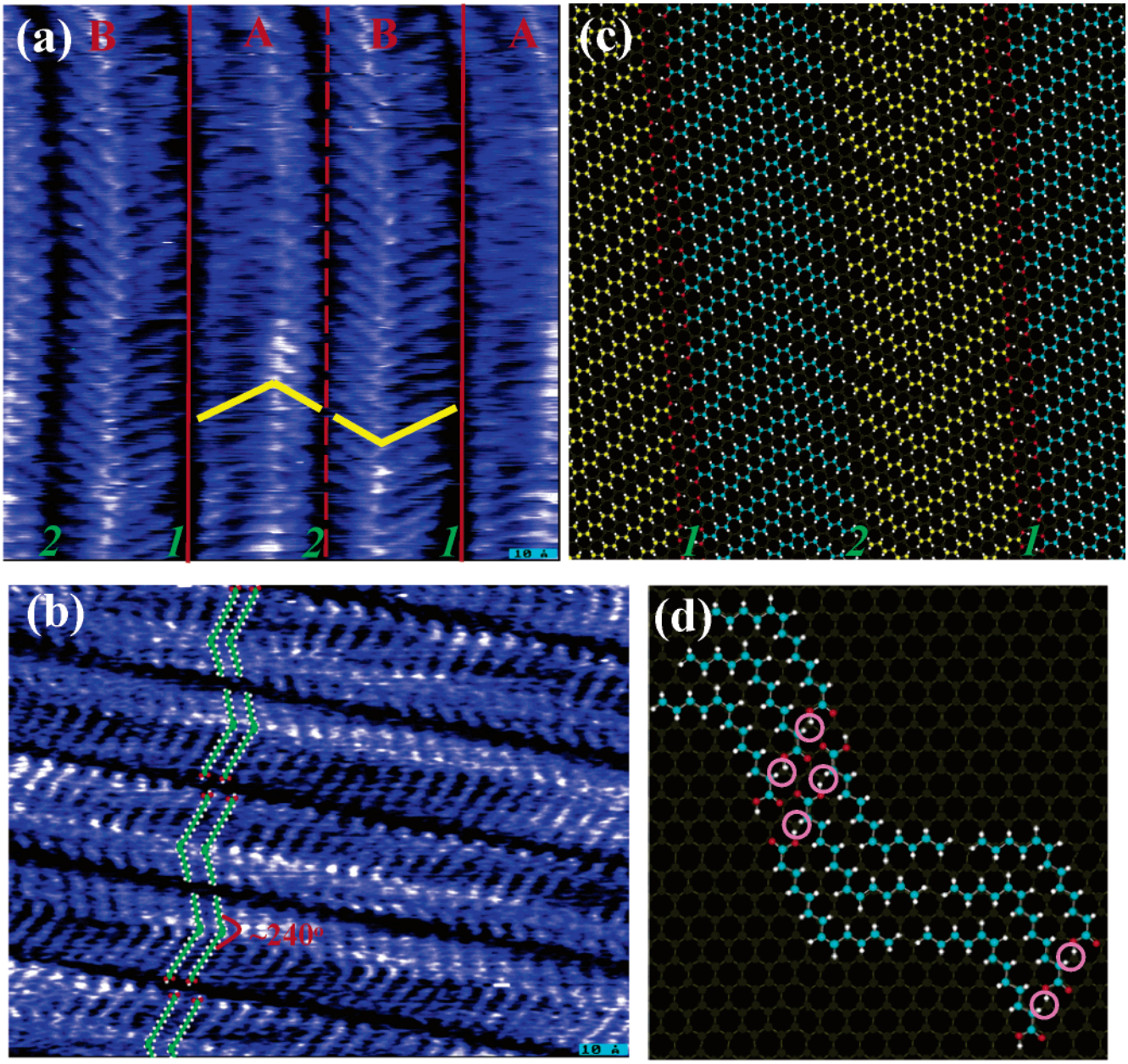

Figure 3. (a and b) STM images of two enantiomers with opposite 2D chirality in which molecules use face 1 and face 2 to pack on HOPG, respectively. Faces 1 and 2 are defined as the faces with angles of ~120° and 240° from short chain to long chain in the clockwise direction. (c) Molecular arrangement of *cis*-15-tetracosenoic acid with its face 1 packed on HOPG. (d) Simulated molecular packing model of *cis*-$CH_3(CH_2)_{p-1}HC{=}CH(CH_2)_{m-1}COOH$ ($p \neq m$, $m = 2n - 1$) on HOPG. The pink circles mark the large steric repulsion.

The second category of *cis*-unsaturated acid is the category containing two alkyl chains with an equal number of all-trans carbon atoms ($p = m$) on both sides of the *cis*-double bond, as in *cis*-$CH_3(CH_2)_{m-1}HC{=}CH(CH_2)_{m-1}COOH$. This category of molecule exhibits another odd−even effect. *cis*-10-Nonadecenoic acid is one example of *cis*-$CH_3(CH_2)_{m-1}$-$CH{=}CH(CH_2)_{m-1}COOH$ (m = even). It forms both enantiomer and racemic domains as shown in Figure 4a and b, respectively. Figure 5 presents the simulated self-assembled patterns of the two enantiomers (Figure 5a,b) and racemic structure (Figure 5c) for the acid with an even number of all-trans carbon atoms on each side of the *cis*-C=C bond. Definitely, there is not any large steric repulsion similar to that predicted in Figures 2c−e and 3c. Thus, this molecule forms a chiral enantiomer structure (Figure 4a) and an achiral racemic structure (Figure 4b). However, for the acid with an odd number of all-trans carbon atoms on each side of the *cis*-C=C bond (*cis*-$CH_3(CH_2)_{m-1}HC{=}CH(CH_2)_{m-1}COOH$, m = odd), the large steric repulsion between two neighboring molecules in each lamella (Figure 6) argues that no stable self-assembled pattern can be predicted for this acid, though a hydrogen-bonding network is possibly formed. Therefore, this second kind of *cis*-unsaturated carboxylic acid also exhibits an odd−even effect on structure and chirality.

2.2. Odd–Even Effect on Packing Structure and Chirality of Terminal Substituted *n*-Carboxylic Acids

As indicated above, the saturated fatty acids $CH_3(CH_2)_{n-2}$-COOH can form racemic and enantiomorphous domains for n = odd and even, respectively, exhibiting an odd−even effect based on alkyl chain length. However, a significantly different odd−even effect is induced if one of the hydrogen

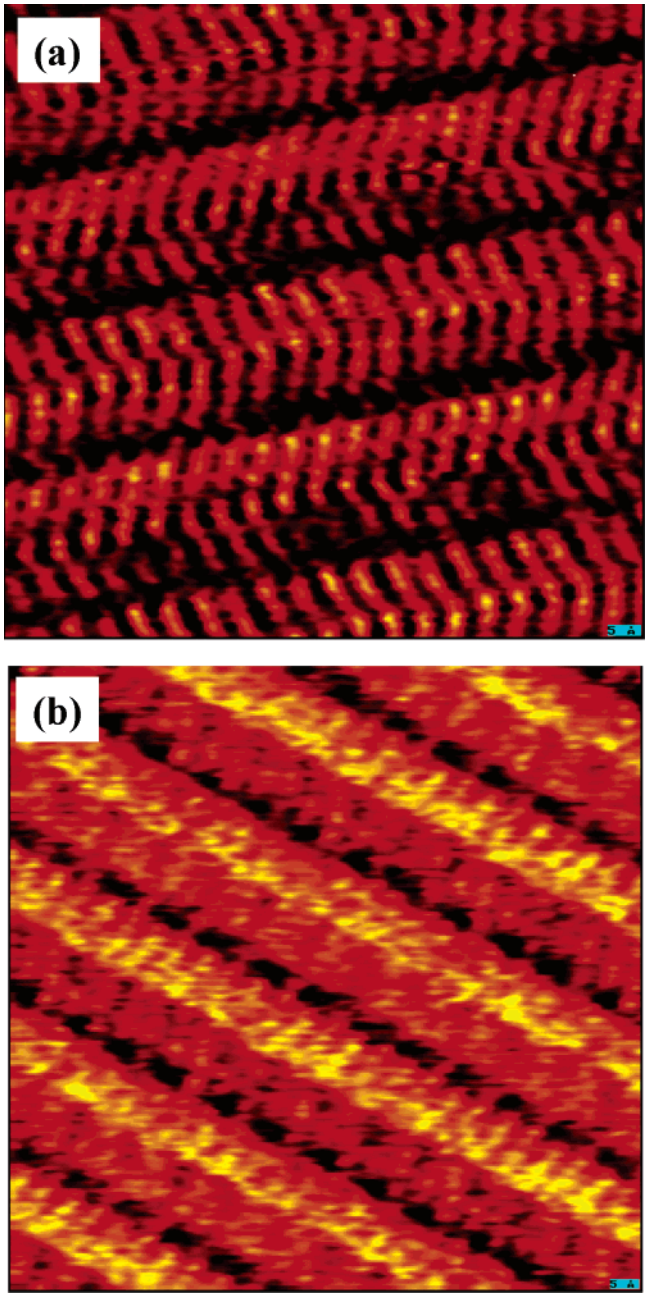

Figure 4. (a) STM images of an enantiomer of *cis*-10-nonadecenoic acid. This acid is one example of *cis*-$CH_3(CH_2)_{m-1}HC{=}CH(CH_2)_{m-1}COOH$ (m = even) (the second category of *cis*-unsaturated acid). (b) STM image of the racemic structure of *cis*-10-nonadecenoic acid.

atoms of the terminal CH_3 of the acid molecule is substituted by a large atom such as bromine.

12-Bromododecanoic acid and 11-bromoandecanoic acid are used to exemplify this odd−even difference.[52] Figure 7a and b shows STM images of $Br(CH_2)_{11}COOH$ and $Br(CH_2)_{10}COOH$, respectively. The two adjacent Br atoms appear as two bright spots[24,25] and pack together as a pair (a twin) bridging over two adjacent lamellae in each image. This common feature for the two representative Br-substituted acids shows that two adjacent Br atoms in a lamella pack together with a head-to-head geometry which is different from the head-to-tail arrangement seen for normal saturated acids. Another interesting feature of the two images is that two or three pairs of bright twin spots possibly pack together as marked with D (double) and T (triple) in Figure 7a,b.

Different from normal carboxylic acid, the two Br-substituted acid molecules are ordered in a direction parallel to but not in the direction perpendicular to the molecular long axis. Between the two images there is a significant difference in the extension direction of the bright pairs in the areas of multiple pairs marked with "D" and "T". For $Br(CH_2)_{11}COOH$, one lower bright pair shifts to the left or right side from its adjacent upper pair (green and blue boxes in Figure 7a). However, the lower pair only shifts to the right side from its adjacent upper pair in the domain of $Br(CH_2)_{10}COOH$ (blue boxes in Figure 7b). This difference is illustrated in their packing structures (Figure 7c,d). The schemes in Figure 8a,b rationalize the origin of this odd−even effect.

As shown in Figure 8a1 Br is on the same side as the OH group along the molecular long axis for $Br(CH_2)_{11}COOH$ but on the opposite side for $Br(CH_2)_{10}COOH$ in Figure 8b1. This difference drives a different assembly pattern for these molecules. $Br(CH_2)_{11}COOH$ assembles along the extension direction of the molecular long axis, alternately up and down (square-wave style as in Figure 8a2 and the black line of Figure 7c). However, $Br(CH_2)_{10}COOH$ assembles only up or down (staircase style as in Figures 8b2 and 7d).

For $Br(CH_2)_{10}COOH$ the next row of molecules can only orient with the same configuration (the same face to pack) as the original one, giving rise to a shift to the right side (Figure 8b3). If one molecule has the other configuration (the other face), which can be obtained by flipping the molecule 180° along its long axis, by which the lower bright pair will shift to the left side compared to the original one, another staircase-like molecular profile assembling in the opposite direction will form. However, there must be a gap between the two staircases extending along different directions, making the monolayer unstable. For $Br(CH_2)_{11}COOH$, however, due to the alternate "up and down" extension along the molecular long axis direction, the next row with the other configuration (Figure 8a4) can assemble together with the original one (Figure 8a3) without a gap via shifting the distance of the molecular length along the molecular long axis as marked with two red arrows between Figure 8a3 and 8a4. Thus, for $Br(CH_2)_{11}COOH$, assembling two profiles with different configurations together results in both a right shift (blue box in Figure 7a and blue arrow in Figure 8a3) and a left shift (green box in Figure 7a and green arrow in Figure 8a4) of one bright Br pair, corresponding to the areas marked with "1" and "2" in the structure pattern of Figure 7c.

This describes the odd−even difference in molecular packing for this category of substituted *n*-carboxylic acid. In addition, these molecules also exhibit an odd−even difference in chirality. The $Br(CH_2)_{11}COOH$ monolayer (Figure 7a) does not display any chirality due to the inhomogeneous distribution of two configurations with opposite chirality. On the other hand, the image of $Br(CH_2)_{10}COOH$ (Figure 7b) is an enantiomer domain because all packed molecules have the same configuration in terms of their 2D chirality.

2.3. Odd–Even Effect on the Chiral Separation of Racemic Mixtures via Coadsorption

Coadsorption of saturated carboxylic acids such as $CH_3(CH_2)_{14}COOH$ and $CH_3(CH_2)_{15}COOH$ with derivatives of normal saturated acids such as $CH_3(CH_2)_{13}CHBrCOOH$ exhibits a new odd−even effect in the self-assembled structures and their chirality. Pure $CH_3(CH_2)_{13}CHBrCOOH$

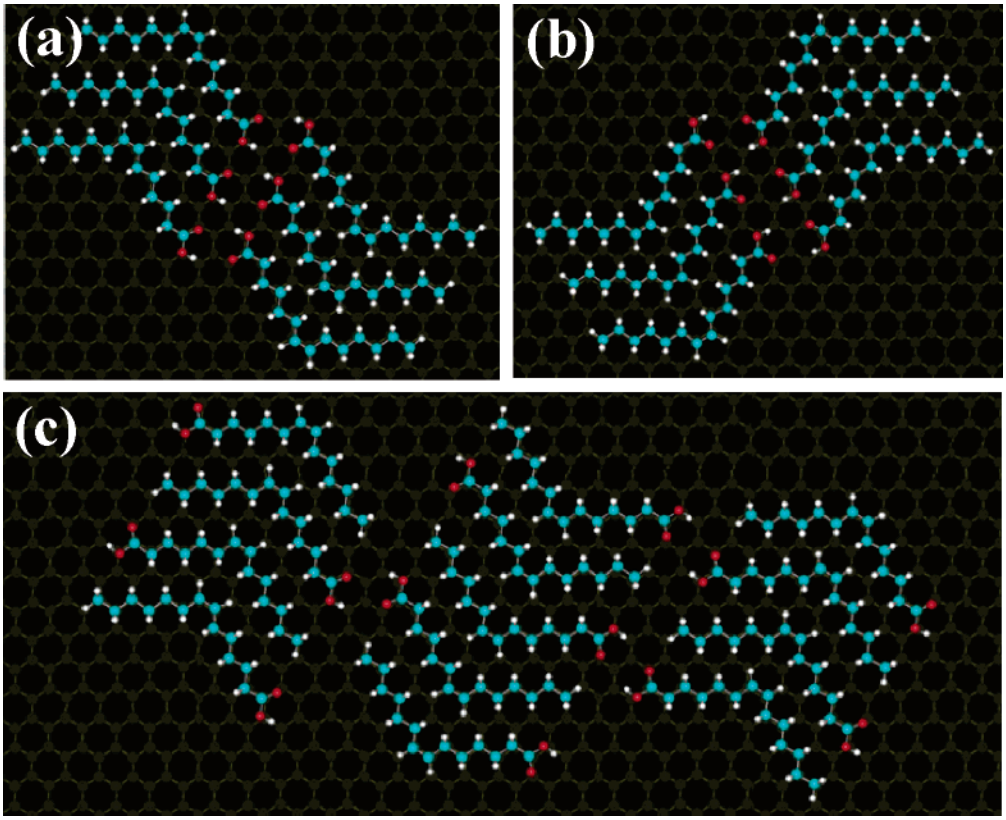

Figure 5. Packing model of *cis*-$CH_3(CH_2)_{m-1}HC{=}CH(CH_2)_{m-1}COOH$ (m = even). (a and b) Structures of the two enantiomers with opposite chirality. (c) Structure of the racemic domain.

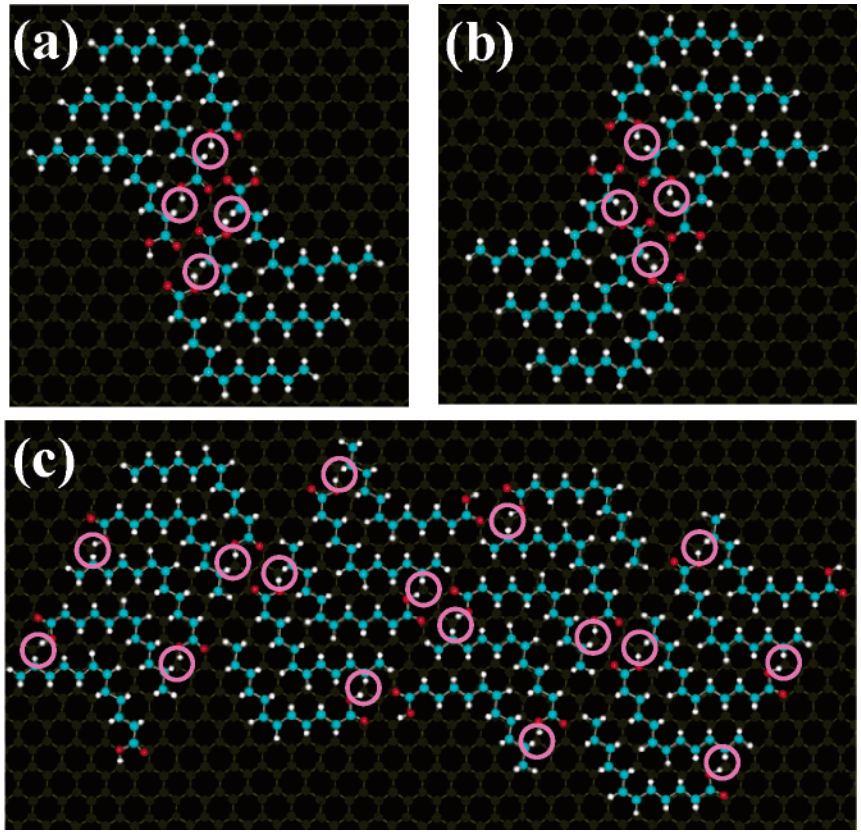

Figure 6. Packing models of *cis*-$CH_3(CH_2)_{m-1}HC{=}CH(CH_2)_{m-1}COOH$ (m = odd). (a and b) Structures of the two enantiomers with opposite chirality. (c) Racemic structure. The pink circles show the large steric repulsion between one H atom of the terminal CH_2 unit and the H atom of the carboxylic acid group of its adjacent molecule in a lamella.

forms domains with a 45° angle between the lamellar direction and molecular long axis,[53] which is distinctly different from the 90° angle seen for $CH_3(CH_2)_{n-2}COOH$.[41,45−49] This special molecular packing structure results from the competi-

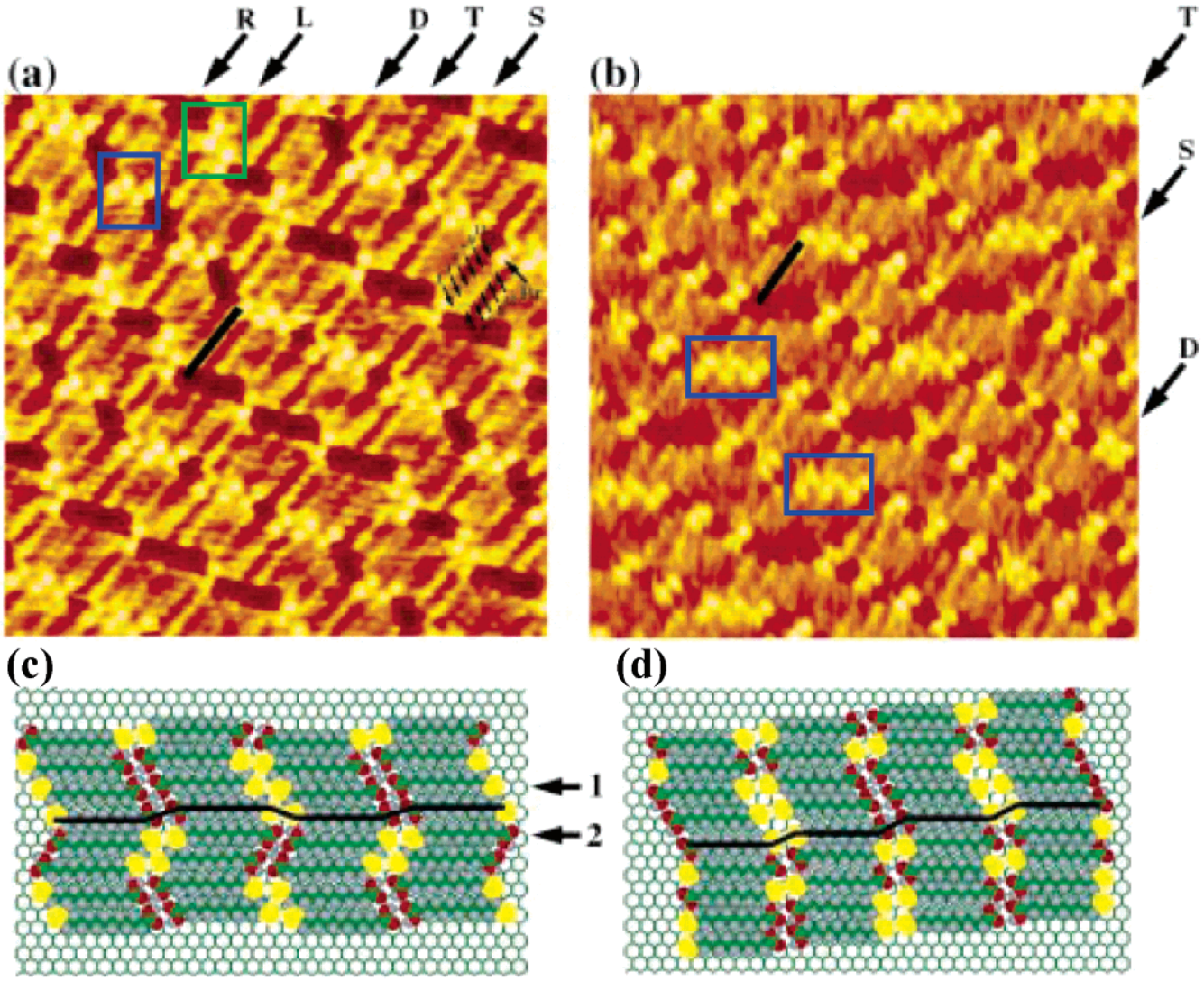

Figure 7. (a) STM image of 12-bromododecanoic acid. One molecular length is indicated by a black bar. Capital letters S, D, and T point to the strips with single, double, or triple pairs of bright spots, respectively. Capital letters R and L point, respectively, to the positions where the lower twin in a strip of double or triple twins shifts right or left relative to the higher twin. (b) STM image of 11-bromoundecanoic acid. (c) Top view of a computer-generated model of the monolayer of 12-bromododecanoic acid in an all-trans conformation. Yellow represents bromine atoms, green represents carbon atoms, gray represents hydrogen atoms, and red represents oxygen atoms. The black lines outline the alternate "up-and-down" profile formed when the twin structures are assumed by 12-bromododecanoic acid. Numbers 1 and 2 refer to two configurations in which the molecules shift right (1) or left (2) relative to the row above. (d) Top view of a computer-generated model of the monolayer of 11-bromoundecanoic acid. The black lines outline the staircase-like profile formed when twin structures are assumed by 11-bromoundecanoic acid on graphite. Reprinted with permission from ref 52. Copyright 1998 American Chemical Society.

tion and balance between the hydrogen-bond interaction of two adjacent carboxylic acid groups and the van der Waals interaction between two bromine atoms. The Br−Br interaction plays a major role, thereby producing a preferred orientation of the bromine atoms. In addition, the racemic $CH_3(CH_2)_{13}CHBrCOOH$ spontaneously self-assembles into two enantiomer domains with opposite chirality.

In the coadsorption system of $CH_3(CH_2)_{14}COOH$ and $CH_3(CH_2)_{13}CHBrCOOH$[54] two different domains are observed as in Figure 9a,b. The black and turquoise bars at the lower right part of Figure 9a mark $CH_3(CH_2)_{14}COOH$ and 2-bromohexadecanoic acid, respectively. Each bright spot corresponds to one bromine atom neighboring one carboxylic group. Each homogeneously arranged dim area (as marked by a green arrow in Figure 9a) in the troughs between lamella is assigned to two adjacent carboxylic acid groups bound together via hydrogen bonds, showing a head-to-tail packing geometry of the acid molecules in each lamella. Each dim area can be roughly considered as a rectangle. Although the bromine atoms are randomly distributed in the coadsorption monolayer, the atom is always located at the left-top or right-bottom of the rectangle as schematically shown in Figure 9c,d. Clearly, formation of a rectangular dim area with one bright spot is due to the interdigital arrangement of two acids in terms of the head-to-tail arrangement of the molecules in a lamella. In the molecular packing model (Figure 9d) all hexadecanoic acid molecules use the same face as do all 2-bromohexadecanoic acid molecules. Thus, Figure 9a is an enantiomorphous domain for the two acids. Interestingly, in another domain of the same coadsorbed monolayer (Figure 9b) the bright spots due to the bromine atoms are located at the right-top or left-bottom of each dim rectangle corresponding to two hydrogen-bonded carboxylic groups, as shown in Figure 9e,f. Compared to Figure 9d, hexadecanoic acid uses the other face to pack as does 2-bromohexadecanoic acid in Figure 9f. Therefore, for both $CH_3(CH_2)_{14}COOH$ and

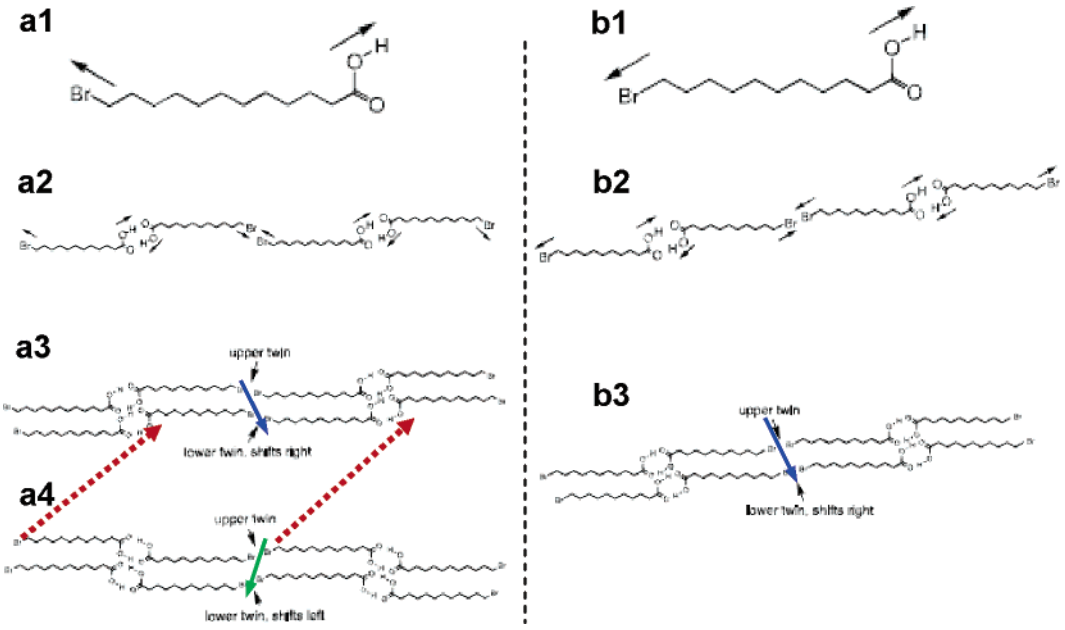

Figure 8. (a1) Structure of 12-bromododecanoic acid molecule in the all-trans conformation. (a2) Four molecules have been arranged to show the "up-and-down" profile described in the text. (a3 and a4) Two groups of molecules have been arranged to show the situation in which the lower twin shifts right or left relative to the upper twin. (b1) Structure of 11-bromoundecanoic acid molecule in the all-trans conformation. (b2) Four molecules have been arranged to show the staircase-like profile described in the text. (b3) The bromine group and the hydroxyl group are on different sides of the long molecular axis, as depicted by the arrows. A group of molecules has been arranged to show the situation in which the lower twin only shifts right relative to the upper twin. Reprinted with permission from ref 52. Copyright 1998 American Chemical Society.

2-bromohexadecanoic acid Figure 9a,b is two enantiomorphous images with opposite chirality. Thus, racemic 2-bromohexadecanoic acid separates into *R*- and *S*-enantiomer domains due to coadsorption with $CH_3(CH_2)_{14}COOH$ on HOPG.

However, 2-bromohexadecanoic acid exhibits distinctly different coadsorption with $CH_3(CH_2)_{15}COOH$ containing an odd number of carbon atoms.[55] Figure 10a is a typical image of this coadsorption system. The troughs between two adjacent lamellae are divided into two types alternately marked with "–" and "*". Each bright spot is located at one corner of a dim rectangle. In the troughs marked with "–", the location of the bromine is top-right or bottom-left of a rectangle, which is the same as that in Figure 9b,e. However, it is located at bottom-right or top-left of the dim rectangle in the "*" troughs of the same domain (Figure 10a), identical to that of Figure 9a,c. Figure 10b is the molecular packing model of this image.[55] Definitely, Figure 10a is a racemic domain for $CH_3(CH_2)_{12}CHBrCOOH$.

Clearly, coadsorption between 2-bromohexadecanoic acid and $CH_3(CH_2)_{n-2}COOH$ with n = even and odd forms chiral enantiomer and racemic domains, respectively, exhibiting an odd−even effect for this coadsorption chemistry. This odd−even effect is associated with and driven by the odd−even effect of the pure $CH_3(CH_2)_{n-2}COOH$ self-assembled monolayers as described in section 2.1. The self-assembled structure of $CH_3(CH_2)_{n-2}COOH$ determines the self-assembly framework of the coadsorption monolayer to which the 2-bromohexadecanoic acid is forced to conform. The 2-bromohexadecanoic acid fits in the 2D lattice of *n*-carboxylic acids such as $CH_3(CH_2)_{14}COOH$ and $CH_3(CH_2)_{15}COOH$, exhibiting an odd−even effect in molecular packing and chirality. Hence, the coadsorbed monolayers display an odd−even difference in self-assembled structure and chirality. This odd−even effect of the coadsorption demonstrates a strategy for designing chiral structures from racemic mixtures and a method of identifying a 2D enantiomer by "tagging" it with a bromine atom which exhibits a bright feature in STM. In addition, coadsorption of the normal saturated acid containing an odd number of carbon atoms, such as $CH_3(CH_2)_{15}COOH$, along with two enantiomers having opposite chirality such as R-$CH_3(CH_2)_{13}C^*HBrCOOH$ and S-$CH_3(CH_2)_{13}C^*HBrCOOH$ in one monolayer suggests a potential method to determine the enantiomeric excess of a chiral molecule.

2.4. Odd–Even Effect on Molecular Conformation Induced by the Length of the Alkyl Spacer

An odd−even chain-length effect was observed early in several categories of three-dimensional crystals including *n*-alkanes,[56] α,ω-alkane diols,[57,58] and α,ω-alkane diacids[59] which have an alternating change in their packing geometry. This odd−even phenomenon is also displayed in the alternating physical properties of liquid-crystalline polymers,[60,61] polyesters,[62] and polyamides.[63]

For example, the crystal structure determination of dicarbamate $CH_3-(CH_2)_7-NH-COO-(CH_2)_n-OOC-NH-(CH_2)_7CH_3$ (n = 4 or 5, abbreviated as 8-4-8 or 8-5-8, respectively)[64,65] shows an odd−even effect in the packing geometries of the 3D crystals. The odd or even length of the middle chain (also called the alkyl spacer, $(CH_2)_n$) determines the extension directions of the two side functional groups. For the 8-4-8 dicarbamate containing an even number of CH_2 units between the two carbamate groups, the two terminal alkyl chains have an anti conformation in terms of a parallel packing geometry for the two side functionalities. However, those of the 8-5-8 dicarbamate have a syn conformation. Recent studies have shown that this 3D odd−even effect can be transferred to the 2D self-assembled monolayer of these molecules on HOPG.[65,66]

Dicarbamates 8-8-8, 8-9-8, and 8-12-8 were used to demonstrate a similar odd−even effect in 2D self-assembled

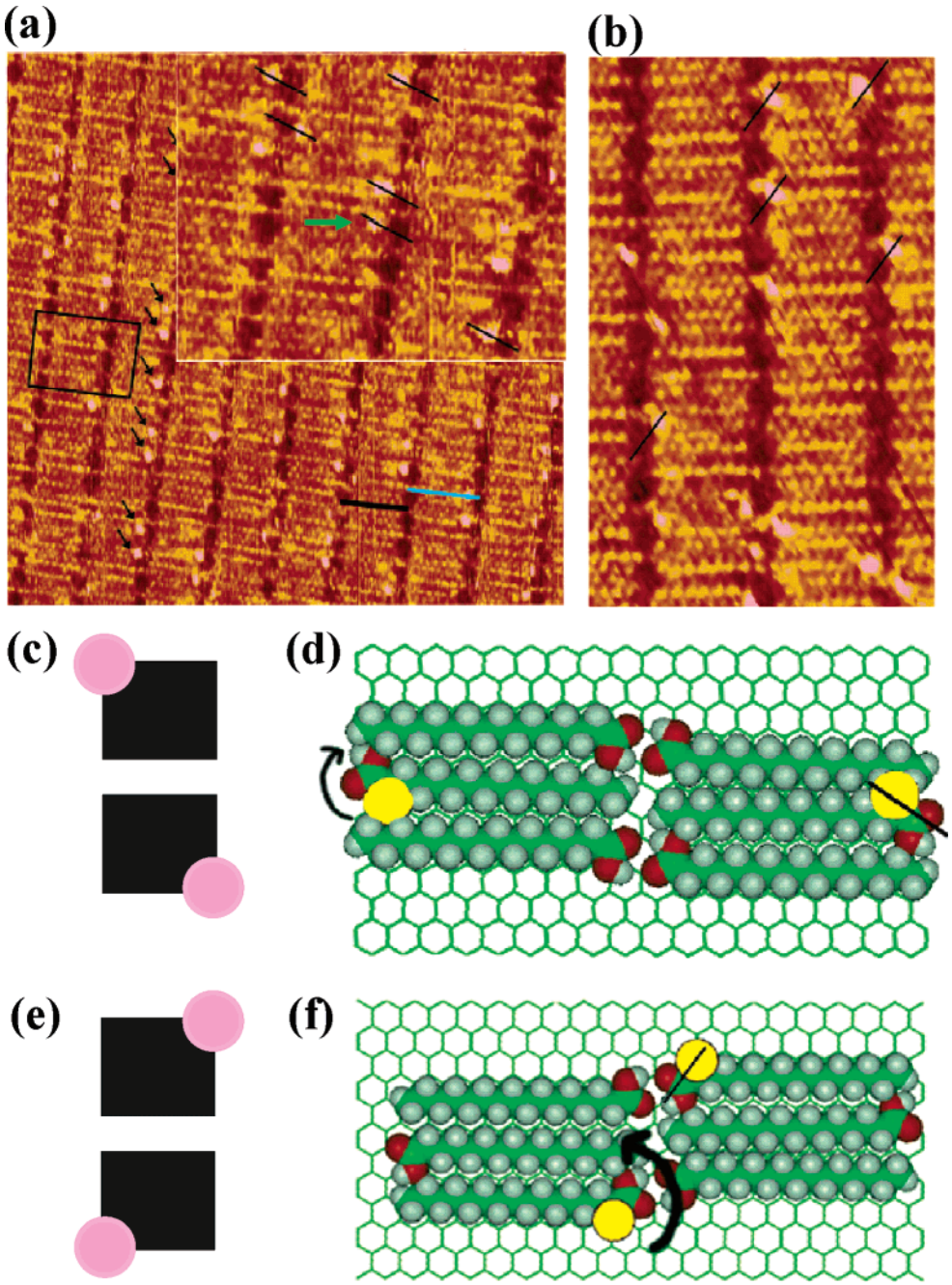

Figure 9. (a) STM image of hexadecanoic acid molecules (black bar) and an occasional (*R*)-2-bromohexadecanoic acid molecule (blue bar), both of which are configured in the all-trans conformation. An enlarged portion (inset of Figure 9a) reveals a consistent orientation of bromine atoms relative to carboxyl groups. A green arrow marks one representative rectangular dim area. Black lines are superimposed onto the dim rectangular area. (b) STM image of a domain of hexadecanoic acid interspersed with (*S*)-2-bromohexadecanoic acid. This orientation of bromine atoms is highlighted by the superimposed black lines. (c) Scheme for the locations (left-top or right-bottom) of Br in a dim rectangle in image a. (d) Top view of a model of hexadecanoic acid interspersed by (*R*)-2-bromohexadecanoic acid physisorbed onto the graphite surface. The black line superimposed on one of the bromine/carboxyl combinations mimics the arrangement found in the STM image (a). An arrow marking the clockwise direction from the bromine to alkyl group via carboxylic acid group classifies the brominated molecules as the *R* conformer. (e) Scheme for the locations (right-top or left-bottom) of bromine atoms in a dim rectangle for image b. (f) Top view of a model of hexadecanoic acid interspersed by (*S*)-2-bromohexadecanoic acid on the graphite surface. An arrow demonstrating the counterclockwise direction from the bromine atom to the alkyl chain via the carboxylic group identifies the brominated molecules as the *S* conformer. Parts a, b, d, and f were reprinted with permission from ref 54. Copyright 2000 American Chemical Society.

monolayers. Figure 11 clearly illustrates the structure difference depending on whether the alkyl spacer has an even or odd number of CH_2 groups. For 8-8-8 and 8-12-8 (Figure 11a,c), the two terminal alkyl chains point in opposite directions. Compared to the dicarbamate with a spacer with an even number of CH_2 units, the two side chains linked at the two ends of the spacer with an odd number of CH_2 groups as in 8-9-8 (Figure 11b) are pointing in the same direction in terms of a syn geometry. Thus, adding or removing one CH_2 unit forms a different conformation in which the two side chains have the same or opposite extension directions.

This odd−even packing also leads to a definite odd−even difference in hydrogen bonding between two adjacent

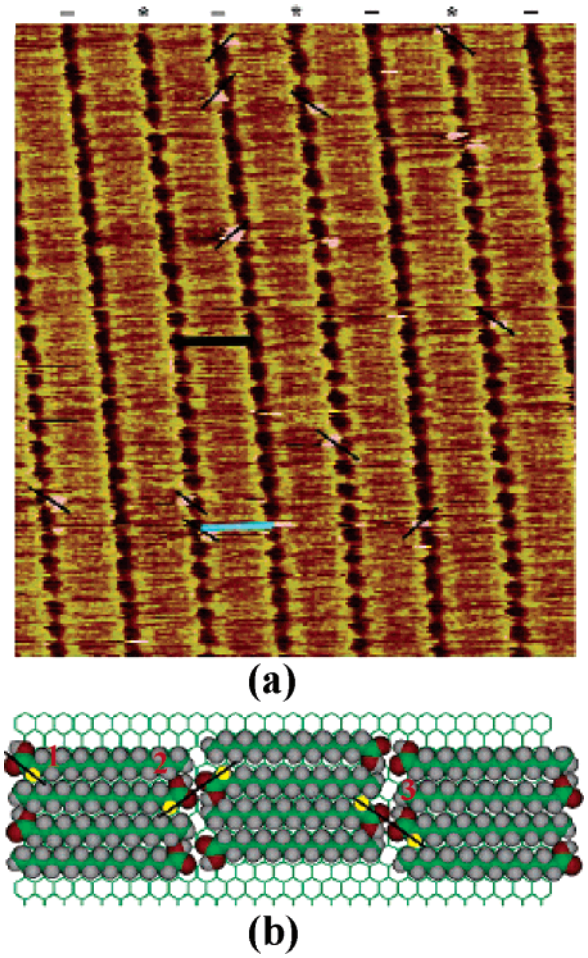

Figure 10. (a) STM image of a 1:1 mixture by volume of heptadecanoic acid with racemic 2-bromohexadecanoic acid. The bright spots (topographical protrusions) that sporadically accompany the troughs are assigned to bromine atoms and hence coadsorbed brominated molecules. Superimposed black lines highlight the bromine/COOH orientations and reflect a mirror-image pattern along alternating troughs. The brominated molecules in the (*) troughs are identified as *R*-2-bromohexadecanoic acid, while those in the (−) troughs are *S*-2-bromohexdecanoic acid. (b) Molecular model depicting a typical domain of a heptadecanoic acid/racemic 2-bromo-hexadecanoic acid mixture. The location of the Br atom in a dim box of two adjacent acid groups is marked by superimposed black bars. For bar 1, the Br atom is at right-bottom of a dim rectangle. For bar 2, the two Br atoms are at left-bottom and right-top, respectively. For bar 3, the two Br atoms are at the left-top and right-bottom, respectively. Reprinted with permission from ref 55. Copyright 2002 American Chemical Society.

molecules of a lamella of this structure.[65] A dicarbamate with a spacer of an even number of CH_2 groups can form stronger hydrogen bonds than the dicarbamate with a spacer of an odd number of CH_2 units. The same odd−even variation in the frame of hydrogen bonds has also been observed in the 3D crystal. It leads to an odd−even difference in the melting points of the 3D crystals.[64,65]

In addition, alkyl-substituted bisurea derivatives are another class of molecule exhibiting a similar odd−even effect in their 2D and 3D packing geometries, depending on the odd or even number of CH_2 units in their middle alkyl chain.[66] In principle, an organic molecule with a general formula like $R_1-(CH_2)_m-R_2$ (R ≠ all-trans alkyl chain, $m = 2n$ and $2n+1$) would be predicted to exhibit a similar odd−even effect.

2.5. Odd–Even Effect on Packing Structure and Chirality Induced by the Length of the Side Chain

The above discussion shows that the odd−even length of the molecular *alkyl spacer* can drive an odd−even difference in the molecular packing pattern on HOPG. In fact, the length of the *side alkyl chain* for molecules such as $CH_3(CH_2)_{n-1}-R-(CH_2)_{n-1}CH_3$ (R ≠ all-trans alkyl chain) possibly induces an odd−even difference in the packing structure and even in the chirality for their self-assembled monolayers on HOPG.

Figure 12 presents two structures of 1,5-substituted anthracene derivatives.[67] Each of the molecules has two equivalent side alkyl chains. Molecules 1 and 2 are substituted with odd-numbered ($C_{11}H_{23}$) and even-numbered ($C_{12}H_{25}$) all-trans alkyl chains, respectively. The STM images of their self-assembled monolayers on HOPG are shown in Figure 13a,b. In each of them the molecules densely pack into a lamella via an interdigitated arrangement similar to that seen for *n*-carboxylic acid, if a lamella is defined as the area between two turquoise dashed lines in Figure 13. For molecule 1, as seen in Figure 13a, the long axes of two adjacent molecules marked with red arrows in a lamella are not parallel and form an angle ≈ 70°. However, they are parallel for molecule 2, as seen in Figure 13b. Thus, there is a clear odd−even difference in the packing structures of molecules 1 and 2. Furthermore, their self-assembled monolayers exhibit an odd−even difference in chirality. The superimposed molecular models on the image of molecule 1 (Figure 13a) shows that two adjacent molecules in a lamella adopt two opposite faces in terms of the packing of two different 2D enantiomers. It forms a racemic structure similar to *n*-carboxylic acid with an odd number of carbon atoms. In contrast, molecule 2 uses the same face to pack and forms an enantiomer phase.

Similar to the odd−even effect seen for *n*-carboxylic acids (Figure 2), the odd−even difference exhibited in the structure of these anthracene derivatives is driven by minimization of intermolecular steric repulsion. Figure 14 shows the packing structure of molecules 1 and 2 on HOPG. For each molecule 2 the ending terminal CH_3-CH_2- moiety marked with a green line is parallel to $-CH_2^{\alpha}-C^1$(of anthracene) labeled with a blue line because its side alkyl chain has an even number of carbon atoms. Thus, the terminal CH_3 group of one molecule points in the same direction as the β-CH_2 group of its adjacent molecule (see the red arrows in Figure 14) with the same face for all molecules in a lamella. For molecule 1, however, the CH_3-CH_2- moiety and $-CH_2^{\alpha}-C^1$(of anthracene) form an angle of ∼70°. To make the CH_3 and β-CH_2 groups point in the same direction as molecule 2 for minimization of intermolecular repulsion, molecule 1 has to use the opposite face to pack compared to its adjacent molecules in the same lamella.

As discussed in section 2.4, the length of the alkyl spacer of a molecule possibly induces an odd−even difference in the extension direction of the two side groups in the packing structure. Considering the alkyl chain between the sulfur atom and the anthracene group as an alkyl spacer, this spacer will possibly result in another odd−even difference in molecular packing structure. Since the sulfur atoms in molecules 1 and 2 do not result in a significant bending for the whole side chain $-(CH_2)_m-S-(CH_2)_{n-1}CH_3$, the two possible odd−even effects for $(CH_2)_m$ and $(CH_2)_{n-1}CH_3$ can be considered together by counting the number of total

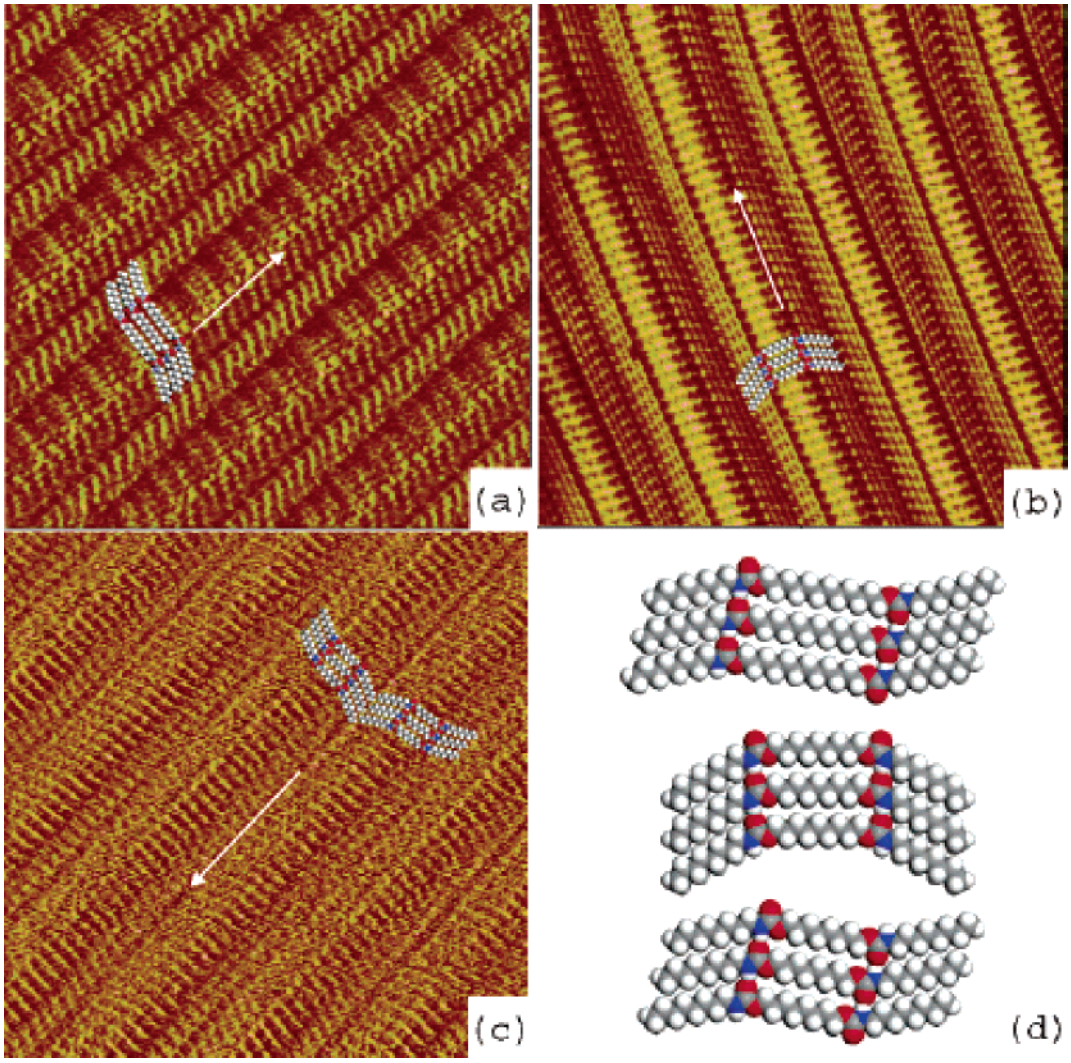

Figure 11. STM images of alkyl dicarbamate physisorbed monolayers. (a) The 8-12-8 dicarbamate has an anti configuration of the two terminal alkyl chains due to the even number of CH_2 units in the alkyl spacer. An optimized molecular model is superimposed on this image to aid visualization of the molecular conformation. White arrows designate the column direction, which is nearly perpendicular with respect to the central alkyl chain and forms an acute angle with the two terminal alkyl chains. (b) The 8-9-8 dicarbamate has a syn configuration of the two terminal alkyl chains due to the odd number of carbons in the alkyl spacer. (c) STM image of 8-8-8 dicarbamate showing an anti configuration of the two terminal alkyl chains as in the case of 8-12-8 dicarbamate. (d) Enlarged molecular models of 8-12-8 (top panel), 8-9-8 (middle panel), and 8-8-8 (bottom panel) dicarbamates. Reprinted with permission from ref 65. Copyright 2005 American Chemical Society.

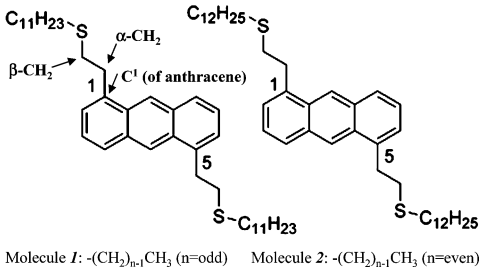

Figure 12. Molecular structures of two 1,5-substituted anthracene derivatives (molecules 1 and 2). Reprinted with permission from ref 67. Copyright 2004 American Chemical Society.

carbon atoms and sulfur atom, $m + n + 1$. Thus, the lengths of the whole side chain of molecules 1 and 2 are 14 and 15, respectively. However, the molecular packing structures will be more complicated if the two sulfur atoms are replaced by two carbamate groups (−NH−COO−). The structural odd−even difference formed by $(CH_2)_m$ and the odd−even alternation produced by $(CH_2)_{n-1}CH_3$ will possibly induce four different packing structures on HOPG. In addition, the odd−even effects on the packing structure and chirality will be maintained if the linking group of the two side chains, the anthracene moiety, is replaced by another functionality which does not make two side alkyl chains extend on the same axis. For example, anhydride $CH_3(CH_2)_{n-1}$−C(=O)-O−(O=C)−$(CH_2)_{n-1}CH_3$ may possibly exhibit a similar odd−even effect upon self-assembly on HOPG. The odd−even effects discussed in sections 2.4 and 2.5 demonstrate that any alkyl chain of a molecule possibly induces an odd−even effect on the packing structure and chirality upon self-assembly on HOPG.

2.6. Odd–Even Effect in the Monolayer Structure of Liquid-Crystal Molecules

The self-assembly chemistry of liquid-crystal molecules *n*-alkyloxy-cyanobiphenyl (*n*OCB) and *n*-alkyl-cyanobiphenyl (*n*CB) on HOPG has been studied.[68−73] These self-assembled monolayers present an odd−even effect in molecular alignment. Figure 15a,b schematically illustrates that

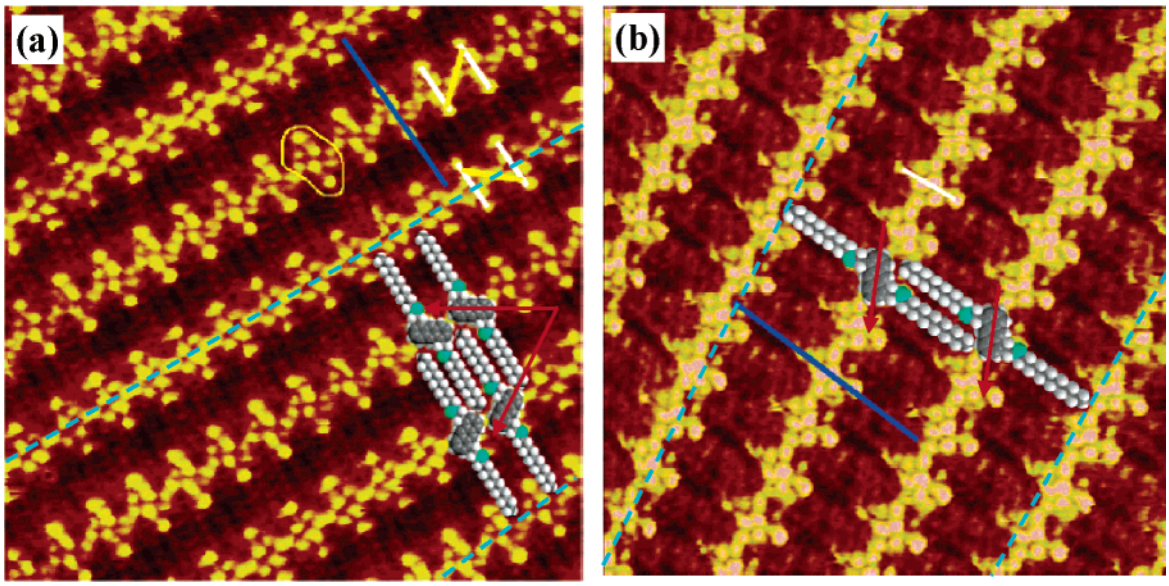

Figure 13. (a and b) STM images of molecules 1 and 2, respectively. The area between two turquoise dashed lines defines a lamella. The red arrows show the relative orientation of two anthracene groups of two adjacent molecules in a lamella. Reprinted with permission from ref 67. Copyright 2004 American Chemical Society.

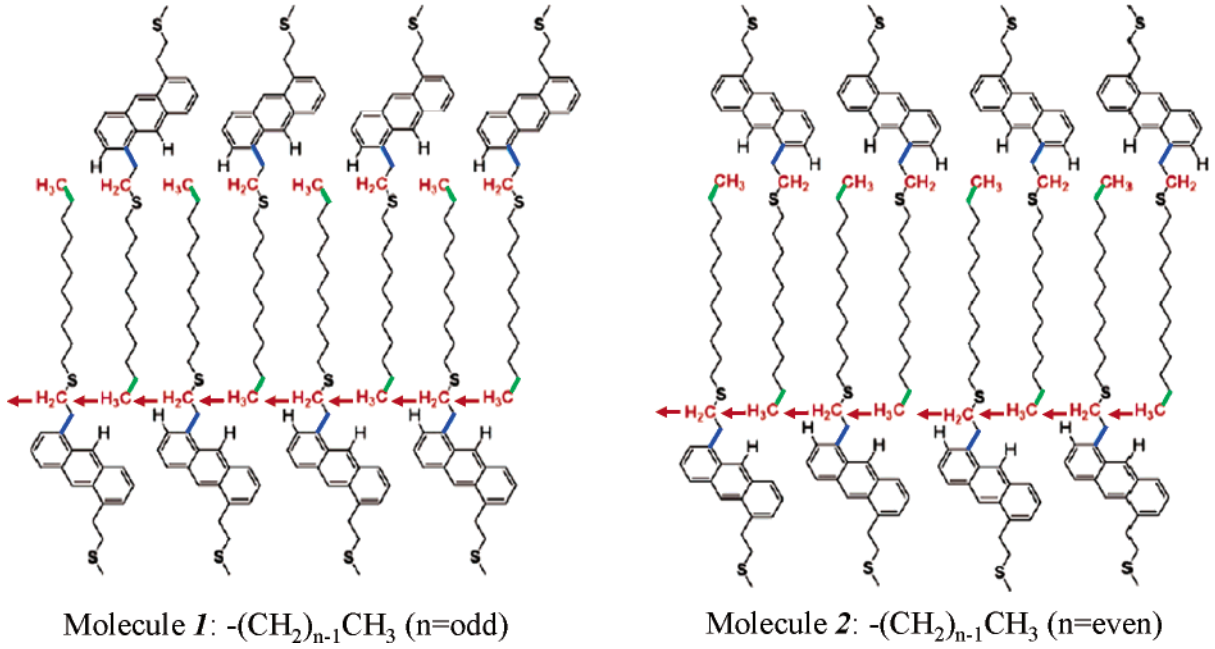

Figure 14. Packing structures of molecules 1 and 2 on HOPG. The ending CH_3 and β-CH_2 groups are highlighted with purple. $CH_2^{\alpha}-C^1$(of anthracene) and CH_3-CH_2 are marked with blue and green lines, respectively. Red arrows show the direction of CH_3 and β-CH_2. Reprinted with permission from ref 67. Copyright 2004 American Chemical Society.

the zigzag carbon backbone of the alkyl chain is perpendicular to the substrate.[72,73] The odd−even difference between two molecules with an even and odd number of CH_2 units is the orientation of the terminal methyl group. In *n*OCB (n = even), the terminal CH_3 points away from the substrate. In contrast, the terminal CH_3 is closely attached to the substrate for *n*OCB (n = odd). The understanding of the odd−even difference in the orientation of the terminal CH_3 is based on distortion in the alkyl chain to form a zigzag pattern perpendicular to the substrate. This structural distortion is supported by molecular dynamics simulations[74] However, there is no substantive evidence for the distortion in the alkyl chain due to the low resolution of the STM images of these self-assembled monolayers.[72,73] In addition, the related orientation between the zigzag pattern of the alkyl chain and the biphenyl plane is not clear.

This difference results in an odd−even alternation in molecular alignment when this molecule self-assembles on HOPG. For *n*OCB (n = odd), the motion of the terminal carbon atom is limited by the strong van der Waals interaction between methyl groups and the substrate. Therefore, this molecule could be well packed via intermolecular van der Waals interactions, similar to the self-assembled *n*-alkanes on HOPG, forming a parallel alignment (Figure 15c). However, the terminal methyl of *n*OCB (n = even) points away from the substrate, offering it the possibility of free motion. The motion of this CH_3 largely weakens the interaction between substrate and alkyl chain, thereby making

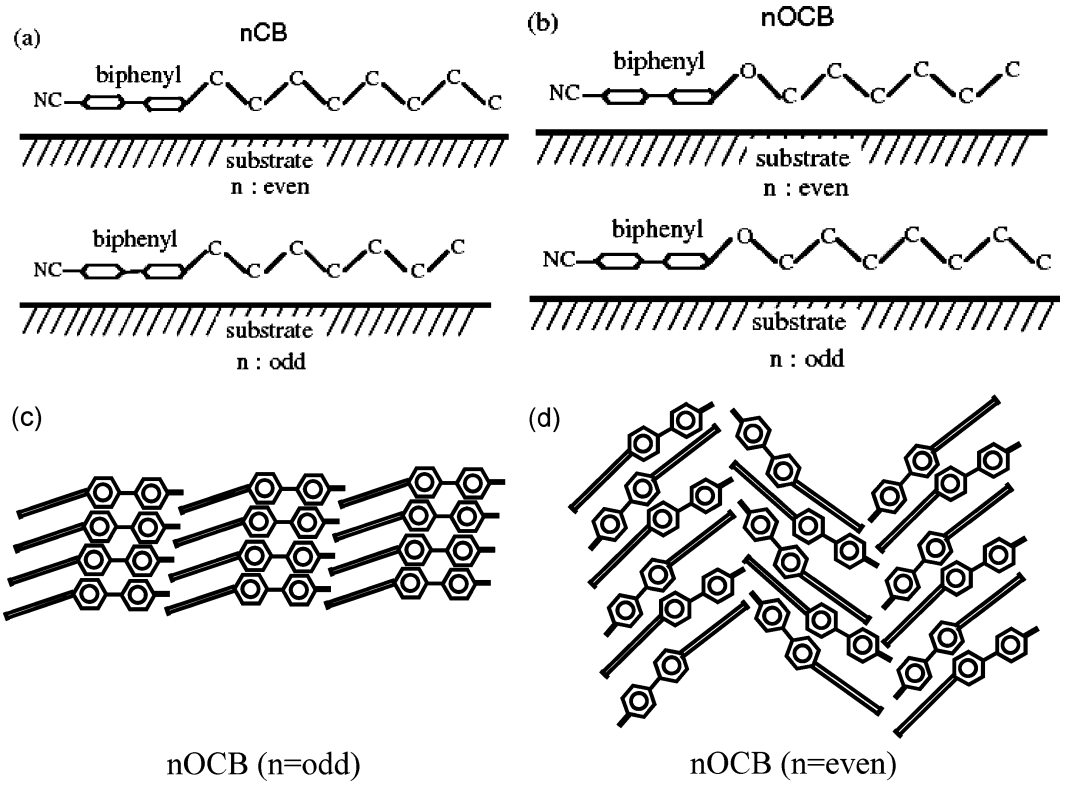

Figure 15. (a and b) *n*CB and *n*OCB molecules on a substrate surface, respectively. (c) Parallel assignment of *n*OCB (*n* = odd) on HOPG. (d) Antiparallel alignment of *n*OCB (*n* = even) on HOPG. Reprinted with permission from ref 72. Copyright 2001 The Japanese Society of Applied Physics.

the intermolecular van der Waals interactions less dominant in determining the molecular alignment. Alternatively, the intermolecular dipole−dipole interaction becomes the main driving force for forming a 2D self-assembled structure on HOPG. Consequently, the *n*OCB (*n* = even) tends to have an *anti*-parallel alignment on the substrate as shown in Figure 15d.

N≡C−$(C_6H_4)_2$−$(CH_2)_{n-1}$−CH_3 (*n*CB) has a similar molecular skeleton less the ether group linking the phenyl ring and alkyl chain. In the formation of a 2D self-assembled monolayer of *n*OCB, the ether group plays the same role as a carbon atom in the alkyl chain. Thus, the terminal CH_3 group of *n*CB (*n* = even) and *n*CB (*n* = odd) are closely attached to and detached from the substrate, respectively (Figure 15a). *n*CB (*n* = odd or even) displays a similar packing structure as *n*OCB (*n* = even or odd), respectively. Thus, it exhibits a reverse odd−even effect compared to *n*OCB but for the same molecular reason.

Interestingly, the similar odd−even effects for liquid-crystal molecules *n*OCB and *n*CB as seen on HOPG were observed on MoS_2.[72,73] MoS_2 in general is described as consisting of a layered structure, like graphite, mica, and other materials, that is composed of stacked planes. All of these layered-structure materials exhibit much stronger bonding within the lateral planes than the interaction between two adjacent planes. Figure 15c,d exemplifies the odd−even difference in packing structure of *n*OCB in their self-assembled monolayers on MoS_2. Observation of the similar odd−even effect regardless of the category of substrate suggests that this odd−even effect is not strongly associated with the molecule−substrate interaction. Instead, it is mainly attributed to the different intermolecular van der Waals interactions resulting from the orientation of the terminal CH_3 group in the adsorbed molecules.

2.7. Odd–Even Effect on Packing Structure of the Bifunctional Molecule $HO(CH_2)_{n-1}COOH$

All the above odd−even effects are associated with single-functional molecules. Bifunctional molecules such as 15-hydroxypentadecanoic acid and 16-hydroxyhexadecanoic acid exhibit an odd−even difference in their self-assembled structures.[75,76] Figure 16a and c presents STM images of the self-assembled monolayers of the two molecules, respectively. Each lamella of $HO(CH_2)_{14}COOH$ forms both an H−O···H−O trough marked with "+" and an H−O−C═O···H−O−C═O trough marked with "*" between adjacent lamellae. The head-to-head packing mode of this molecule is shown in Figure 16b. However, $HO(CH_2)_{15}COOH$ self-assembles into a distinctly different structure (Figure 16c). Between two adjacent lamellae there are ordered large dark areas. Each area is roughly a rectangle. Figure 16d is the proposed model of the monolayer of $HO(CH_2)_{15}COOH$. Further examination shows that all dark areas can be classified as two types by the angle from the long axis of one dark rectangle to the molecular long axis along the clockwise direction. One category is T1 and T2 (120°) marked with red lines in Figure 16c,d. Another one is T3 and T4 (60°) marked with yellow lines in Figure 16c,d. Clearly, each dark area is formed by two acid groups and two hydroxyl groups. The four groups are assembled together through six hydrogen bonds to form a tetramer. Notably, the two categories of dark areas are mirror images of each other. For example, T1 (or T2) and T3 (or T4) use opposite faces to pack, suggesting the opposite chirality in the two categories of dark tetramers. Clearly, $HO(CH_2)_{14}COOH$ and $HO(CH_2)_{15}COOH$ self-assemble into different structures on HOPG.

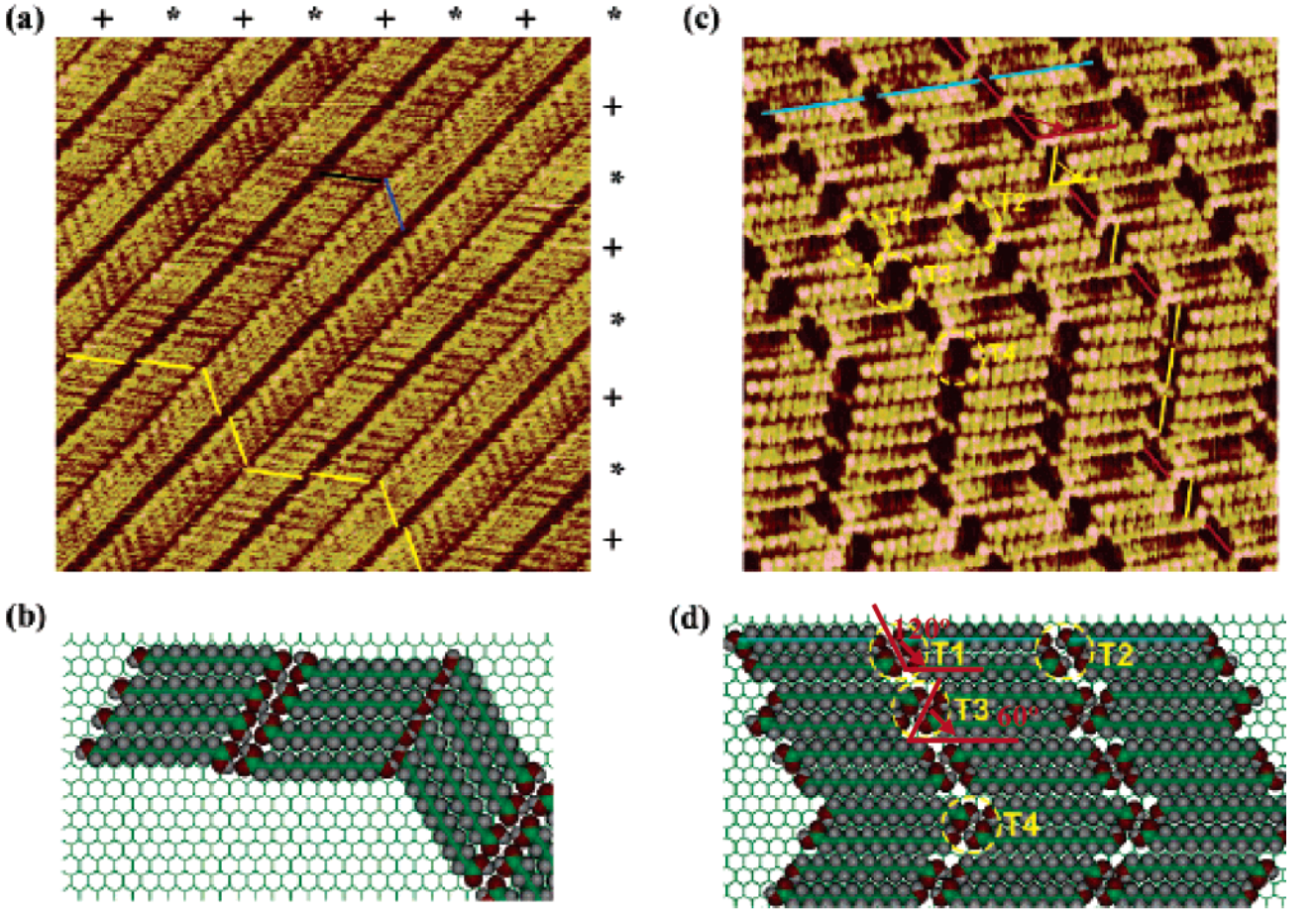

Figure 16. (a) STM image of 15-hydroxypentadecanoic acid at the interface of a 1-nonanol solution and the basal plane of graphite. The asterisks (*) mark troughs that are composed of carboxylic acid groups, and the pluses (+) mark troughs that are composed of alcohol functional groups. (b) Top view of a computer-generated model of 15-hydroxypentadecanoic acid on a graphite surface. (c) STM image of 16-hydroxyhexadecanoic acid in a hexanol solution on graphite. One molecular length is indicated by one of the blue bars. These blue bars are collinear, indicating that the fatty acids occupy the same graphite lattice rows. The dark spot T1 is identical to T2 and corresponds to a tetramer of two −COOH functions and two −OH functions connected through hydrogen bonding. The red and yellow bars depict the two different orientations observed for the dark spots. For example, T3 and T4 have the same orientation but are tilted from that of T1 and T2. (d) Top view of a model of 16-hydroxyhexadecanoic acid on a graphite surface. T1−T4 correspond to the −COOH and −OH functional groups that are hydrogen bonded and to the STM image in Figure 16c. Note that the orientations of T1 and T2 are identical and that T3 and T4 are identical. Furthermore, T1 and T2 are mirror images of T3 and T4. Reprinted with permission from ref 75. Copyright 2003 American Chemical Society.

This is a classic example of a significant change of the packing structure driven by a subtle difference in molecular length. In fact, this odd−even effect originates from a basic principle for 2D self-assembly of all molecules on solid substrates in terms of the optimization of surface−adsorbate and adsorbate−adsorbate interactions. The difference of chain length for the two molecules is only 7.7%, which can only result in a very small difference in the overall energetics of the surface structures due to the contribution from intermolecular van der Waals forces. Thus, the driving force for the odd−even difference in the self-assembled structure must be attributed to the intermolecular hydrogen bonds. Figure 17 clearly presents the difference in the hydrogen bonding of the structures. The −OH terminations of $HO(CH_2)_{n-1}COOH$ (n = odd) are in a favorable orientation to form an H−O···H−O hydrogen bond with the adjacent molecules in a lamella (green box in Figure 17a). However, for the molecules with an even number of carbon atoms, the added CH_2 group adjacent to the terminal OH creates an unfavorable conformation whose OH group cannot form a hydrogen bond with the OH group of its adjacent molecules in a lamella (red box in Figure 17b). To maximize the hydrogen-bond density of the self-assembled monolayer of $HO(CH_2)_{n-1}COOH$ (n = even), every four molecules form a tetramer (the dark areas in Figure 16c and yellow boxes in Figure 17c) where the molecules adopt a head-to-tail arrangement.

This odd−even effect is different from the others discussed. It results from maximizing attractive hydrogen-bonding density. However, other odd−even effects associated with carboxylic acid molecules are driven by reducing intermolecular repulsions.

2.8. Odd–Even Effect on Melting Behavior of *n*-Alcohol Monolayers

In organic chemistry the melting and boiling points of molecules such as unbranched alkanes exhibit an obvious odd−even effect.[1] The effect of chain length of the alkane in an adsorbed monolayer on its melting behavior has also been considered.[77] Recent studies revealed that the 2D self-assembled monolayers of *n*-alcohols with less than seven carbon atoms present an odd−even difference in their melting behaviors.[78] The saturated monolayer of *n*-alcohol with an

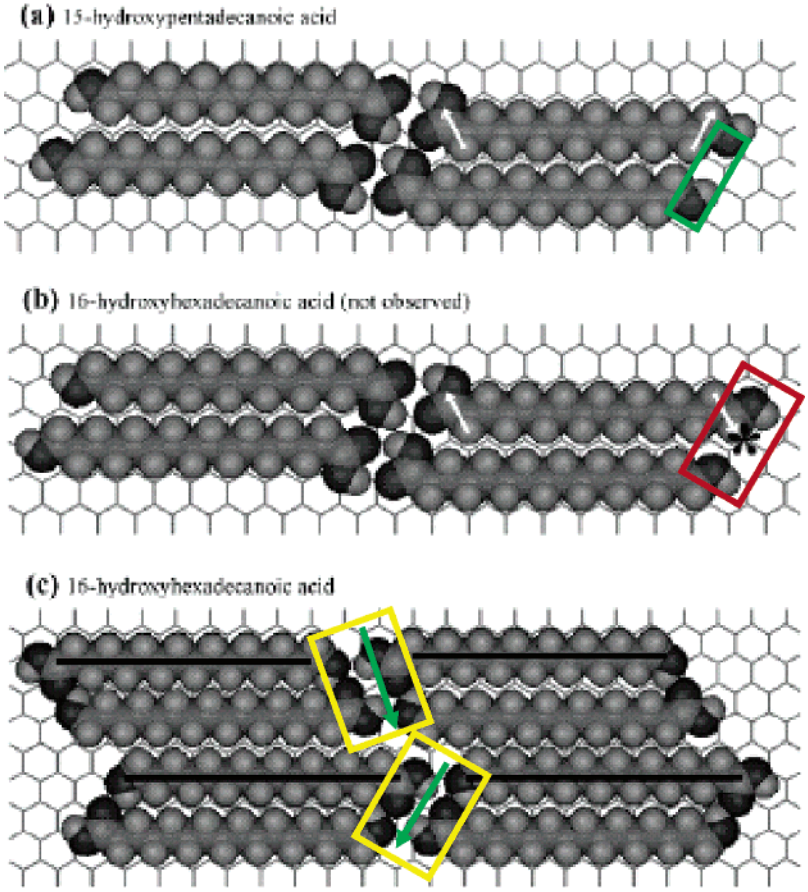

Figure 17. Top views of models describing a similar arrangement of four molecules of 15-hydroxypentadecanoic acid (a) and four molecules of 16-hydroxyhexadecanoic acid on a graphite surface (b). In a) the OH of one alcohol molecule is in a favorable orientation (see green box) to form a hydrogen bond to give the pattern shown in Figure 16a. (b) The OH groups of the two adjacent molecules in a lamella are in an unfavorable orientation (because one extra methylene group marked by a black asterisk lies between the two hydroxyl groups) and cannot hydrogen bond with the two adjacent lamellae. (c) Top views of models describing the arrangement of one tetramer of 16-hydroxyhexadecanoic acid where the superimposed black line shows the direction of the alkyl chain and the green arrow points to the long axis of the rectangular dim area. In c, the chemical functionalities −OH and −COOH are close to each other, forming a densely packed tetramer of hydrogen-bonded H-donor and H-acceptor groups. Reprinted with permission from ref 75. Copyright 2003 American Chemical Society.

odd number of carbon atoms melts through a 2D smectic mesophase in contrast to directly melting via a footprint reduction mechanism for the *n*-alcohol with an even number of carbon atoms. The melting behavior of *n*-alcohols with more than seven carbon atoms does not show this odd−even effect as the subtle differences in energetics are overcome by the increasing chain length.

The monolayers of *n*-alcohols on HOPG adopt a herringbone packing pattern via a head-to-head arrangement. The OH and terminal CH_3 have a cis conformation for the *n*-alcohols with an even number of carbon atoms, while they have a trans conformation for the *n*-alcohols with an odd number of carbon atoms. The difference in molecular conformation results in an odd−even difference in the packing of the terminal CH_3 on HOPG, though a herringbone structure is in general formed for the self-assembled monolayers of all *n*-alcohols. The difference in molecular conformation results in a slightly closer packing of the terminal CH_3 in individual lamellae for $CH_3(CH_2)_{n-1}OH$ (n = even) than for $CH_3(CH_2)_{n-1}OH$ (n = odd).[78] As shown in Figure 18 a dense packing of the terminal CH_3 is formed for *n*-alcohol molecules with an even number of carbon atoms (a) and a slightly looser packing for *n*-alcohol molecules with an odd number of carbons (b). Definitely, the latter gives an enhanced out-of-plane motion of the terminal CH_3 due to rotation of the terminal CH_3 around its adjacent C−C bond or even formation of a gauche conformation at the molecule end. In the center of two adjacent lamellae all the OH groups are still packed together through a hydrogen-bond network, though the terminal CH_3 groups at the two sides of one herringbone unit made of two adjacent lamellae have an enhanced out-of-plane motion. This structural feature may cause a random displacement of a pair of lamellae along the lamella direction without breaking the hydrogen bonding in this pair. The random displacement results in a random stacking of pairs of lamellae and thereby contributes to formation of a smectic mesophase for $CH_3(CH_2)_{n-1}OH$ (n = odd), as seen by X-ray diffraction patterns of the self-assembled monolayers.[78]

Originating from the real microscopic difference in the packing of the terminal CH_3, *n*-alcohols with an even number of carbon atoms do not melt via the 2D smectic mesophase. Moreover, the melting behavior of the partial monolayer of the molecules with an even number of carbon atoms does not display coverage dependence. In this case, melting may proceed via a footprint reduction mechanism[78] similar to the self-assembled monolayers of butane and hexane on graphite.[79−81] In this mechanism, motion of the adsorbate molecules normal to the substrate surface (footprint reduction) induces vacancies in the monolayer, therefore providing

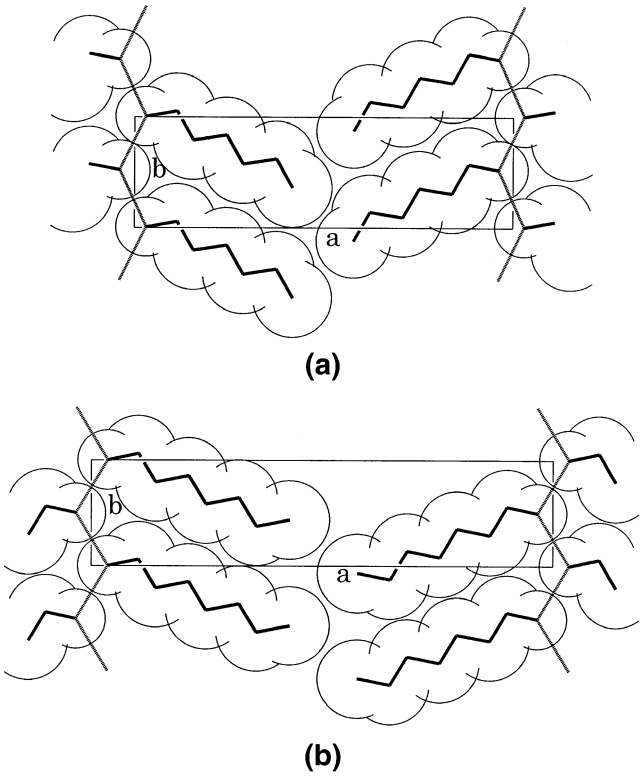

Figure 18. Structures of the crystalline monolayer of *n*-hexanol (a) and *n*-heptanol (b) adsorbed on graphite. They demonstrate a slightly different molecular packing density between *n*-alcohols with even and odd number of carbon atoms. Reused with permission from Kunimitsu Morishige and Takako Kato, *Journal of Chemical Physics*, *111*, 7095 (1999). Copyright 1999, American Institute of Physics.

sufficient space on the surface to make molecules disorder both translationally and rotationally during melting. The footprint reduction could be obtained by changing the molecular conformation or tilting molecules away from the surface. Therefore, the self-assembled monolayers of *n*-alcohols exhibit odd−even differences in their melting behaviors.

3. Odd–Even Effects in Organic Self-Assembled Monolayers on Au(111) and Ag(111)

The surprising interest and tremendous efforts in the self-assembly of organic molecules on metal surfaces were motivated by a wide spectrum of technological requirements. Compared to other thin film techniques such as molecular beam epitaxy and chemical vapor deposition, molecular self-assembly can controllably incorporate various organic functionalities and form highly ordered and oriented monolayers with fine chemical control at the molecular level. The self-assembled organic surfaces on metal substrates are currently of promising technological applications[82,83] such as corrosion inhibition and coating,[84] lubrication,[85] adhesion,[86] molecular electronics,[87] catalysis,[88] and sensor devices.[89−91] In addition, chemical attachment of organic layers on metal surfaces is an excellent approach to tuning surface composition, physical and chemical properties, and surface and interfacial functions via controllable tailoring of molecular functional groups and surface structure.[9]

For the self-assembled monolayers of organic molecules on HOPG (and MoS_2) exhibiting diverse odd−even effects on structure and chirality, the interactions between organic molecules and substrate are primarily weak van der Waals interactions. All molecules of one monolayer lie on the substrate, and the planes of the molecular carbon skeletons are parallel to the substrate. For organic molecules containing head groups with a chemical affinity for the solid substrate such as Au(111), however, all molecules stand upright on the metal surface with a specific tilt angle. In this case the interaction between the head group of the organic molecule (such as the sulfur atom of a thiol) and the metal atom is a chemical bond with a strength of ∼50 kcal/mol on Au(111).[92,93] As expected, the strong chemical binding between organic molecules and the metal substrate possibly plays a more important role in molecular self-assembly and determining the odd−even effects.

For organic self-assembled monolayers formed via chemical reaction with a substrate such as thiolate monolayers on Au(111), the terminal group/moiety, the head group/moiety, and the length and geometry of the all-trans alkyl chains between the terminal and head groups/moieties significantly impact their surface structures and various properties. This influence exhibits a number of structural odd−even effects which further induce corresponding odd−even alternation in various chemical, physical, and interfacial properties of these interesting self-assembled monolayers.

3.1. Surface Structures and Adsorption Sites on Au(111) and Ag(111)

The most widely used substrates for growth of organic self-assembled monolayers through chemical binding are thin films of coinage metals supported on mica or silicon single crystals. Generally, the grown films on these substrates have a dominant (111) texture for the fcc coinage metals. For example, Au and Ag films grow epitaxially into a strongly oriented (111) surface structure on the (100) surface of mica. The fabricated Au(111) and Ag(111) films have the same structure as shown in Figure 19a, though their lattice parameters are slightly different. The distance between the two adjacent Au atoms is 2.88 Å. There are three categories of adsorption sites including the on-top site, 2-fold bridge site, and 3-fold hollow site. The separation of the two adjacent hollow sites is ∼2.9 Å. For the (111) surface of coinage metal substrates such as Au(111) and Ag(111) films, the head group sulfur atom of the organosulfur marked with a light-aqua toroid in Figure 19b typically bonds on a 3-fold hollow site.

3.2. Odd–Even Effect on Structure of Organic Monolayers on Au(111)

Self-assembly of organic monolayers on Au(111) films is a model of developing self-assembled organic monolayers on metal substrates. It is historically the most studied system, and a complete discussion of the many systems investigated is well beyond the scope of this review. One important reason for focus on the Au(111) film is that the Au(111) film is not oxidized at a temperature lower than its melting point. However, many metal substrates such as Cu(111) and Al(111) films can easily be oxidized at room temperature and under ambient conditions.

The self-assembled $CH_3(CH_2)_nS-Au$ monolayer is taken as a model of organic monolayers on metal substrates for defining molecular geometry upon self-assembly. Figure 20 schematically describes the geometry of methyl-terminated alkanethiolate self-assembled on the metal substrate. The self-assembled monolayer exhibits a $(\sqrt{3} \times \sqrt{3})R30°$ surface structure. The surface geometry of the all-trans alkyl chain

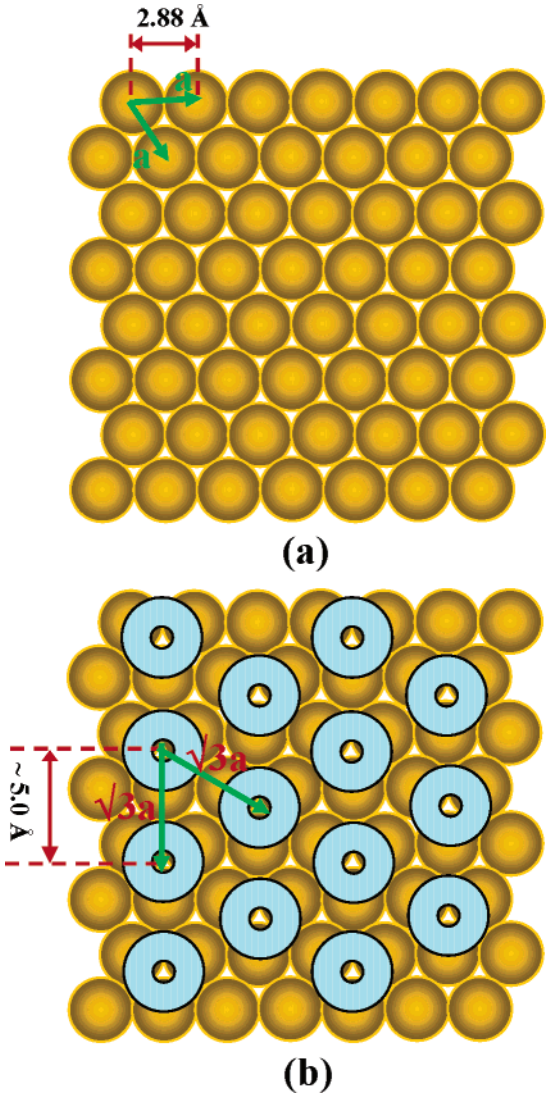

Figure 19. Structures and adsorption sites of Au(111) and Ag(111) surfaces. (a) Top view of a clean (111) substrate. (b) Top view of an organic self-assembled monolayer with $\sqrt{3} \times \sqrt{3}R30°$ surface structure. Each light-green circle represents one organic molecule which chemically binds to a 3-fold adsorption site of the (111) substrate. The labeled structure parameters are for Au(111).

attached to the surface through a Au−S bond can be described by a tilt angle, α, and a twist angle, β, as shown in Figure 20a. The angle α is defined as the angle between the molecular long axis in the plane containing the all-trans zigzag carbon skeleton and the surface normal. The angle of chain twist, β, is defined as the rotation of the plane containing the zigzag carbon chain along the long axis of the alkyl chain (Figure 20a). If α is 0°, the terminal CH_3 of a chain with either an even or an odd number of CH_2 units has the same projection along the surface normal (Figure 20b,e), showing no odd−even effect of terminal CH_3 orientation and subsequent properties. When α is not 0°, the alkyl chain with an even number of CH_2 units has a different orientation of the terminal CH_3 and CH_3-CH_2- moiety in terms of a larger exposure of the topmost CH_2 unit compared to the molecules with an odd number of CH_2 groups (Figure 20c,f). Figure 20d,g shows the geometry of the alkyl chain after rotating an angle β along the long axis of the alkyl chain. For an alkanethiol whose terminal moiety or head moiety is substituted by another functionality such as a

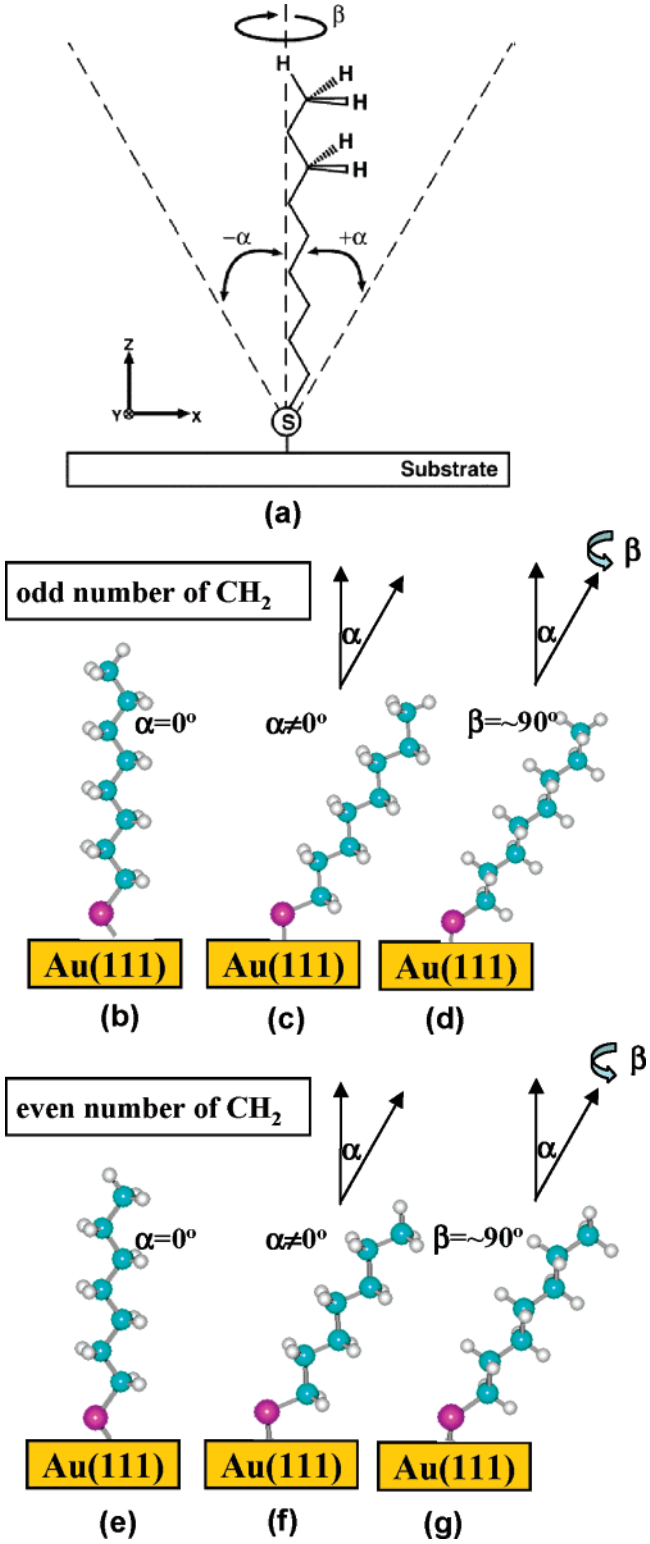

Figure 20. (a) Scheme showing the definition of tilt angle (α) and twist angle (β) of all-trans alkyl chains of organic molecules self-assembled on solid surfaces. (b−d) Geometries of alkyl chains of $CH_3(CH_2)_nS-Au$ monolayer (n = odd). (b) $\alpha = 0°$, $\beta = 0°$. (c) $\alpha \neq 0°$, $\beta = 0°$. (d) $\alpha \neq 0°$, $\beta \neq 0°$. (e−g) Geometries of alkyl chains of $CH_3(CH_2)_nS-Au$ monolayer (n = even). (e) $\alpha = 0°$, $\beta = 0°$. (f) $\alpha \neq 0°$, $\beta = 0°$. (g) $\alpha \neq 0°$, $\beta \neq 0°$. Figure 20a was reprinted with permission from ref 9. Copyright 2005 American Chemical Society.

phenyl ring or carboxylic acid group, respectively, the geometry of their alkyl chain can still be described with these two parameters, α and β.

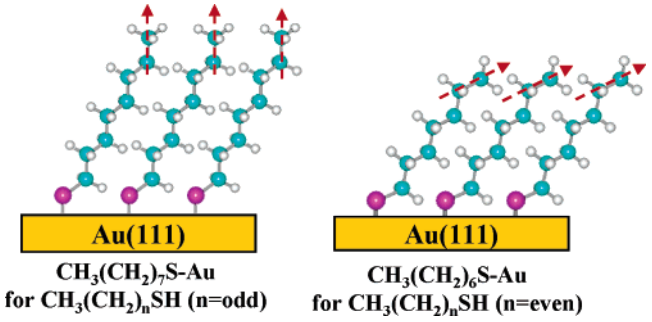

Figure 21. Illustration of the odd−even effect on the orientation of the terminal methyl group and CH_3-CH_2- moiety for the self-assembled *n*-alkanethiolate monolayers on Au(111).

3.2.1. $CH_3(CH_2)_nSH$

Alkanethiol $CH_3(CH_2)_nSH$ is the simplest example to demonstrate the odd−even chain-length effect on the structure of organic self-assembled monolayers on metal surfaces. On the basis of the sp^3 hybridization of the bonded sulfur atom upon chemical binding, the alkyl chain has an orientation of ~30° from the normal of an Au(111) surface and a twist angle $\beta \approx 50°$.[12,94−96] Depending on the even or odd number of CH_2 units of the all-trans alkyl chains, the terminal CH_3 groups have different orientations (Figure 21) under an assumption that the self-assembled monolayer exhibits a 2D crystal ordering. The expected odd−even effect on the orientation of the terminal CH_3 group which in turn is evidence of the 2D crystallization of $CH_3(CH_2)_nSH$ on Au had been confirmed by vibrational spectroscopy and other techniques.[97−100]

Vibrational signatures of the self-assembled monolayers of $CH_3(CH_2)_nS-Au$ obtained from high-resolution electron energy loss spectroscopy (HREELS) provide clear evidence for the odd−even difference in the orientation of the terminal CH_3 group. The terminal CH_3 can be identified by its vibrational signatures including the *s*-deformation mode at ~1380 cm^{-1} and the *d*-deformation mode at ~1460 cm^{-1} as well as the symmetric and asymmetric stretching modes around ~2850−3000 cm^{-1}.[98] Figure 22 shows a series of vibrational spectra corresponding to the self-assembled monolayers of alkanethiolates with 10−16 carbon atoms on the Au surfaces. This figure clearly shows that the appearance and absence of the CH_3 *s*-deformation mode at ~1380 cm^{-1} completely depends on whether the number of CH_2 units of an alkyl chain is odd or even, respectively. The appearance and absence in fact rely on the orientation of the terminal CH_3-CH_2- moiety. For $CH_3(CH_2)_nS-Au$ with n = odd or even, the terminal CH_3-CH_2- tends to be parallel to the surface normal or tilt from it, largely enhancing or weakening the dipole scattering and producing the difference in the vibrational features of the terminal CH_3 group (Figure 22). In addition, the intensity of the CH_3 rocking mode also alternately changes for molecules with an even or odd number of CH_2 units. In fact, the infrared spectra with a higher resolution than HREELS show an odd−even effect on intensity of $\nu_{sym}(CH_3)$, $\nu_{asym}(CH_3)$, and the intensity ratio between them for the self-assembled monolayers of $CH_3(CH_2)_nS-Au$.[100] The odd−even alternation of intensity of the CH_3 stretching mode further supports that the orientation of the terminal CH_3 is dependent on whether the number of CH_2 groups is even or odd.

Contact angle measurement on the $CH_3(CH_2)_nS-Au$ monolayers using methylene diiodide and nitrobenzene

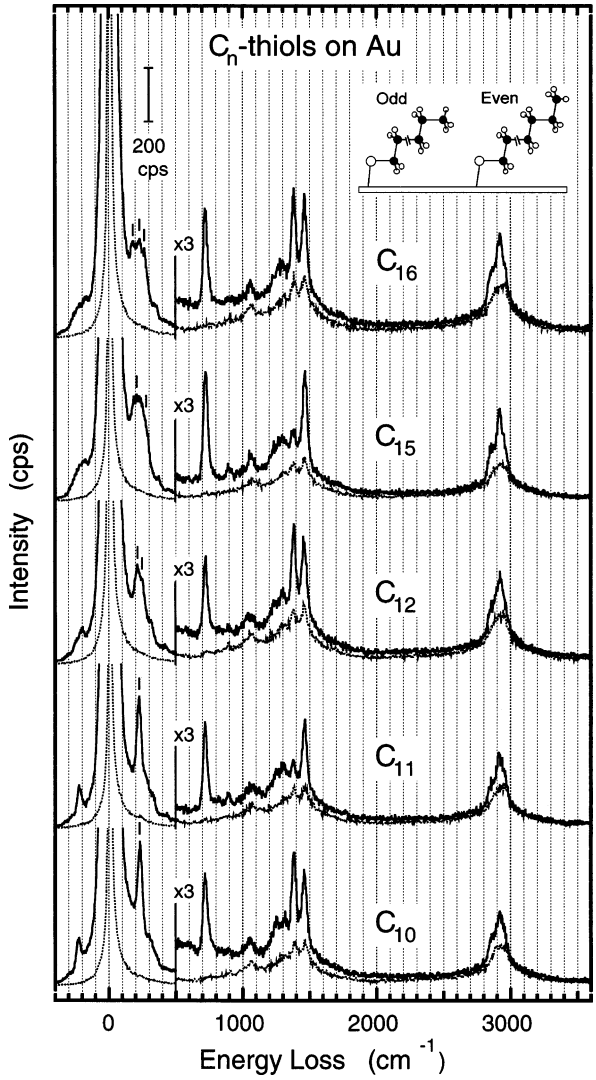

Figure 22. HREEL spectra of $CH_3(CH_2)_nS-Au$ monolayers (n = 9, 10, 11, 14, 15) on Au. (Inset) Schematic models of molecules with odd and even carbon number on Au. Notably, *m* in the label C_m around each spectrum presents the total number of carbon atoms of one molecule. Reprinted with permission from ref 98. Copyright 2002 American Chemical Society.

confirmed the odd−even effect on the orientation of the terminal CH_3 (or CH_3-CH_2-) (Figure 23). The alkanethiolate monolayer with an odd number of CH_2 units has a larger contact angle in terms of a lower wettability compared to the monolayer with an even number of CH_2 units.[79] For a monolayer of $CH_3(CH_2)_nS-Au$ (n = odd), the surface is predominantly composed of methyl groups because its terminal CH_3-CH_2 bond is perpendicular to the substrate. The terminal CH_3-CH_2- moiety of the $CH_3(CH_2)_nS-Au$ monolayer (n = even) is tilted away from the surface normal, producing a surface that is composed of methyl groups and topmost methylene groups. The contact angles of $CH_3(CH_2)_nS-Au$ (n = even) are lower because the exposure of the underlying methylene units increases the number of attractive dispersive contacts with the area of the liquid drop compared to the monolayers of $CH_3(CH_2)_nS-Au$ (n = odd).

3.2.2. $CH_3(CH_2)_nCS_2H$

To test whether different binding chemistry of head groups to the hexagonal lattice of the Au(111) surface can change the structural feature and modify the odd−even effect of the

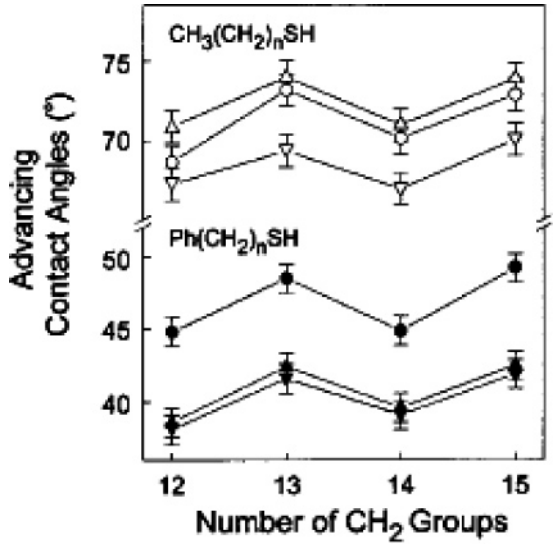

Figure 23. Advancing contact angles measured on the $CH_3(CH_2)_nS-Au$ and $C_6H_5(CH_2)_nS-Au$ monolayers using methylene iodide (○ and ●), nitrobenzene (▽ and ▼), and dimethyl formamide (Δ and ▲) as contacting liquids. Open symbols for $CH_3(CH_2)_nS-Au$. Solid symbols for $C_6H_5(CH_2)_nS-Au$. Reprinted with permission from ref 79. Copyright 2001 American Chemical Society.

self-assembled monolayers, aliphatic dithiocarboxylic acids $CH_3(CH_2)_nCS_2H$ ($n = 8-17$) were selected as a probe.[101,102] Figure 24a shows the molecular structure of this category of molecule. Upon adsorption, the S−H bond dissociates on the Au(111) film and both sulfur atoms of the head group equivalently bond to the Au surface as shown in Figure 24b. In the self-assembled thiolate monolayer $CH_3(CH_2)_nS-Au$ the separation between two adjacent tethered sulfur atoms is ~5.0 Å (Figure 19b). Compared to $CH_3(CH_2)_nS-Au$, the distance between the two sulfur atoms in one $CH_3(CH_2)_nCS_2H$ molecule is ~2.9 ± 0.3 Å,[101] suggesting a different chemical binding on the Au(111) film. In contrast to the alkanethiolate monolayer, this gives rise to a modified odd−even effect.

The vibrational evidence for the alternating variation in the intensity of CH_3 vibrational modes for the dithiocarboxylic acids with odd and even number of CH_2 units suggests that the terminal CH_3 groups have different orientations.[101] The terminal CH_3-CH_2- moiety of molecules with an odd number of CH_2 units tilts from the surface normal; in contrast, that of molecules with even number of CH_2 groups appears to be normal to the surface. This odd−even alternation of the CH_3-CH_2- orientation is further supported by contact angle measurements.[101] The value of the contact angles of monolayers with an even number of CH_2 units is higher than that with an odd number of CH_2 groups (Figure 24c). The difference of contact angles between the even series and the odd series for $CH_3(CH_2)_nCS_2-Au$ monolayers[101] is dramatically greater than that for $CH_3(CH_2)_nS-Au$[100] as shown in Figure 24c, indicating that the geometries of the alkyl chains in $CH_3(CH_2)_nS_2-Au$ are different from those of the alkanethiolate monolayers. It may be partially due to the different binding configuration of the tethered group Au−S−C−S−Au for dithiocarboxylic acid compared to Au−S of the alkanethiol. Compared to $CH_3(CH_2)_nS-Au$ monolayer, the chelation effect of two terminal sulfur atoms bonded to two nearest 3-fold hollow sites largely enhances the structural constraints in terms of torsional stiffening, increasing the odd−even difference in the orientation of the

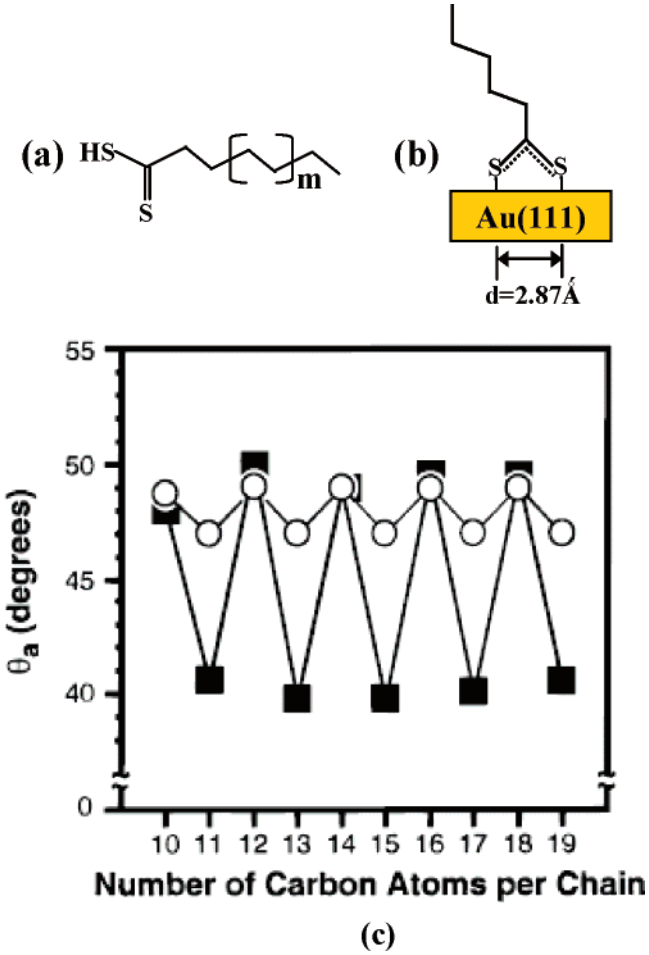

Figure 24. (a) Aliphatic dithiocarboxylic acids $CH_3(CH_2)_nCS_2H$. (b) Binding geometry of dithiocarboxylic acid group on Au surface. (c) Advancing contact angles of hexadecane on self-assembled monolayers of $CH_3(CH_2)_nCS_2-Au$ (filled squares) and $CH_3(CH_2)_nS-Au$ (empty circles). Notably, the *X* axis shows the number of all carbon atoms in a molecule of $CH_3(CH_2)_nCS_2-Au$ or $CH_3(CH_2)_nS-Au$. Figure 24c was reprinted with permission from ref 101. Copyright 1998 American Chemical Society.

terminal CH_3-CH_2- moiety for $CH_3(CH_2)_nS_2-Au$ monolayers.

Generally, the odd−even effects on wettability of the monolayer of alkanethiolate and its derivatives are understood as a greater exposure of the topmost CH_2 groups of the self-assembled monolayer having an even number of CH_2 units giving a lower contact angle in terms of stronger wettability.[29,100,103,104] Thus, the larger exposure of the topmost CH_2 resulting from the larger separation between two adjacent chains in $CH_3(CH_2)_nCS_2-Au$ monolayers with an odd number of carbon atoms compared to $CH_3(CH_2)_nS-Au$ monolayers with an odd number of carbon atoms gives a smaller contact angle, increasing the odd−even difference in measured contact angle for the $CH_3(CH_2)_nCS_2-Au$ series. A comparison of odd−even effects between the $CH_3(CH_2)_nS-Au$ series and the $CH_3(CH_2)_nCS_2-Au$ series indicates that the different binding configuration of the head group and geometry of the alkyl chain on Au(111) may modify the odd−even effect of these self-assembled monolayers.

3.2.3. $C_6H_5(CH_2)_nSH$

To determine the possible change of the odd−even effects of alkanethiolate monolayers depending on different terminal

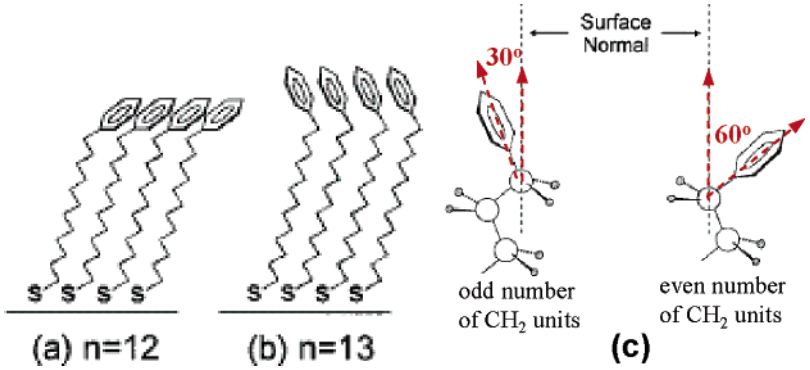

Figure 25. Schemes of phenyl-terminated self-assembled monolayers of 12-phenyldodecanethiolate (a) and 13-phenyltridecanethiolate (b). (c) Average tilt angles of the terminal phenyl groups of $C_6H_5(CH_2)_nS-Au$ monolayers with odd number (left panel) and even number (right panel) of CH_2 units. Reprinted with permission from ref 79. Copyright 2001 American Chemical Society.

groups, the odd−even effect of phenyl-ring-terminated alkanethiolates $C_6H_5(CH_2)_nS-Au$ ($n = 12-15$) was investigated.[79] $C_6H_5(CH_2)_nSH$ bonds to the Au surface via the same chemical binding as the alkanethiol. Vibrational analysis and contact angle measurement show an odd−even effect of the orientation of the terminal phenyl ring. It was determined that the C^1-C^4 ring axis of the phenyl ring is oriented from the surface normal by ~30° for molecules with an odd number of CH_2 units.[79] However, it is ~60° for molecules with an even number of CH_2 groups. This odd−even difference is schematically shown in Figure 25.

The contact angle measurements confirmed the odd−even difference in the orientation of the terminal phenyl ring.[79] Measurements using methylene iodide, nitrobenzene, or dimethyl formamide as the contacting liquid exhibit an odd−even alternation of advancing contact angles on the odd and even numbers of CH_2 units in the alkyl chains (Figure 23). The contact angle of $C_6H_5(CH_2)_nS-Au$ is always smaller than that for $CH_3(CH_2)_nS-Au$ when the same contacting liquid is used for the measurements (Figure 23),[100] which possibly implies different origins of the odd−even effects in wettability. For $CH_3(CH_2)_nS-Au$, as mentioned above, the odd−even difference of contact angles results from the greater exposure of the topmost CH_2 groups for molecules with an even number of CH_2 units.[29,100,103,104] In contrast, the dependence of contact angles of $C_6H_5(CH_2)_nS-Au$ monolayers on the odd and even number of CH_2 groups is mainly determined by the orientation of the terminal phenyl ring due to the blocking effect of the large phenyl ring on the topmost CH_2 group.

IR results for the $C_6H_5(CH_2)_nS-Au$ monolayers suggest a novel odd−even difference in the twist angle of the alkyl chain. This odd−even difference is not observed for $CH_3(CH_2)_nS-Au$ monolayers. Figure 26 shows that the intensity ratio between $\nu_{sym}(CH_2)$ and $\nu_{asym}(CH_2)$ varies alternately depending on the odd and even number of CH_2 groups in the $C_6H_5(CH_2)_nS-Au$ monolayers.[79] The lower ratio of the intensity for molecules with an even number of CH_2 units indicates that the molecules in these self-assembled monolayers have a larger twist of the backbone chain,[100,105] though the contribution of chain tilting cannot be excluded entirely. This odd−even difference in chain twist is proposed to be possibly related to the different degree of interaction among the terminal phenyl groups such as $\pi-\pi$ stacking or/and steric repulsion associated with the distinctly different orientation of the phenyl group of the molecule with an odd or even number of CH_2 units. For example, the different extent of $\pi-\pi$ overlap as shown in Figure 25a,b possibly

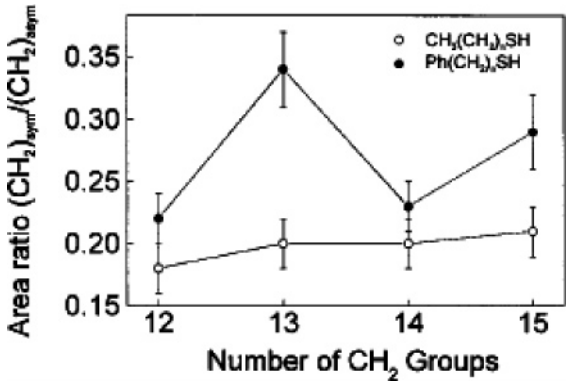

Figure 26. Ratio of intensity between $\nu_{sym}(CH_2)$ and $\nu_{asym}(CH_2)$ as a function of the number of CH_2 units for $C_6H_5(CH_2)_nS-Au$ and $CH_3(CH_2)_nS-Au$ self-assembled monolayers. Reprinted with permission from ref 79. Copyright 2001 American Chemical Society.

leads to a different degree of chain twist between molecules with an even or odd number of CH_2 units. It could be considered as a new odd−even effect induced by a substituted terminal group such as a phenyl ring. In addition, the much lower intensity ratio between $\nu_{sym}(CH_2)$ and $\nu_{asym}(CH_2)$ of $CH_3(CH_2)_nS-Au$ compared to that of $C_6H_5(CH_2)_nS-Au$ in Figure 26 indicates a larger twist angle for the alkyl chains of normal alkanethiolate monolayers, though there is no odd−even difference in the chain twist. Compared to $CH_3(CH_2)_nS-Au$, the small chain twist of $C_6H_5(CH_2)_nS-Au$ may result from the blocking effect of their large phenyl rings on the rotation of the alkyl chains in this monolayer.

Although the odd−even effect of phenyl-ring-terminated alkanethiolate monolayers is somewhat different from that of the methyl-terminated alkanethiolate monolayers, their chemical bonding, lattice spacing of the backbone chain, lattice ordering, and surface coverage are indistinguishable from one another.

3.2.4. $C_6H_5-(C_6H_4)_2-(CH_2)_n-SH$

Compared to $C_6H_5(CH_2)_nSH$, 4, 4′-terphenyl-substituted alkanethiol $C_6H_5-(C_6H_4)_2-(CH_2)_n-SH$ (TP_n, $n = 1-6$) has two more phenyl rings. Its self-assembled structure and interfacial properties on Au(111) were studied using XPS, HREELS, IRAS, NEXAFS, contact angle measurement, AFM, and STM.[105−112] Identical to the odd−even effect of the orientation of the phenyl ring of $C_6H_5(CH_2)_nS-Au$, the terphenyl moieties of the molecules with an even number

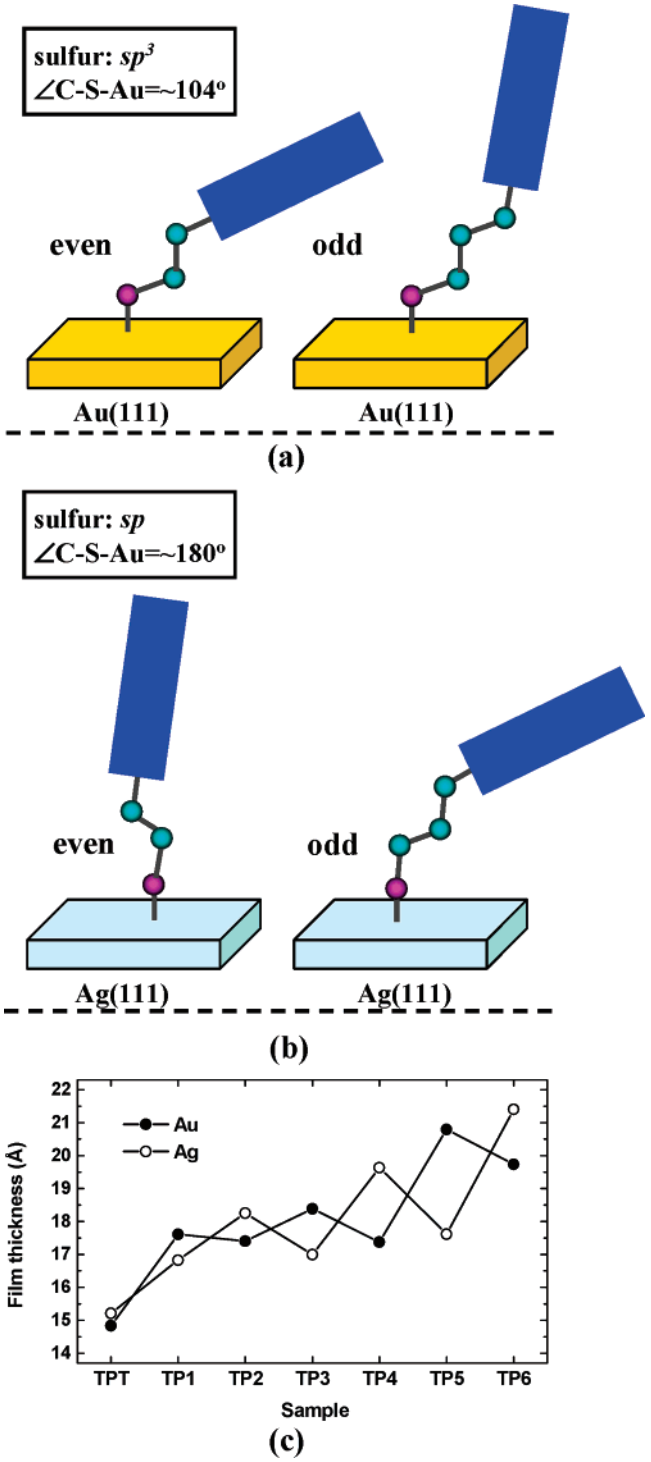

Figure 27. Schemes showing the orientation of the terminal terphenyl rings and the binding geometry of TP_n monolayers on Au(111) (a) and Ag(111) (b). (c) Effective film thickness of TP_n/Au(111) and TP_n/Ag(111) derived from the ellipsometry data. Figure 27c was reprinted with permission from ref 106. Copyright 2004 American Chemical Society.

of CH_2 units tilt from the surface normal by a larger angle than those with an odd number of CH_2 groups as schematically illustrated in Figure 27a. The odd−even oscillation of tilt angles of the terminal terphenyl moieties is supported by IRAS and NEXAFS. This odd−even effect is also consistent with the odd−even alternations of the molecular packing densities and effective film thickness of the self-assembled monolayers obtained from high-resolution XPS (HRXPS) and ellipsometry data (Figure 27c), respectively.[106] Similar odd−even effects in molecular packing density and effective film thickness are expected for $C_6H_5(CH_2)_nS-Au$, though there is no report on them.

The odd−even variation of intensity of the CH_2 stretching mode of $C_6H_5-(C_6H_4)_2-(CH_2)_n-S-Au$ possibly indicates a slight odd−even alternation of the orientation of the alkyl chain in terms of chain tilt.[106] This possibly results from an odd−even change of $\pi-\pi$ repulsion of two adjacent molecules in the self-assembled monolayers. However, it is not conclusive due to the small odd−even difference in the intensity of the CH_2 stretching mode. No similar odd−even effect reported for $CH_3(CH_2)_nS-Au$, $CH_3(CH_2)_nS_2-Au$, and $C_6H_5(CH_2)_nS-Au$ is possibly due to the absence of large $\pi-\pi$ repulsion in these self-assembled monolayers.

No pronounced odd−even changes in the contact angles were observed for $C_6H_5-(C_6H_4)_2-(CH_2)_n-S-Au$ monolayers when the contacting liquid was water,[106] suggesting the complexity of the origin of the wetting property. The weaker and weaker odd−even difference for contact angles from $CH_3(CH_2)_nS_2-Au$, $CH_3(CH_2)_nS-Au$, $C_6H_5(CH_2)_nS-Au$, to $C_6H_5-(C_6H_4)_2-(CH_2)_n-S-Au$ indicates that the wetting property is at least partially determined by the exposure of the topmost CH_2 group in the self-assembled monolayers. Notably, a weak odd−even effect of contact angle for $C_6H_5-(C_6H_4)_2-(CH_2)_n-S-Au$ monolayers is possibly observed if different contacting liquids such as methylene iodide or nitrobenzene are used. The reason is that a contacting liquid with a small dipole moment such as H_2O did not reveal an odd−even difference for monolayers such as $C_6H_5(CH_2)_n-S-Au$, but an obvious odd−even effect was observed when a strongly dipolar liquid such as methylene iodide or nitrobenzene was used.[79]

Overall, $C_6H_5-(C_6H_4)_2-(CH_2)_n-S-Au$ exhibits odd−even effects similar to $C_6H_5(CH_2)_nS-Au$. Compared to the two series $C_6H_5-(C_6H_4)_2-(CH_2)_n-S-Au$[106] and $CH_3-(C_6H_4)_2-(CH_2)_n-S-Au$[113−116] to be discussed in the next section, $CH_3(CH_2)_nS-Au$ monolayers do not exhibit the odd−even effect of molecular packing density. However, a pronounced odd−even effect of wetting properties was observed in $CH_3(CH_2)_nS-Au$ monolayers, which is only weakly observed in phenyl-ring-substituted alkanethiolate monolayers. These differences in the odd−even effects between methyl-terminated alkanethiolates and phenyl-ring-terminated alkanethiolates demonstrate that structures and properties such as packing density and wettability of the organic self-assembled monolayer as well as their odd−even effects may be modified by substituting the terminal group of the self-assembled molecule.

3.2.5. $CH_3-(C_6H_4)_2-(CH_2)_n-SH$

Compared to the organosulfur molecules discussed above, odd−even effects for methyl-terminated biphenyl-substituted alkanethiols $CH_3-(C_6H_4)_2-(CH_2)_n-SH$ (BP_n, $n = 1-4$) were systematically studied using various experimental techniques coupled with theoretical calculation, particularly employing synchrotron-based HRXPS and STM.[63,113−116] In addition to the odd−even alternation of packing density and effective thickness, new odd−even effects such as an odd−even difference in the inhomogeneity of adsorption sites of $CH_3-(C_6H_5)_2-(CH_2)_n-S-Au$ were revealed.

The C1s photoemission feature of BP_n self-assembled monolayers on Au is a main peak at ~284.0 eV and a small shoulder at the side of higher binding energy (BE). The

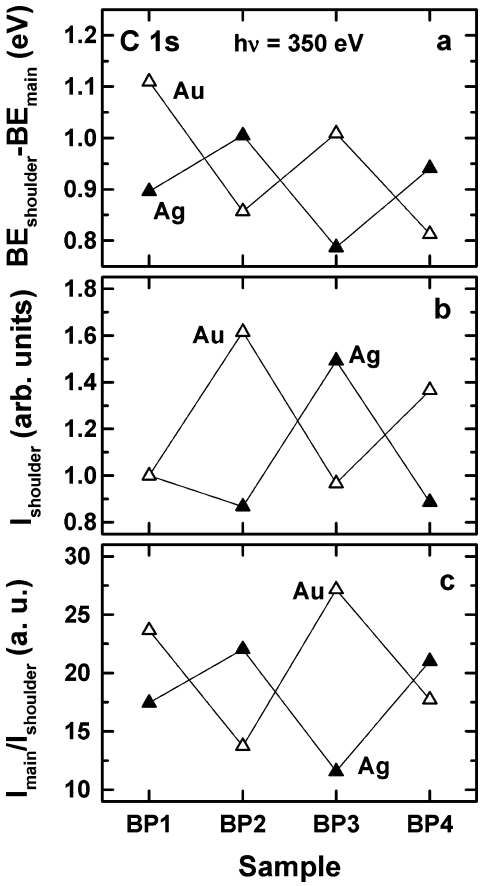

Figure 28. C1s photoemission features of BP_n self-assembled monolayers on Au(111) and Ag(111). (a) BE position of the shoulder compared to its corresponding main C1s peaks; the *Y* axis shows how much the shoulder shifts from the main peak of the same spectrum. (b) Intensity of the shoulder of C1s photoemission feature. (c) Ratio of C1s photoemission intensity between the shoulder and its corresponding main peaks. Reprinted with permission from ref 113. Copyright 2001 American Chemical Society.

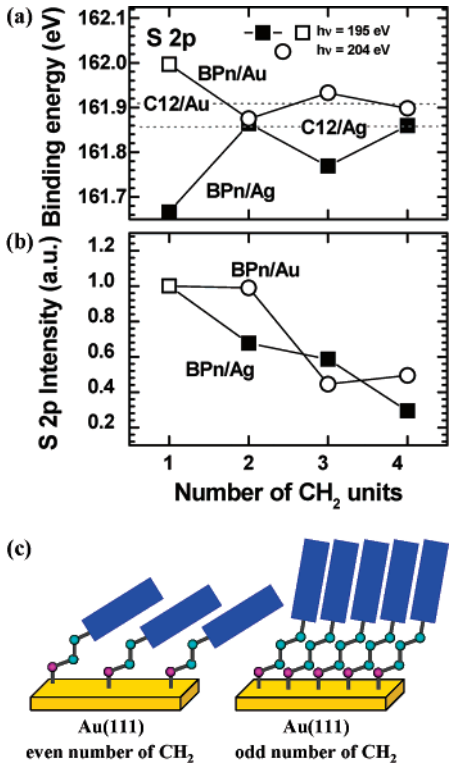

Figure 29. (a) BE position of the S2p doublet derived from the S2p photoemission spectra of $CH_3-(C_6H_4)_2-(CH_2)_n-S-Au$ and $CH_3-(C_6H_4)_2-(CH_2)_n-S-Ag$ monolayers. Two dashed lines show the BE of S2p of $CH_3(CH_2)_{11}S-Au$ and $CH_3(CH_2)_{11}S-Ag$ monolayers. (b) Normalized intensity of the S2p doublet. (c) Schematic drawings of the orientation and packing of the $CH_3-(C_6H_4)_2-(CH_2)_n-S-Au$ monolayers with odd and even number of CH_2 units in the alkyl part. Note that for clarity the large intermolecular distance for the case of unfavorable packing in the self-assembled monolayer BP_n (n = even) is exaggerated. Parts a and b were reprinted with permission from ref 113. Copyright 2001 American Chemical Society.

position and intensity of the shoulder with respect to the main C1s peak of $CH_3-(C_6H_4)_2-(CH_2)_n-S-Au$ presents a pronounced odd−even alternation as seen in the XPS.[113] On the basis of the odd−even variation in the peak position and intensity (Figure 28a,b), the higher BE shoulder results from the low-energy shake up excitation in the aromatic matrix. Considering the high surface sensitivity of synchrotron-based HRXPS obtained by choosing optimal excitation energy to enhance photoemission from biphenyl groups, this assignment of the higher BE shoulder is reasonable. Therefore, the odd−even variation of the position and intensity of the C1s shoulder reflects the odd−even difference of the tilt angle of the biphenyl ring moiety.

Although the sulfur atoms of $CH_3-(C_6H_4)_2-(CH_2)_n-SH$ bond to Au(111) via the same sp^3 hybridization, the BE and intensity of the S2p exhibit an obvious odd−even alternation with the length of the alkyl chain as shown in Figure 29a,b.[113] The odd−even effect of S2p BE suggests an odd−even variation of Au−S binding configuration which is possibly driven by the odd−even difference in the molecular packing density and biphenyl orientation as a function of the number of CH_2 units in the molecule. The odd−even variation of the S2p intensity which gradually decreases with increasing length of the alkyl chain may be attributed to two opposite effects. The odd−even change of packing density of the tethered sulfur atoms in terms of molecular absolute coverage on the Au surface (Figure 29c) directly determines that the S2p intensity exhibits an odd−even effect. From this point the S2p intensity of BP_n (n = odd) is higher than that of BP_n (n = even) due to its higher packing density. On the other hand, the effective film thickness of BP_n (n = odd) is larger than that of BP_n (n = even) due to the orientation of the biphenyl moieties (Figure 29c), resulting in a higher photoionization cross section for each sulfur atom of a molecule with an even number of CH_2 units. Overall, the effect (decreasing surface coverage of sulfur atom) of decreasing S2p intensity from odd (m) to even ($m + 1$) is nearly overcompensated by the second effect (decreasing effective film thickness) of increasing S2p intensity due to the increase of photoionization probability from odd (m) to even ($m + 1$). Thus, from BP_m (m = odd) to BP_{m+1} ($m + 1$ = even), the S2p intensity remains constant or is slightly enhanced as compared to the average downward trend (Figure 29b). From even ($m + 1$) to odd ($m + 2$) the effect of packing density on increasing S2p intensity is overcompensated by the effect of the effective film thickness in decreasing the S2p intensity, thereby resulting in an overall decrease of the S2p intensity from BP_{m+1} to BP_{m+2}. Although an odd−even effect of S2p intensity for $C_6H_5-(CH_2)_n-S-Au$ and $C_6H_5-(C_6H_4)_2-(CH_2)_n-S-Au$ monolayers was not reported, a similar trend is predicted since they have the same odd−even difference in the orientation of terminal

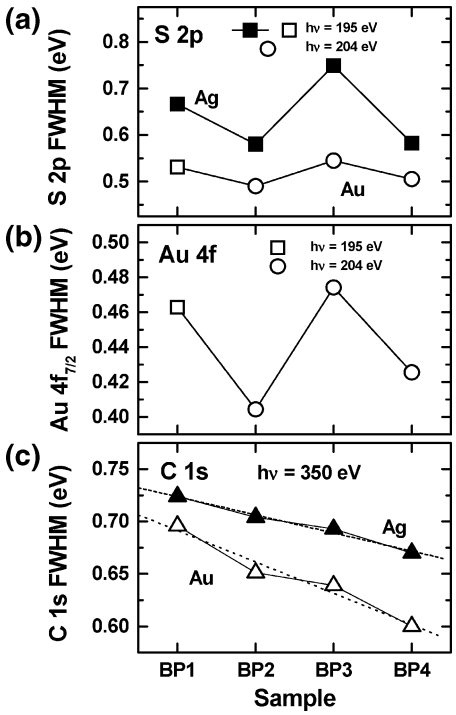

Figure 30. fwhm of the S $2p_{3/2,1/2}$ (a), Au $4f_{7/2,5/2}$ (b), and main C 1s (c) XPS peaks for $CH_3-(C_6H_4)_2-(CH_2)_n-S-Au$ and $CH_3-(C_6H_4)_2-(CH_2)_n-S-Ag$ monolayers. The dashed lines in a show the fwhm of S2p for $CH_3(CH_2)_{11}S-Au$ and $CH_3(CH_2)_{11}S-Ag$. The dashed lines in c are only a guide for the eyes. Reprinted with permission from ref 113. Copyright 2001 American Chemical Society.

phenyl rings and similar molecular geometry and self-assembled structure.

Strikingly, the fwhms of all core-level photoemission features (Figure 30) including $Au4f_{7/2}$, S2p, and C1s display synchronous odd−even effects.[113] The odd−even effects of $Au4f_{7/2}$ and S2p fwhms are driven by a difference in the extent of inhomogeneity of the surface adsorption sites dependent on whether the molecule has an odd or even number of CH_2 units. In addition, the consistent odd−even variations of fwhms of various atoms suggest that the inhomogeneity of molecular adsorption sites influences the whole molecule. Compared to BP_n (n = even), the larger fwhm for BP_n monolayer (n = odd) shows a higher extent of inhomogeneity of adsorption sites. The overall decreasing trend of C1s fwhm is possibly related to a better localization of the C1s core-hole placed further away from the surface with the increase of the alkyl chain length. The better localization decreases the influence of inhomogeneity of adsorption sites on the C1s photoionization probability, leading to a C1s peak with a smaller width.

Considering the existence of two larger-size phenyl ring groups, the odd−even difference in the inhomogeneity of adsorption geometry may associate with the different distance between two adjacent tethered sulfur atoms on the Au surface induced by the odd−even alternation of the orientation of the phenyl ring groups (see Figure 29c). Notably, compared to the S2p fwhm of the alkanethiolate monolayer, the small odd−even difference in fwhm of S2p for BP_n implies that the inhomogeneity of adsorption sites does not mean really different chemical binding sites. Considering the less densely packed BP_n monolayers (n = even) compared to alkanethiolate monolayers, the inhomogeneity may result from a slightly different shift of the binding positions of the sulfur atoms from the 3-fold sites of the Au(111) film or slightly different spacing of those sulfur atoms from the substrate. This new odd−even effect on *the extent of inhomogeneity* of the adsorption geometry was not observed for the $CH_3(CH_2)_nS-Au$ monolayers, possibly due to the absence of the terminal phenyl rings which contribute to this odd−even effect. It is expected that TP_n possibly exhibits a similar odd−even effect, though there is no high-resolution XPS reported on this series of organothiolate monolayers.

STM and LEED studies of the monolayer structure of BP_3 and BP_4 confirm the odd−even effect of molecular packing density and intermolecular distance driven by the odd−even difference in the orientation of the terminal biphenyl ring.[116] Figure 31a and b shows the structural models of the $(2\sqrt{3} \times \sqrt{3})$ overlayer of $CH_3-(C_6H_4)_2-(CH_2)_3-S-Au$ and $(5\sqrt{3} \times \sqrt{3})$ overlayer of $CH_3-(C_6H_4)_2-(CH_2)_4-S-Au$, respectively. The black box in Figure 31a shows the unit cell with a size of $a = 4.8 \pm 0.25$ Å and $b = 10.0 \pm 0.45$ Å. Each unit cell has two molecules with an area of 21.6 Å^2 per molecule. However, the unit cell of $CH_3-(C_6H_4)_2-(CH_2)_4-S-Au$ in Figure 31b is definitely different from that of $CH_3-(C_6H_4)_2-(CH_2)_3-S-Au$. If each molecule in Figure 31b occupies the same 21.6 Å^2 area as the $CH_3-(C_6H_4)_2-(CH_2)_3-S-Au$ in Figure 31a, each unit cell of Figure 31b should have 10 molecules. However, the high-resolution STM image of the $CH_3-(C_6H_4)_2-(CH_2)_4-S-Au$ monolayer (Figure 31c) shows only eight molecules in each unit cell, demonstrating a less dense molecular packing for $CH_3-(C_6H_4)_2-(CH_2)_4-S-Au$. The low packing density of $CH_3-(C_6H_4)_2-(CH_2)_4-S-Au$ shows that $CH_3-(C_6H_4)_2-(CH_2)_4-S-Au$ definitely adopts adsorption sites different from $CH_3-(C_6H_4)_2-(CH_2)_3-S-Au$. The odd−even difference in binding sites is reasonable since the energy difference between different sulfur adsorption sites for thiolate on Au(111) is fairly small[117−120] and less dense packing of $CH_3-(C_6H_4)_2-(CH_2)_4-S-Au$ offers the flexibility of slightly moving the sulfur atom away from the $\sqrt{3} \times \sqrt{3}$ site.

3.2.6. 4′-$CH_3(CH_2)_mOC_6H_4C_6H_4$-4-$CH_2SH$, 6-$CH_3(CH_2)_m$-$OC_{10}H_6$-2-$CH_2SH$, and 4′-$CH_3(CH_2)_mOC_6H_4C_6H_4$-4-SH

The above discussion involves the normal alkanethiols $CH_3(CH_2)_nSH$ and phenyl-ring-substituted alkanethiols at their terminal moieties. The documented difference in the odd−even effects of the two categories of molecules (normal alkanethiol and substituted alkanethiol) demonstrates that replacing the terminal group/moiety can alter the odd−even effects of $CH_3(CH_2)_nS-M$ (M = Au or Ag) and induce new odd−even effects. The terminal moiety containing one or more phenyl rings introduces larger $\pi-\pi$ steric repulsion at the upper part of the self-assembled monolayer for molecules with an odd number of CH_2 units than molecules with an even number of CH_2 units. For example, the different $\pi-\pi$ steric repulsion of the terminal phenyl rings possibly slightly modifies the adsorption sites of the tethered atoms to a different extent, leading to a new odd−even difference in the inhomogeneity of the adsorption sites for sulfur atoms on the Au surface.

In this section three series of molecules with different head moieties but the same upper part as alkanethiol, 4′-alkoxybiphenyl-4-methanethiol, 4′-$CH_3(CH_2)_mOC_6H_4C_6H_4$-4-$CH_2SH$ (series I), (6-alkoxynaphth-2-yl)methanethiol, 6-$CH_3(CH_2)_mOC_{10}H_6$-2-CH_2SH (series II), and 4′-alkoxybiphenyl-4-thiol, 4′-$CH_3(CH_2)_mOC_6H_4C_6H_4$-4-SH (series III) (Figure 32) were chosen for discussing how the different head moiety

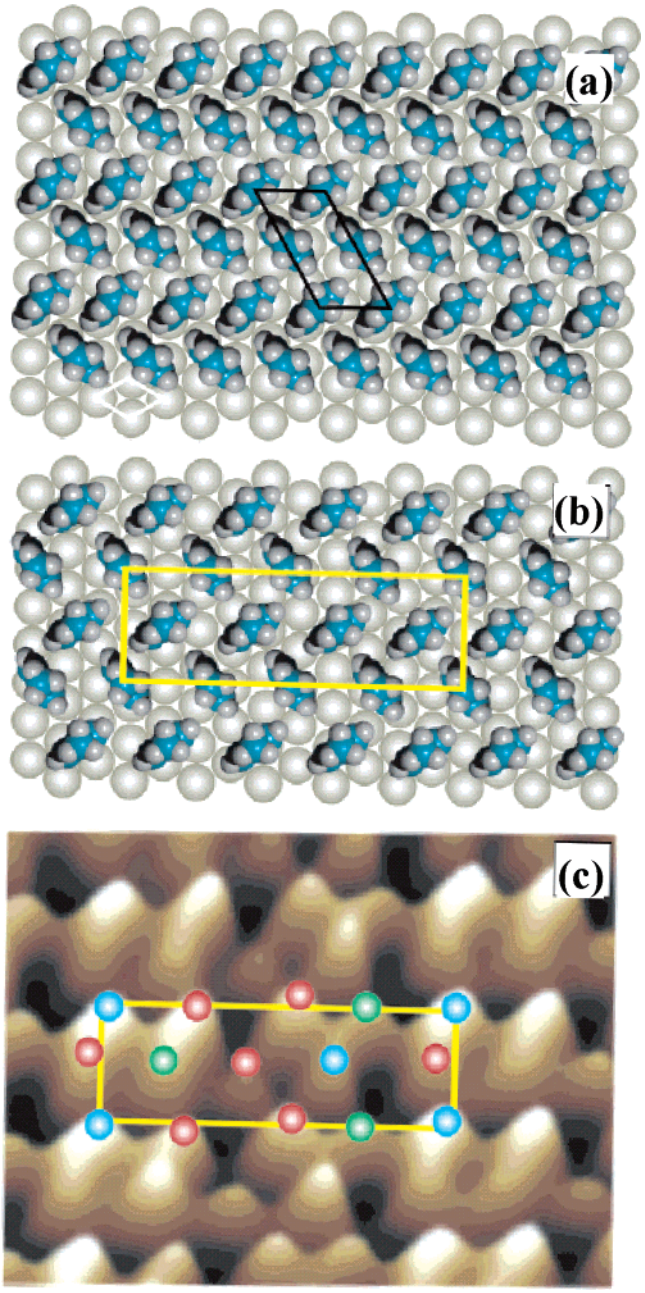

Figure 31. (a) Top view of a structural model for the ($2\sqrt{3} \times \sqrt{3}$) overlayer of a BP_3 monolayer on Au(111). (b) Top view of a structural model for the ($5\sqrt{3} \times \sqrt{3}$)rect overlayer of a BP_4 monolayer on Au(111). (c) 3D STM image where three different heights observed in the unit cell of BP_4 are marked with different colors. Reprinted with permission from ref 116. Copyright 2003 American Chemical Society.

modifies the odd−even effect for organosulfur on the Au surface or even whether these head groups could induce new odd−even effects for the self-assembled monolayer on Au.[100] In addition, the long spacer of the all-trans alkyl chain above the phenyl rings was used to probe the ordering of the chain packing and possible odd−even effects. Thus, they are good templates for examining the interplay of various interactions involved in the process of self-assembly and its association with various odd−even effects.

For the monolayers of the series I, II, and III their static advancing contact angle θ_a(hexadecane) presents a strong dependence on the odd or even number of CH_2 units in their alkyl chains, $(CH_2)_n$.[100] The contact angles of monolayers of series I, II, and III with an odd number of CH_2 units ($m = 15$) are 8−10° greater than those with an even number of CH_2 groups ($m = 16$). This odd−even effect on wettability is similar to that of normal alkanethiolates due to the same terminal long alkyl chain. Notably, this odd−even difference in contact angle for series I, II, and III is much larger than that seen for normal alkanethiolate monolayer (series IV), though all four series have the same hexagonal lattice ($\sqrt{3} \times \sqrt{3}$)R30°. This is related to the biphenyl and naphthalene of the head moieties. An eclipsing effect of the O−C_{alkyl} bond on the aromatic-group plane[121−123] induces a rotation barrier to the alkyl chain which results in a lower twist angle, β, under the same tilt angle of the alkyl chain, α. This is in contrast to the *n*-alkanethiolate on Au(111) because the eclipsing effect is definitely absent in the case of the alkanethiolate monolayers. In addition, IR studies revealed a larger odd−even difference in the orientation of the terminal CH_3 for series III compared to normal alkanethiolate monolayers.

As seen previously, the stretching mode of the terminal CH_3 is an indication of odd−even structural alternation. For molecules of series I on Au, the intensity of $\nu_{sym}(CH_3)$ is larger for molecules with m = odd than that of molecules with m = even, whereas the reverse is true for the ν_{asym}-(CH_3) mode. Series II and III exhibit the same odd−even variation as series I. Because the extent of this odd−even effect is related to the absolute direction of the terminal CH_3 and the extent of chain tilt and twist, these similar odd−even effects indicate a very similar geometry of the alkyl chain in terms of chain tilt and twist among series I, II, and III, even though their head groups are different.

Since the molecules of series I and II have a similar tilt angle of the alkyl chains upon self-assembly and the same orientation of the S−C bond relative to the long axis of the alkyl chain (two red arrows for each molecule in Figure 32), their head sulfur atoms must bond on Au(111) through the same sp^3 hybridization and form the same C−S−Au bond angle. As shown in Figure 33, both molecules I and II bond to Au(111) films with sp^3 hybridization and assemble with a herringbone packing.[100] Although the alkyl chain of series III has a tilt angle similar to that of series I and II upon self-assembly, its sulfur atom has to adopt different hybridization because the orientation of the S−C bond relative to the long axis of the alkyl chain is different from that of series I and II as shown in Figure 32. Due to the absence of one carbon atom between the sulfur atom and the biphenyl rings in series III, to have a similar orientation of the alkyl chain in the self-assembled monolayer requires a Au−S−C bond angle of ~180°, suggesting sp hybridization for the sulfur atom of series III on the same ($\sqrt{3} \times \sqrt{3}$)R30° lattice (Figure 33e). This demonstrates that slightly different head moieties may significantly alter the chemical binding of the sulfur atom on the substrate. A significant change for the binding chemistry of the sulfur atom driven by slightly modifying the terminal group was not observed in the series $C_6H_5(CH_2)_n$-SH, $C_6H_5-(C_6H_4)_2-(CH_2)_n-SH$, and $CH_3-(C_6H_4)_2-(CH_2)_n-$SH, which have the same head group but different terminal groups. Thus, it is understandable that the terminal group and head group play different roles in determining the chemical binding, structure of self-assembled monolayer, and observed odd−even effects for organosulfur monolayers on Au.

In addition, a trend of decreasing odd−even difference in the orientation of the terminal CH_3 and wettability with

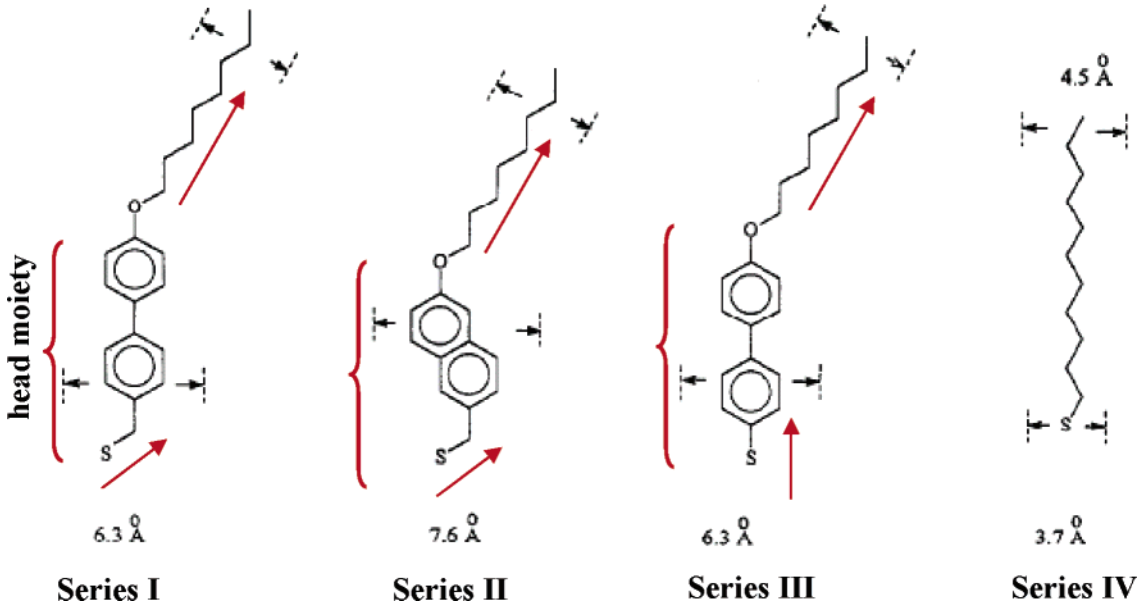

Figure 32. Molecule structures of 4′-$CH_3(CH_2)_mOC_6H_4C_6H_4$−4-$CH_2SH$ (series I), 6-$CH_3(CH_2)_mOC_{10}H_6$−2-CH_2SH (series II), 4′-CH_3-$(CH_2)_mOC_6H_4C_6H_4$−4-SH (series III), and $CH_3(CH_2)_nSH$ (series IV).

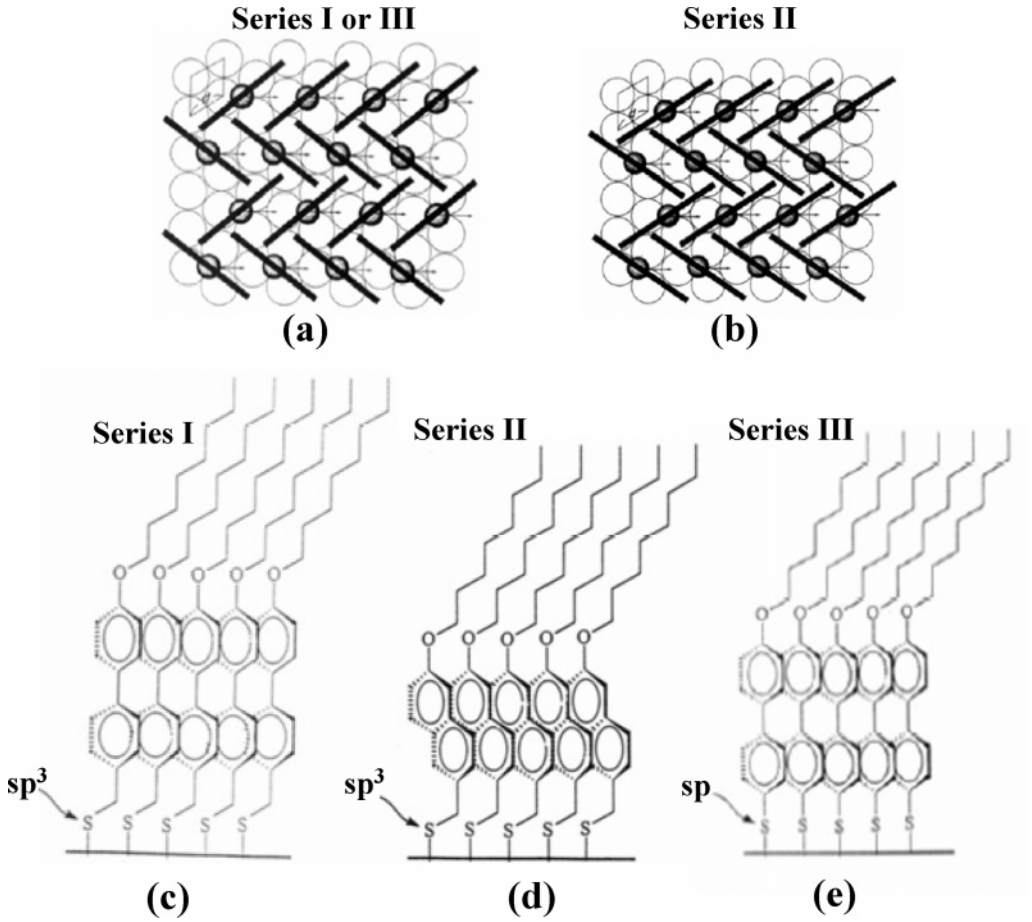

Figure 33. (a) Top view of proposed structures of monolayers of series I (and III) on the ($\sqrt{3} \times \sqrt{3}$)R30° overlayer of Au(111) and Ag(111) films. (b) Top view of proposed structures of monolayers of series II on the ($\sqrt{3} \times \sqrt{3}$)R30° overlayer of Au(111) and Ag(111) films. Each superimposed small circle shows one bonded organothiolate molecule. Each black line crossing one small circle indicates the tilting direction of the alkyl chains. (c, d, and e) Side views of monolayers of series I, II, and III on Au(111) and Ag(111) films. They have the same orientation and packing of terminal alkyl chains and biphenyl rings/naphthenes. Reprinted with permission from ref 100. Copyright 1994 American Chemical Society.

increasing length of the alkyl chain is observed for *n*-alkanethiol monolayers on Au.[100] This trend is suggested to be associated with the rotation of the alkyl chains of the molecules. Because the rotation of the alkyl chain is progressive, the end of a longer chain may rotate more than that of a short chain. Rotation of the alkyl chain can obscure the odd−even difference in the orientation of the terminal methyl. Because the odd−even effects in vibrational features

and wetting properties are directly associated with the odd−even difference in the orientation of the terminal methyl and the exposure of the topmost CH_2, respectively, these odd−even effects decrease with increasing length of the molecular chain. However, this trend does not hold for molecules with a terminal molecular moiety containing a larger group such as $C_6H_5(CH_2)_nSH$, $C_6H_5-(C_6H_4)_2-(CH_2)_n-SH$, and $CH_3-(C_6H_4)_2-(CH_2)_n-SH$. The reason is that the large terminal group can block rotation of the alkyl chain.

3.2.7. $CF_3(CH_2)_nSH$

The above sections show that the substitution of a functional group at different regions of a normal alkanethiol molecule results in a different impact on various odd−even effects observed for organosulfur molecules on the Au substrate. This might be called an effect of substitution at the level of a functional group. Another substitution is at the level of an atom in a molecule. For example, replacement of hydrogen atoms at the terminal methyl with fluorine atoms for normal alkanethiols forms fluoroalkyl-terminated alkanethiolates.

Self-assembled monolayers of $CF_3(CH_2)_nS-Au$ were systematically examined.[103,124] The tilt angle of the terminal CF_3 group displays the same odd−even effect as for methyl-terminated alkanethiolates. Both of the series exhibit the same odd−even effect on advancing contact angle if the contacting liquid is water or glycerol. This odd−even effect on wettability is associated with the different exposure of the topmost CH_2 group depending on whether the carbon number of the alkyl chain is odd or even.[30]

The odd−even effect on wettability measured using a strong dipolar liquid such as acetonitrile (molecular dipole moment 3.47 D[125]) or dimethyl formamide (3.6−3.7 D[126]) is more pronounced than that seen for a weak dipolar liquid such as H_2O (2.4−2.6 D[127]). Definitely, substitution of CH_3 with CF_3 introduces a strong dipole at the monolayer termination. The self-assembled monolayer terminated with CF_3 has an ordered array of the oriented dipoles. The interaction between this ordered array of dipoles in the self-assembled monolayer and the dipole of the strongly polar contacting liquid can enhance the wettability (decreasing the advancing contact angle).

However, the fluorine-substituted and nonsubstituted alkanethiolate monolayers exhibit reverse odd−even effects for advancing contact angles in terms of wettability when the contacting liquid acetonitrile, dimethyl formamide, or nitrobenzene is used. Those reverse odd−even effects are ascribed to two different mechanisms. Substitution of trifluoroalkyl groups for the terminal methyl groups in an alkanethiolate monolayer creates an oriented force field which is distinctly different for $CF_3(CH_2)_nS-Au$ (n = odd) and $CF_3(CH_2)_nS-Au$ (n = even), leading to an alternating difference of interaction with contacting liquid molecules.[128] Figure 34 shows two schemes of the self-assembled monolayers of $CF_3(CH_2)_{11}S-Au$ and $CF_3(CH_2)_{10}S-Au$, respectively. For CF_3-terminated alkanethiolate with an even number of CH_2 groups such as $CF_3(CH_2)_{10}S-Au$, the terminal dipoles (marked with a double arrow in Figure 34a) are far away from the surface normal. They can partially compensate each other. However, for CF_3-terminated alkanethiolates with an odd number of CH_2 units such as $CF_3(CH_2)_{11}S-Au$, the terminal dipoles are oriented almost normal to the substrate and parallel to each other. Thus, the monolayers with an odd number of CH_2 groups have a larger

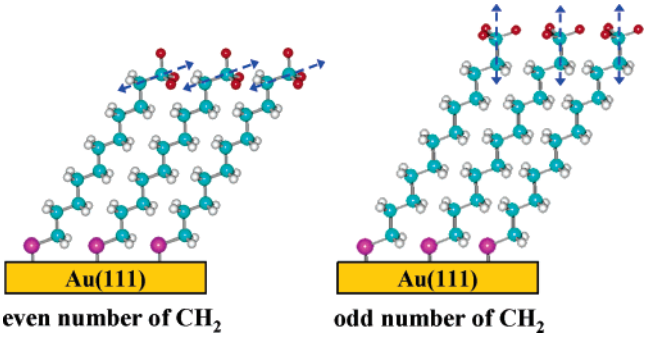

Figure 34. Scheme for the odd−even alternation of the orientation of terminal CF_3, the orientation of the CF_3-CH_2- moiety, and the surface dipole of CF_3-CH_2- in CF_3-terminated alkanethiolate monolayers on Au surfaces.

interaction with the strongly polar contacting liquid than monolayers with an even number of CH_2 units. Definitely, the orientation of the CF_3 dipole plays a dominant role in the wettability of this system.

Notably, for methyl-terminated alkanethiolate monolayers, the interaction with strongly dipolar contacting liquid is not a main driving force for formation of an odd−even alternation in contact angle because the surface dipole is weak. As discussed before, the larger exposure of CH_2 in $CH_3(CH_2)_nS-Au$ (n = even) contributes to a lower contact angle than $CH_3(CH_2)_nS-Au$ (n = odd). Thus, this comparison indicates that introduction of a polar terminal moiety may tune the surface properties and modify the odd−even effect in the self-assembled monolayer.

3.2.8. Diamidothiols

Diamidothiol, $HS(CH_2)_2NHCO(CH_2)_nCOOHCONHCH_3$, contains amino acid groups at the head and terminal end separated by an alkyl spacer. One end of the molecule is terminated with a thiol group. Figure 35a presents four diamidothiol molecules with differing length alkyl group spacers. Similar to alkanethiols and substituted alkanethiols, diamidothiol molecules self-assemble onto the Au substrate via forming a Au−S−C bond.[129] Different from other organothiols, however, the amino acid groups can form intermolecular hydrogen bonds which modify the odd−even effect of the self-assembled monolayers.

Figure 35b,c schematically shows the self-assembled monolayer of diamidothiol with an even or odd number of CH_2 groups in the alkyl chain between the two amino acid groups. The tilt angle of the alkyl chain from the surface normal in the diamidothiolate monolayers was suggested to be ~18°,[129] though it is ~30° for alkyl chains of alkanethiolates tightly packed on Au(111).[130,131] For monolayers of diamidothiolates with n = even, two hydrogen bonds C═O···H−N form between two adjacent molecules (Figure 35b). However, only one hydrogen bond is formed between two molecules with n = odd because the two C═O of one molecule are on the same side of the molecular carbon skeleton (Figure 35c). In addition, to maintain the linearity of C═O···H−N hydrogen bonds in these self-assembled monolayers, the tilt angle of the alkyl chain could be ~18° or even slightly lower than ~18°. The absence of a hydrogen bond between two adjacent terminal groups of diamidothiolate monolayers with n = odd results in a much less crystalline and ordered layer than for the monolayers with n = even. Furthermore, the structural odd−even difference in formation of intermolecular hydrogen bonds and the extent

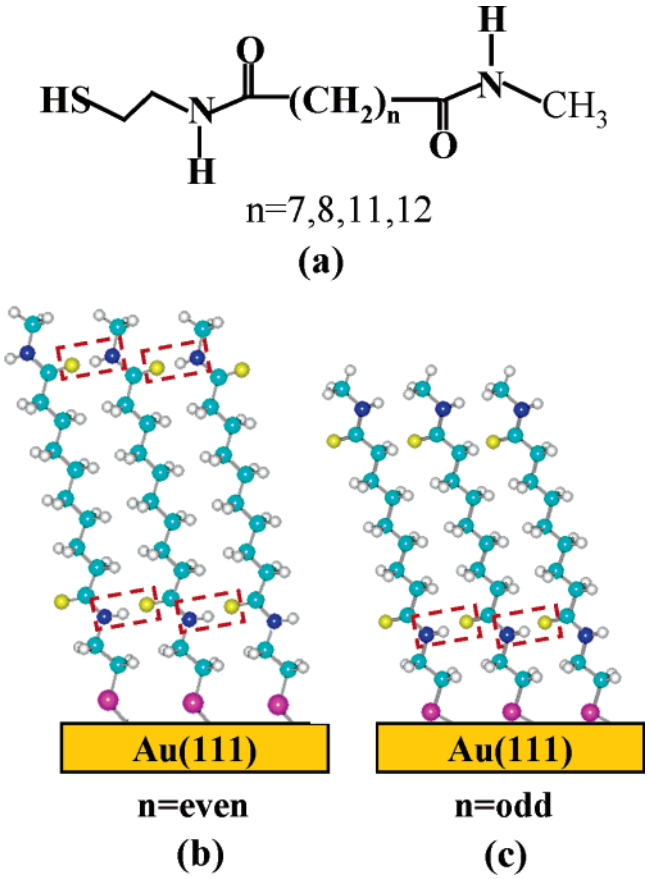

Figure 35. (a) Molecular structures of diamidothiols. *n* is the number of CH_2 groups between the two C═O in the molecule. (b) Molecules with an even number of CH_2 units between two C═O groups can form two intermolecular hydrogen bonds between molecular chains at the head moiety and terminal moiety. (c) Molecules with an odd number of CH_2 groups between two C═O groups only form one intermolecular hydrogen bond at the head moiety.

of crystalline ordering of these self-assembled monolayers induces an odd−even difference in the conductivity of these monolayers which will be discussed in section 3.5.6.

3.2.9. Influence of the Deposited Metal Monolayer on the Odd–Even Effect of Organic Molecules on Au

Previous studies have shown that the chemisorption of sulfur atoms of organosulfurs on Ag and Cu single-crystal surfaces is stronger and more stable than on Au single-crystal surfaces in vacuum.[132−137] However, due to the chemical inertness of the Au film under ambient conditions, the excellent reproducibility in preparing high-quality organothiolate monolayers on the Au substrate and the easy partial oxidation of Ag and Cu surfaces, Au is a better substrate for self-assembly of organic molecules under ambient conditions. Recently, the technique of underpotential deposition (UPD)[138−142] was used to controllably deposit a submonolayer or a full monolayer of foreign metals such as Ag or Cu in the Au substrate.[143−147] More importantly, these studies show that no oxide is formed on the deposited atomic layer and the bonded external atomic layer on Au is more stable than its bulk form. Thus, the UPD metallic layer such as Ag, Cu, Bi, and Hg on Au could be used to modify the binding geometry, molecular packing, and surface properties of the self-assembled monolayers on Au.[148] Some odd−even effects different from those seen for organothiols directly self-assembled on bare Au were also revealed.

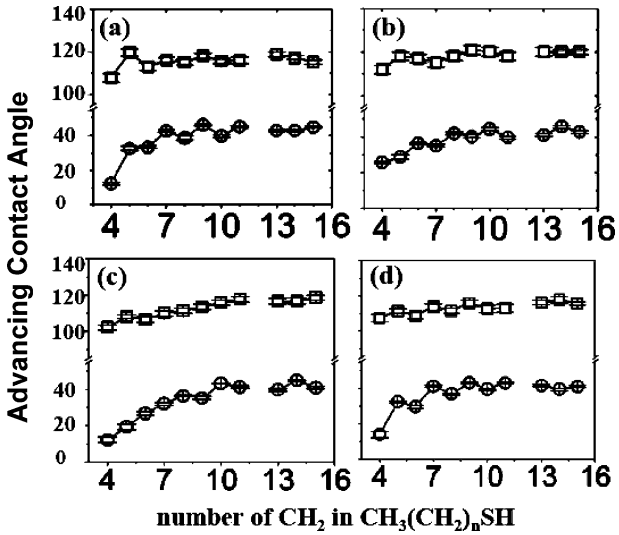

Figure 36. Advancing contact angles for self-assembled monolayers of *n*-alkanethiolates on (a) Au(111) films, (b) Ag/Au (upd, 454 mV), (c) Cu/Au (upd, 108 mV), and (d) Bi/Au (upd, 220 mV). The probe liquids are water (square) and hexane (circle). Reprinted with permission from ref 148. Copyright 2004 American Chemical Society.

Figure 36a presents the odd−even effect of the contact angles of $CH_3(CH_2)_nS$−Au (n = 4−11, 13−15) self-assembled monolayers on bare Au(111) films. However, the odd−even effect of these molecules on UPD Ag layer deposited on Au(111) films (Figure 36b) is opposite to that on the pure Au(111) films but the same as that on pure Ag(111) films.[148] This odd−even effect is associated with the sp hybridization of the sulfur atom bonded on the Ag(111) film to be discussed in section 3.3. For alkanethiolates on the UPD Cu layer on Au(111) films (Figure 36c), the same odd−even effect and sulfur hybridization as for alkanethiolate monolayers on Ag deposited on Au(111) (Ag/Au) were revealed. However, self-assembled monolayers of alkanethiolates on Bi/Au (Figure 36d) exhibit the same odd−even effect as those on pure Au(111) films.

Notably, although there is no obvious odd−even effect found for the self-assembled monolayer of alkanethiolate on Hg/Au from the contact angle measurements, the IRAS clearly shows odd−even effects for UPD Hg on Au.[148] As shown in Figure 37b at low coverage of Hg on Au, the absorbance intensities of $\nu_{asym}(CH_3)$ and $\nu_{sym}(CH_3)$ exhibit the same odd−even effect as those on bare Au(111) films (Figure 37a). The bonded sulfur atoms for a low coverage of Hg have sp^3 hybridization. An in-situ XRD study revealed an open structure of a $(\sqrt{3} \times \sqrt{19})$ adlattice formed from bisulfate-stabilized Hg_2^{2+} dimers.[142] However, on a full monolayer coverage of UPD Hg on Au (Figure 37c) the monolayer displays an odd−even effect opposite to that at low coverage and the bonded sulfur has sp hybridization. This coverage dependence of the odd−even effect for alkanethiolates on UPD Hg deposited on Au(111) films demonstrates that the structure of the self-assembled monolayer and binding of the head group could be modified by controlling the coverage of the deposited foreign atomic layer. In addition, these observed odd−even effects of contact angles for alkanethiolates on Ag/Au, Cu/Au, and Bi/Au were confirmed by the IRAS data in Figure 37d, e, and f, respectively. The hybridization of bonded sulfur atoms on deposited Ag, Cu, and Bi is sp, sp, and sp^3, respectively. The structural odd−even effects of the monolayers on

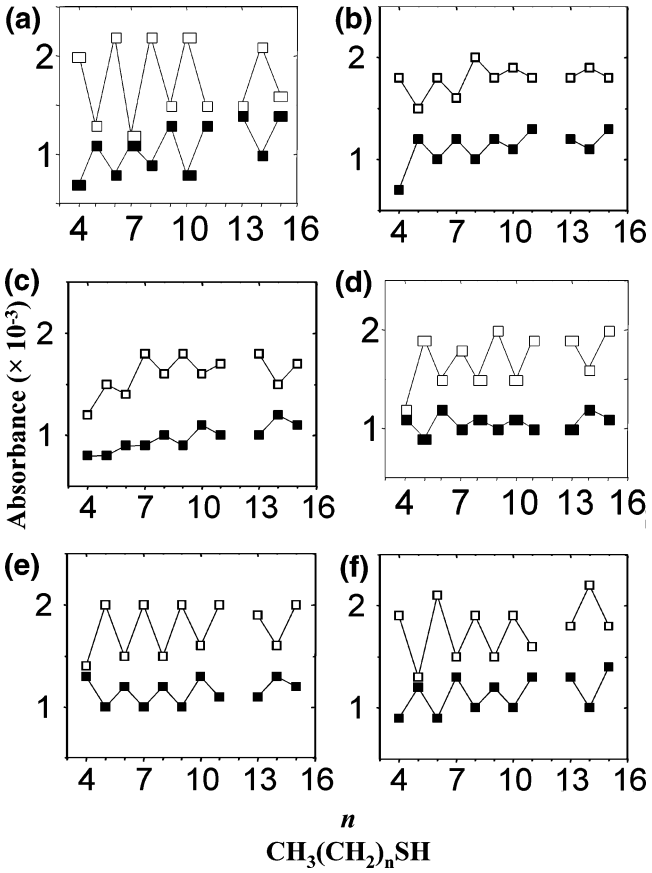

Figure 37. Absorbance of $\nu_{asym}(CH_3, ip)$ and $\nu_{sym}(CH_3)$ versus the number of CH_2 units for self-assembled monolayers of *n*-alkanethiolates on (a) bulk gold, (b) Hg/Au (upd, 887 mV), (c) Hg/Au (upd, 527 mV), (d) Ag/Au (upd, 868 mV), (e) Cu/Au (upd, 8 mV), and (f) Bi/Au (upd, 220 mV). The open and solid circles denote intensities of $\nu_{aym}(CH_3, ip)$ and $\nu_{sym}(CH_3)$, respectively. Reprinted with permission from ref 148. Copyright 2004 American Chemical Society.

Ag/Au, Cu/Au, and Bi/Au do not exhibit coverage dependence. These investigations clearly show that the odd−even effect of organothiolates on Au can be altered by depositing a submonolayer or saturated monolayer of foreign metal atoms on the Au surface before self-assembling the organothiol monolayer. In addition, the stability of the self-assembled monolayer on the substrate could be improved by underpotential deposition of metal atomic layers between the self-assembled organic monolayer and the original substrate. Notably, there are still some open issues about the self-assembly of organic molecules on a metal atomic layer deposited on a solid substrate such as Au(111), including the role of the original substrate such as the Au(111) film in molecular self-assembly, the chemical binding of different deposited metal atomic layers, and the driving force of the coverage-dependent odd−even effects and the corresponding switch of sulfur hybridization.

3.3. Odd–Even Effect on Structure of Organic Monolayers on Ag(111)

3.3.1. $CH_3(CH_2)_nSH$

Compared to the alkanethiolate monolayers on Au(111) films, the largest difference in molecular packing on Ag(111) is the tilt angle of the alkyl chains from the surface normal. On the evaporated Ag thin film surface it is only ∼13°,[149] whereas it is ∼30° on Au(111).[94,95] This difference results from the different chemical binding of the sulfur atoms in these monolayers: sp^3 on Au and sp on Ag.

A structural odd−even effect is seen in the wetting properties and intensity of the $\nu_{asym}(CH_3)$ and $\nu_{sym}(CH_3)$ modes for *n*-alkanethiol with short chain $CH_3(CH_2)_nSH$ ($n = 3-9$) on Ag(111).[149] However, this odd−even effect is quite weak for alkanethiolates with longer chains ($n = 10-15, 17$), which is possibly associated with the diminution of the odd−even difference for alkanethiolates with long alkyl chains reported in the self-assembled monolayers of alkanethiolates on Ag(111).[149] It is understandable that the rotation of the alkyl chain can weaken the difference in the orientation of the terminal methyl between chains with an odd or even number of carbon atoms. Since the rotation can be progressive, the CH_3 of the longer chain may rotate more than that of a shorter one. In fact, the $CH_3(CH_2)_nS-Au$ monolayers also exhibit a trend of a weakening of the odd−even difference in the orientation of the terminal CH_3 group with an increase of chain length.[100]

The existence of an odd−even effect for $CH_3(CH_2)_nS-Ag$ with a short alkyl chain is controversial. The odd−even variation of the contact angles of $CH_3(CH_2)_nS-Ag$ measurements[100,149] and IR spectra[29,149] was not obvious in another study.[29] Whether an odd−even effect can be observed or not is possibly associated with the adventitious oxidation of the evaporated Ag films prior to adsorption of the *n*-alkanethiol. It was noted that there is some difficulty in preparing high-quality monolayers of alkanethiolates with a short chain.[29,149]

Notably, compared to the odd−even effect on Au(111), the odd−even effect of *n*-alkanethiolate monolayers on Ag(111) is offset by one CH_2 group. For example, the monolayer of $CH_3(CH_2)_nS-M$ (M = Au or Ag) with $n =$ even for Au and $n =$ odd for Ag exhibits a higher $\nu_{asym}(CH_3)$ absorbance than monolayers with $n =$ odd for Au and those with $n =$ even for Ag, respectively.[100,149] More straightforwardly, the CH_3-CH_2- moiety of both $CH_3(CH_2)_nS-Au$ ($n =$ odd) and $CH_3(CH_2)_nS-Ag$ ($n =$ even) monolayers has smaller a tilt angle than that of the chains with an even number of CH_2 units for Au and chains with an odd number of CH_2 groups for Ag (Figure 38). The driving force for this specific offset of the two odd−even effects on Au(111) and Ag(111) films is the chemical bonding of the sulfur atom to the metal substrate. As has been well studied, the geometry of the alkyl chain of the alkanethiolate on Au(111) is rationalized with a bond angle Au−S−C of ∼110°[95] in terms of sp^3 hybridization for the bonded sulfur atoms. Figure 38a,b schematically presents the bonding of alkanethiolate on Au(111) via a Au−S−C angle of ∼110°.[95] The offset of the odd−even effect by one CH_2 unit for alkanethiolate on the Ag substrate suggests that the Ag−S−C bond is a nearly linear configuration because of sp hybridization upon bonding (Figure 38c,d).[100,149]

The driving force for the difference in bonding of sulfur atoms with Au(111) and Ag(111) films is not quite understood. The different electron-accepting ability of the two metals is believed to play an important role. A number of physical parameters of the metal substrate such as work function,[150] ionization potential,[150] electronegativity,[151] and electronic band structure[152] suggest that the Ag(111) surface has a higher trend toward oxidation than the Au(111) surface. Ag is a stronger Lewis acid than Au. The bonding of thiols on Ag is more ionic in nature; thereby, the attachment to

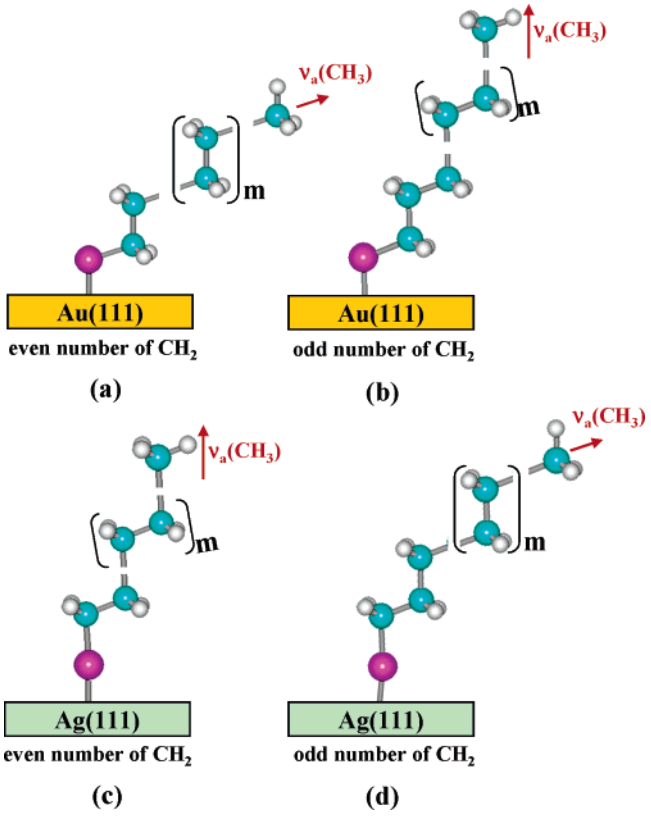

Figure 38. Scheme of binding geometry of the sulfur atom, orientation of the terminal CH_3 group of $CH_3(CH_2)_nS-Ag$, and $CH_3(CH_2)_nS-Au$ monolayers with an even or odd number of CH_2 units.

Ag will be more dependent on bonding through the lone pair of the sulfur atom.

3.3.2. $C_6H_5-(C_6H_4)_2-(CH_2)_n-SH$

Compared to the simple organosulfur molecule $CH_3(CH_2)_n$-SH, substituting the terminal methyl with terphenyl leads to new odd−even effects for the monolayers of TP_n ($n = 1-6$) on Ag as well. Two pronounced odd−even effects with respect to the number n of CH_2 units of the alkyl spacer were noted.[106] A clear odd−even difference of 10−15% of the packing density of the terphenyl films was determined using HRXPS.[106] The change of packing density is closely associated with the odd−even alternation of the terphenyl orientation. IRAS and NEXAFS data further show that the tilt angle of the terminal terphenyl exhibits a pronounced odd−even difference by 7−14°.[106] In fact, as mentioned before, a similar odd−even effect was observed for this series of molecules on the Au(111) film,[106] which however is reverse to the effect seen on the Ag(111) film. A larger inclination of the terphenyl moieties and a lower packing density was seen for TP_n with an even number of CH_2 units on Au(111) and for TP_n with an odd number of CH_2 units on Ag(111).

Similar to normal alkanethiolate on Au(111) and Ag(111) films,[100] the offset of one CH_2 unit for TP_n on the two substrates originates from the different bonding of the sulfur atoms on them in terms of the hybridization of the sulfur atoms and the C−S−M (M = Au or Ag) bond angle. Figure 27a,b schematically presents the difference in binding configuration of 4,4′-terphenyl-substituted alkanethiolate monolayers on Au(111) and Ag(111) films.

Compared to TP_n monolayers self-assembled on Au(111) and Ag(111), no odd−even variation of packing density as a function of the number of CH_2 units was observed for normal alkanethiolate self-assembled monolayers on the two substrates. Again, this difference demonstrates an approach for tuning packing structure and surface properties of the self-assembled thin film on a metal surface by tailoring the terminal group.

3.3.3. $CH_3-(C_6H_4)_2-(CH_2)_n-SH$

HRXPS, IRAS, and NEXAFS were used to study the adsorption structure of the self-assembled monolayers of BP_n ($n = 1-4$) on Ag(111).[113,115] The combination of these techniques offers a precise characterization of both the monolayer/metal interface and the interior of the monolayer. Odd−even effects similar to that of TP_n monolayer on Ag(111) film were revealed for BP_n. The odd−even alternations of BE and intensity of the C1s main peak and its shoulder and the S2p intensity in XPS suggest that the odd−even effects of packing density in terms of molecular coverage and effective monolayer thickness on Ag(111) film are opposite to those on Au(111). Clearly, the opposite odd−even effects are driven by the M−S−C (M = Au and Ag) bonds at the surface. The fwhms of C1s and S2p photoemission peaks also exhibit odd−even effects on Ag(111), suggesting a slight difference in the extent of heterogeneity of the adsorption geometries. Interestingly, these odd−even effects of the fwhm of S2p and C1s are consistent with but not opposite to those on Au(111). The synchronicity of all these fwhm (C1s, S2p, Au3d/Ag3d) alternations as a function of alkyl length in either BP_n/Au or BP_n/Ag suggests that the inhomogeneity of adsorption sites influences the whole molecule.[115,153]

Notably, no odd−even effects on the fwhms of S2p and C1s were observed in the alkanethiolate monolayers on Au(111) and Ag(111) films. This indicates that the odd−even difference in the orientation of the terminal phenyl rings is possibly the driving force for the odd−even change of the C1s and S2p fwhms and the existence of the inhomogeneity of adsorption geometries.

The above discussion for the molecular packing and geometry of the alkyl chain of the normal alkanethiolate and phenyl-ring-terminated alkanethiolates on Ag(111) films shows that modification of a terminal group can tune the molecular packing density, effective film thickness, orientations of the terminal group, and geometry of the alkyl chain and even slightly vary the adsorption site of the binding group.

3.3.4. 4′-$CH_3(CH_2)_mOC_6H_4C_6H_4$-4-$CH_2SH$, 6-$CH_3(CH_2)_m$-$OC_{10}H_6$-2-$CH_2SH$, and 4′-$CH_3(CH_2)_mOC_6H_4C_6H_4$-4-SH

Three categories of molecules, series I, II, and III (Figure 32), were investigated for probing the impact of the head moiety on odd−even effects in molecular packing and monolayer structures.[100] For the same reason as discussed in section 3.2.6, the odd−even difference of contact angles of the monolayers of series I, II, and III on Ag(111) films, respectively, is definitely larger than that seen for $CH_3(CH_2)_nS-Ag$ monolayers.[100]

A nearly identical odd−even effect for the orientation of the terminal CH_3 group was observed for series I, II, and III on Ag(111) films, indicating a similar geometry of the alkyl chains for these molecules, though they have different head moieties as shown in Figure 32. Molecules of series I and II bond on the Ag(111) film through sp^3 hybridization of sulfur atoms. However, molecules of series III chemically bind to

Ag(111) via sp hybridization of the sulfur atom. The different hybridization of molecules of series I and III is driven by the extra CH_2 group between the biphenyl group and the sulfur atoms in the molecules of series I.

Notably, for any of the three series the same odd−even effect in packing density, chain tilting, and binding configuration is exhibited in terms of the same hybridization of the sulfur atom on both Au(111) and Ag(111) (series I and II, sp^3 for both Au and Ag; series III, sp for both Au and Ag); all three series of molecules have head moieties much larger than CH_2 units. However, the odd−even effects on Au(111) and Ag(111) films are opposite for the self-assembled monolayers of phenyl-ring-substituted alkanethiols such as $C_6H_5(CH_2)_nSH$ (series a), $C_6H_5-(C_6H_4)_2-(CH_2)_n-SH$ (series b), $CH_3-(C_6H_4)_2-(CH_2)_n-SH$ (series c), and $CH_3(CH_2)_nSH$ (series d) because each series of these molecules has different chemical binding (sp^3 on Au and sp on Ag). Furthermore, each of the four series (a, b, c, and d) having different binding (sp^3 for Au and sp for Ag) is related to their small head moiety CH_2 units compared to large biphenyl or naphthalene in series I, II, and III. For example, the least sterically demanding alkanethiolates allow a greater density of packing on Ag(111) but not on Au(111).

3.3.5. $CH_3(CH_2)_nCOOH$

All of the above-discussed molecules chemically bind to Au(111) and Ag(111) films via the sulfur atom. *n*-Alkanoic acids can also form stable self-assembled monolayers on Ag(111) via chemical binding of the carboxylic acid group. The carboxylic acid dissociatively chemisorbs on the Ag(111) film in an ordered array.[30] The two oxygen atoms of one carboxylate bond are nearly symmetric on the surface. More importantly, the orientation of the terminal CH_3 group and the wettability of monolayers exhibit odd−even effects similar to those of alkanethiolate monolayers on Ag(111) films.

Monolayers of acid molecules with alkyl chains having an odd number of CH_2 units (corresponding to an odd number of carbon atoms) have a lower contact angle than those having an even number of carbon atoms when the contact angle is measured with hexadecane and bicyclohexyl. In addition, the intensities of the vibrational mode of the terminal CH_3 show an obvious odd−even alternation as schematically shown in Figure 39. The intensity of $\nu_{asym}(CH_3)$ (~2965 cm^{-1}) is higher for a chain with an odd number of carbon atoms.[30] Correspondingly, the intensity of $\nu_{sym}(CH_3)$ is higher for the chain with an even number of carbon atoms. These results consistently confirm the difference in the orientation of the terminal methyl group based on the same tilt angle of the alkyl chain for $CH_3(CH_2)_nCOOH$ bonded on the Ag(111) surface. For the chain with an even number of carbon atoms, the CH_3-CH_2- moiety is closer to the surface normal. However, for the chain with an odd number of carbon atoms, its CH_3-CH_2- points away from the surface normal. Since the number of total carbon atoms counts the two carbon atoms of the terminal methyl and bound carboxylic acid group, this odd−even effect is consistent with that of $CH_3(CH_2)_nSH$ on Ag(111) film (Figure 38c,d) but opposite to that of $CH_3CH_2)_nSH$ on Au(111) (Figure 38a,b). Thus, the carboxylate binding group is perpendicular to the substrate as shown in Figure 39, which schematically presents the geometry of the molecular chains with an even and odd number of CH_2 units on Ag(111), respectively.

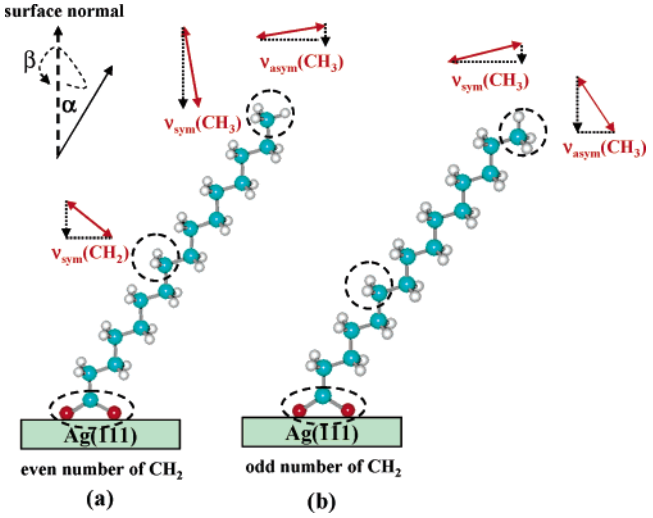

Figure 39. Proposed structure of *n*-alkanoic acid monolayers with an even and odd number of CH_2 units on the Ag(111) surface. Represented with permission from ref 30. Copyright 1993 American Chemical Society.

Notably, the odd−even difference of the methyl vibrational modes of the carboxylic acid on Ag(111) is much more pronounced than that for alkanethiol on Au(111) and Ag(111) films. For $CH_3(CH_2)_nS-Ag$, the intensity of the $\nu_{asym}(CH_3)$ or $\nu_{sym}(CH_3)$ of the molecule with an odd number of CH_2 units is 1.3 or 0.7 of that of the molecule with an even number of CH_2 groups, respectively. For *n*-alkanoic acid on Ag(111), however, the ratio is 2.2 or 0.5 for $\nu_{asym}(CH_3)$ or $\nu_{sym}(CH_3)$, respectively. It is proposed that a considerable population of gauche conformations exists in the $CH_3(CH_2)_nS-Ag$ monolayer, but chains of acid monolayers on Ag(111) films are more ordered with fewer gauche defects along the molecular chains. On the other hand, the difference in odd−even effects between $CH_3(CH_2)_nCO_2-Ag$ and $CH_3(CH_2)_nS-Ag$ monolayers is also associated with the different binding configurations of the carboxylic acid and thiol groups. As shown in Figure 39, the bonded carboxylate group limits the conformation of the CH_2 next to it and so the rest of the alkyl chain. That is, since the bonded carboxylate moiety cannot rotate, its alkyl chain cannot rotate or at least it experiences much limitation. However, this constraint does not exist for alkanethiolate on Au(111) and Ag(111) films because the sulfur atom bonds to the Au or Ag atom via a Au−S or Ag−S single bond which can easily rotate. This results in a large population of gauche defects in $CH_3(CH_2)_nS-Au$ monolayers and $CH_3(CH_2)_nS-Ag$ monolayers. Thus, these monolayers exhibit a weaker odd−even effect than that seen for *n*-alkanoic acid monolayers on Ag. This difference demonstrates that a different anchoring configuration of the binding group may modify the odd−even effect of monolayer structures, further tuning surface and interfacial properties of the self-assembled monolayers.

3.4. Self-Assembly of Organic Molecules on Cu, Al, Hg, Al_2O_3, and SiO_x/Si Substrates

The self-assembled monolayers of alkanethiol and *n*-alkanoic acid formed on Cu,[29,30] Al,[30] Al_2O_3,[31] Hg,[33,34] and SiO_x/Si[34−36] surfaces under ambient conditions have been studied as well. However, measurement of wettability shows no odd−even effect on these substrates.

In the RAIS spectra of the self-assembled monolayers of *n*-alkanoic acids on Cu, the ratio of intensity between $\nu_{asym}(CH_3)$ around 2964 cm^{-1} and $\nu_{sym}(CH_3)$ around 2877 cm^{-1} stays nearly the same for molecules with an odd number (n) of CH_2 units and molecules with an even number ($n \pm 1$) of CH_2 groups. This suggests that the projection of transition dipoles along the surface normal is the same for these molecules. Definitely, these results show no odd−even effect for *n*-alkanoic acid on Cu. Very similar results obtained from alkanoic acid on Al and alkanethiol on Cu suggest the absence of an odd−even effect.

Compared to various odd−even effects observed on Au(111) and Ag(111) films, the absence of an odd−even effect on Cu and Al surfaces shows that the surface chemistry and structure of Cu and Al substrates must be different from those of Au(111) and Ag(111) films, as supported by XPS studies of these substrates.[29,102] XPS data clearly show that the Cu substrate under ambient conditions is not metallic but a hydrous surface oxide related to Cu_2O. This kind of oxide layer is highly active for CO_2 and other reactive impurities. The formed oxide layer is not chemically and structurally homogeneous. Definitely, the quality of this surface with an unevenly distributed oxide layer cannot ensure formation of a well-ordered self-assembled monolayer exhibiting an odd−even effect of the orientation of the terminal group.

In fact, alkanethiol dissociatively chemisorbs on the clean Cu(111) surface via forming a Cu−S chemical bond in ultrahigh vacuum (UHV).[154,155] In this case, we expect that the self-assembled monolayers of alkanethiols on clean Cu(111) in UHV would display a clear odd−even effect similar to that on Au(111) and Ag(111) films under ambient conditions.

Similarly, there is no odd−even effect observed for the organic self-assembled monolayers on oxidized aluminum and silicon oxide surfaces. The major reason is the rough surface structure and heterogeneous surface chemistry of these substrates because they are formed under ambient conditions. The importance and requirement for the surface of a substrate on which organic self-assembled monolayer exhibiting odd−even effects in structure and interfacial property will be discussed in sections 4 and 5.

3.5. Odd–Even Effect on Interfacial Properties

As mentioned before, self-assembly of organic molecules to form organic thin films is an important strategy for modification of chemical and physical properties of the solid surface. It is one of the main approaches for functionalization of solid surfaces as the properties and functions of the attached organic layers are generally absent for inorganic substrates. More importantly, this organic modification and functionalization allows surface and interfacial properties to be tailored controllably, since myriad organic molecules are available and the structure and property of organic materials can be systematically varied. This advantage is based on the principle that the surface and interfacial structures determine surface properties and functions. In fact, the significant structural dependence is evidenced by the observed odd−even effects in interfacial properties such as wettability, surface work function, adhesion, exchange kinetics, friction, and electron transfer. This section demonstrates how the odd−even effects of interfacial properties are dominated by the odd−even difference in surface and interfacial structural issues including intermolecular interactions, binding configuration of head groups, and interactions between terminal groups.

3.5.1. Odd–Even Effect on Wettability

The wettability was extensively studied for various organic self-assembled monolayers on Au(111) and Ag(111) films via measuring the contact angle of contacting liquids on the self-assembled monolayers.[82] The wetting properties of a number of organic monolayers on Au(111) and Ag(111) films[79,96,103,124,156−159] exhibit odd−even effects of chain length as discussed in sections 3.2 and 3.3. The above sections summarized the dependence of the odd−even difference in contact angles on molecular functional groups at head and terminal moieties and on the geometry of the alkyl chains. The wettability of these organic monolayers is strongly associated with the contacting area of the self-assembled monolayers with the contacting liquid.[29,100,103,104] It is in general determined by the exposure of the topmost CH_2, the orientation and dipole of the terminal group, and the geometry of the alkyl chain. It is also associated with the geometry of the head moiety and even the binding chemistry of the tethered functional group.

3.5.2. Odd–Even Effect on Surface Work Function

Chemical attachment of organic molecules on solid surfaces is an important approach for modification of solid surface physical properties. One general strategy for this modification is to tailor the molecular structure or functional group of organic layers, which is confirmed by the experimentally observed changes of surface potential resulting from variation of the molecular chain length or terminal functional groups with different electronic affinity.[103,160−167]

One specific example of the surface modification of organic layers is tuning the surface work function by varying the surface dipole with a self-assembled monolayer. The dependence of the work function on the surface organic layer is due to the electron distribution at the surface. It is known that the electron density oscillates near the surface before decaying slowly into vacuum, which produces an electrostatic dipole layer at the surface. Referring the electrostatic potential to the mean potential in the bulk gives an expression for the work function in terms of the surface dipole, $\phi = D - E_F$ (or $\Delta\phi = \Delta D - E_F$). The surface dipole, D, is a function of the surface structure and adsorbate. Since E_F, the Fermi level, is a bulk property, modification of the surface with a self-assembled monolayer in terms of changing the surface dipole will directly tailor the surface work function. An STM study of $CH_3C_{n-1}H_{2n-1}S-Au$ and $CF_3C_{n-1}H_{2n-1}S-Au$[17] suggested that the dipole can be expressed as dipoles at both the organic/solid interface and the organic/vacuum interface. Compared to a clean metal surface, the change of surface potential upon adsorption of an organic layer can be approximately considered as a combination of three contributions: $\Delta U = eD_{chemisorption} + eD_{molecule} + e\Delta D_{metal}$. $D_{chemisorption}$ is the dipole moment contributed by the charge transfer based on formation of new chemical bonds at the organic/metal interface such as the Au−S bond; $D_{molecule}$ is the dipole moment of the chemisorbed molecules; $e\Delta D_{metal}$ is the change of metal surface potential resulting from addition of the adsorbed molecules. The last term is mainly dependent on the nature of the metal but not strongly on the identity of the attached molecules.[120,168,169] For a series of alkanethiolate monolayers ($C_nH_{2n+1}S-Au$) and fluorine-substituted monolayers ($C_nH_{2n+1-m}F_mS-Au$) there is no

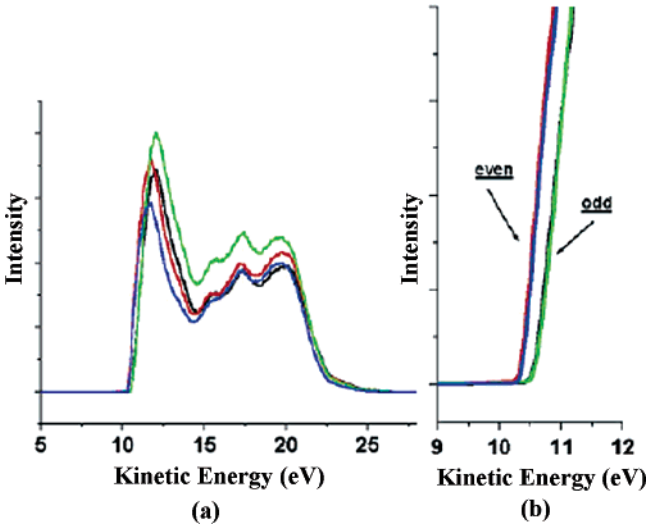

Figure 40. UV photoemission spectra for a series of alkanethiolate monolayers having a single CF_3 termination with either an odd or an even number of carbon atoms in the molecular chain. The low-KE edge region in a has been expanded to show the difference in KE of this edge for even- and odd-numbered carbon chains in b. Reprinted with permission from ref 96. Copyright 2003 American Chemical Society.

Table 2. Shifts in Measured Effective Work Function and Calculated Dipole Moments for Au(111) Films upon Formation of Self-Assembled Au−S(CH$_2$)$_n$CF$_3$ Monolayers (from ref 96)

molecule	monolayer	low-KE cutoff (eV)	change of effective work function (eV)	dipole along normal axis (D)
	Au	10.45	0.00	0
$HS(CH_2)_{12}CF_3$	$Au-S(CH_2)_{12}CF_3$	10.57	0.12	−0.7
$HS(CH_2)_{13}CF_3$	$Au-S(CH_2)_{13}CF_3$	10.34	−0.11	−1.8
$HS(CH_2)_{14}CF_3$	$Au-S(CH_2)_{14}CF_3$	10.64	0.19	−0.7
$HS(CH_2)_{15}CF_3$	$Au-S(CH_2)_{15}CF_3$	10.33	−0.12	−1.8

significant difference in the total of $eD_{chemisorption} + e\Delta D_{metal}$ since these monolayers have the same chemical linkage Au−S bond and the same solid surface Au(111). Thus, the difference in the variation of surface dipole moment (ΔU) for different alkanethiolate and fluorine-substituted alkanethiolate monolayers is mainly the $eD_{molecule}$. This is evidenced by the continuous increase in the shift of effective vacuum level with the increased extent of fluorination at the chain terminus in the order $CH_3(CH_2)_{15}S-Au$, $CF_3(CH_2)_{15}S-Au$, $CF_3(CF_2)(CH_2)_{14}S-Au$, $CF_3(CF_2)_9(CH_2)_6S-Au$.[96]

Just as with the important contribution of the adsorbed molecule for the variation of the surface dipole, an odd−even effect on the change of surface dipole depending on the chain length of $CF_3(CH_2)_nS-Au$ has been seen. Figure 40 shows the UV photoemission feature for $Au-S(CH_2)_n-CF_3$ monolayers with either an even or an odd number of carbon atoms in the molecule.[96] The low-kinetic energy cutoff for these valence spectra is greater for molecules with an odd number of carbon atoms than for molecules with an even number of carbon atoms by ~0.3 eV. Table 2[96] lists the measured dipole moments of alkanethiolate and partially fluorinated alkanethiolate monolayers compared to the clean Au(111) surface and the calculated dipole along the normal axis. The surfaces of the self-assembled monolayer with molecular chains having an odd number of carbon atoms have a larger effective work function than those having an even number of carbon atoms for these fluoromethyl-terminated monolayers. The odd−even effect on the surface work function results from the odd−even difference in the dipole along the surface normal (listed in Table 2 and illustrated in Figure 34), which is induced by the odd−even difference in the orientation of the terminal CF_3 group as schematically shown in Figure 34. This interpretation is based on the fact that the dipole along the most exposed C−F bonds dominates the probability for the escape of the low-kinetic-energy photoelectron.[96] In addition, atomic substitution of H by F for methyl-terminated alkanethiolate monolayers induces odd−even effects of interfacial properties such as wettability[96] as discussed in section 3.5.1 and probe ion neutralization probabilities[170] as discussed in section 3.6.1.

3.5.3. Odd–Even Effect on Maximum Adhesion

As demonstrated above, the surface structure can be controllably tuned at the atomic scale by tailoring the terminal functional group of the self-assembled monolayer on the substrate. This ability offers applications in the development of molecular electronics, nanotribology, and nanografting. One specific application is chemical force microscopy in which surface functional groups are used to identify chemical inhomogeneity of the surface. Many of these applications involve interfacial properties such as adhesion and friction. Thus, the chemical effects on the adhesion and friction between two self-assembled alkanethiolate monolayers $X(CH_2)_nS-Au$ (X = CH_3, OH, COOH) were studied using molecular dynamic simulations.[171] Some odd−even effects as a function of chain length of the self-assembled alkanethiolate monolayers were revealed.

$Au-S(CH_2)_nX$ (X = CH_3, OH, COOH, n = 8, 9, 12, 13, 16, and 17) self-assembled monolayers on Au were investigated by molecular dynamics simulations.[171] Figure 41 shows two self-assembled monolayers of $HOOC(CH_2)_8-S-Au$ with different relative displacement to exemplify how the adhesion and friction of the self-assembled monolayers $Au-S(CH_2)_nX$ were studied. For adhesion and friction studies a second layer mirroring the first one was included in the calculation with an initial vacuum gap, S, of 10 Å between the outermost hydrogen atoms in the terminal groups (Figure 41a). D is defined as the relative displacement of the two monolayers which could be equal to the vacuum gap, S, or not. For example, at this starting state both S and D equal 10 Å. Figure 41a−c shows the structures of the alkanethiolate monolayers at various relative displacements. These simulations were performed with the COMPASS force field.[93,172] The sulfur atom was kept frozen during the simulation. The binding of thiol on the Au substrate was considered constant under the condition of the simulation due to the strong Au−S bond length of ~50 kcal/mol.[93] Al least three structures for the self-assembled alkanethiolate monolayers on Au including $(\sqrt{3} \times \sqrt{3})R30°$, herringbone, and $c(4 \times 2)$ were used as templates for these simulations. However, the force−separation curve does not depend on the choice of the original structure of the alkanethiolate self-assembled monolayer on the Au substrate.

The normal pressure of each of the two monolayers shown in Figure 41 is 0 at a separation greater than the cutoff distance for the nonbonded interaction (12 Å). When brought together, they are attractive due to the Coulomb and van der Waals interactions between their terminal COOH groups. It is understandable that an attractive minimum in the normal pressure−separation curves occurs at a small separation in all cases.

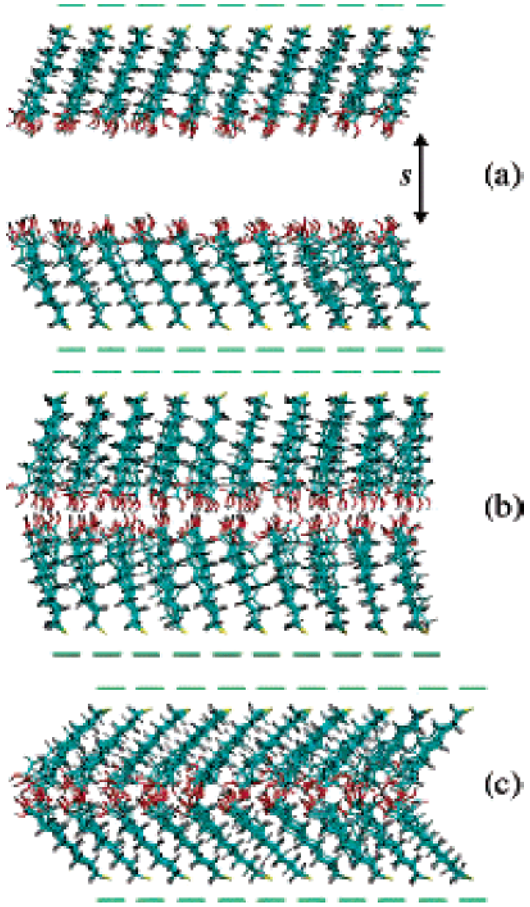

Figure 41. Structure of two self-assembled monolayers of Au−S(CH$_2$)$_8$COOH···HOOC(CH$_2$)$_8$S−Au at various relative displacements: (a) at the separation S = 10 Å, (b) at the maximum attraction, D = 2.9 Å, and (c) at a highly compressed position D = −4 Å. The H atoms are gray, the C atoms are cyan, the O atoms are red, and the S atoms are yellow. The distance S is the average separation between the terminal carbon atoms of two self-assembled monolayers. While S and D are almost equal in a, they are different in b, S = 3 Å, and in c $S \cong$ 2 Å. Reprinted with permission from ref 171. Copyright 2003 American Chemical Society.

Figure 42 demonstrates the odd−even dependence of the maximum attractive pressure (P_{max}) calculated as a function of the number of CH$_2$ units of the three series of substituted alkanethiolate monolayers Au−S(CH$_2$)$_n$X (X = CH$_3$, OH, and COOH). Although the values of P_{max} for a monolayer terminated with CH$_3$ (marked with circles) are much smaller than those for monolayers terminated with OH (triangle) and COOH (square) monolayers, there is still a slight odd−even difference for the three pairs of CH$_3$(CH$_2$)$_n$S−Au (n = 8 versus n = 9, n = 12 versus n = 13, and n = 16 versus n = 17). P_{max} of the monolayer with n = odd is larger than that of the monolayers with $n \pm 1$. The odd−even difference for self-assembled monolayers (n < 13) terminated with the COOH group is large. For $n \geq 13$ however this odd−even effect becomes weaker, which will be rationalized at the end of this section. The odd−even effect for n < 13 is attributed to the difference in the orientation of the terminal COOH group which impacts the possibility of forming hydrogen bonds.

Another important factor is the specific arrangement of the atoms of the terminal COOH group which influences formation of interlayer hydrogen bonds. Figure 43 presents the calculated models for HOOC(CH$_2$)$_8$S−Au and HOOC-(CH$_2$)$_9$S−Au at a tilt angle of 15° with a cell having four

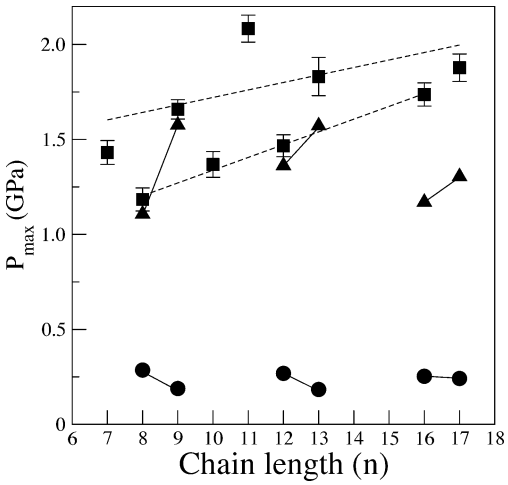

Figure 42. Chain length dependence of maximum attractive normal pressure (P_{max}) for (CH$_2$)$_n$−X monolayers, X = CH$_3$ (●), OH (▲), COOH (■). Pressures were determined from equilibrium simulation at the minimum position. Solid lines connect every odd−even pair for CH$_3$ and OH. For COOH, the least-squares fit for the even and odd series is given with two dashed lines. Error bars are shown for the COOH. Reprinted with permission from ref 171. Copyright 2003 American Chemical Society.

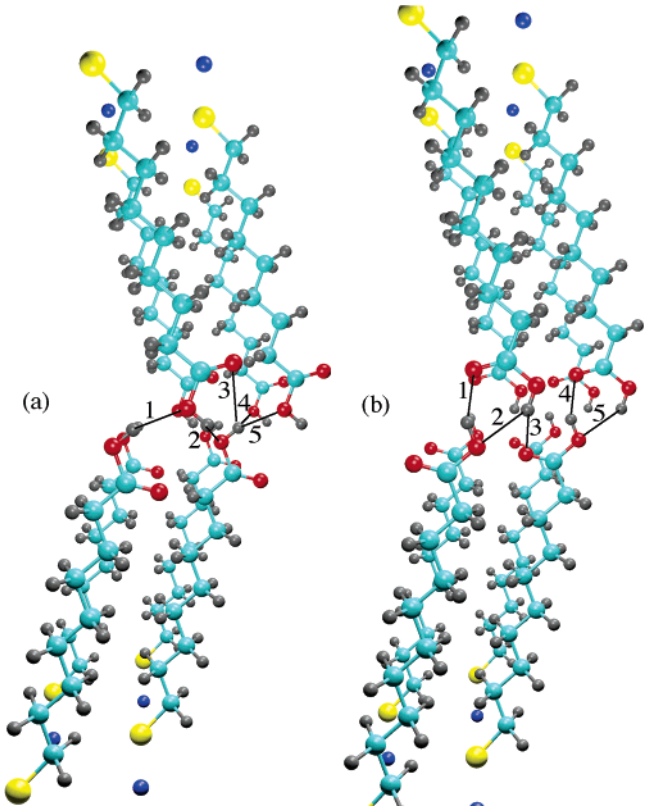

Figure 43. Four-chain cells of HOOC(CH$_2$)$_n$S−Au showing oxygen−hydrogen separation. (a) Cell made of four HOOC-(CH$_2$)$_8$S−Au molecules. (b) Cell made of four HOOC(CH$_2$)$_9$-S−Au molecules. The distances labeled 1−5 are given in Table 3. Coloring is the same as in Figure 41. Reprinted with permission from ref 171. Copyright 2003 American Chemical Society.

molecules. The interlayer separation between the terminal carbon atoms (the carbon atoms of COOH groups of the two self-assembled monolayers) is 4 Å, which approximately is the separation at P_{max}. Table 3 lists the separation between the H and O atom from two carboxylic acid groups in this model. Definitely, all the labeled five pairs (1, 2, 3, 4, and

Table 3. H−O Distances in the Calculated Models of Figure 43 (from ref 171)

	distance (Å)	
label	HOOC−$(CH_2)_8$−S−Au	HOOC−$(CH_2)_9$−S−Au
1	2.1	1.9
2	2.8	2.3
3	3.5	3.1
4	5.4	1.9
5	2.1	2.3

5) of the hydrogen acceptor and hydrogen donor in the system of Au−$S(CH_2)_9COOH\cdots HOOC(CH_2)_9S$−Au (Figure 43b) can form hydrogen bonds. However, only two of five pairs can form hydrogen bonds for the system of HOOC−$(CH_2)_8$−S−Au (Figure 43a). This difference in the interlayer hydrogen bonding suggests that P_{max} between two HOOC−$(CH_2)_9$−S−Au monolayers is larger than that between two Au−$S(CH_2)_8COOH\cdots HOOC-(CH_2)_8$−S−Au monolayers, consistent with the odd−even effect shown in Figure 42.

In fact, a slight deformation of the alkyl chain (only tenths of 1 Å) can obviously increase the number of hydrogen bonds in HOOC−$(CH_2)_n$−S−Au (n = even). It is understandable that the longer chain needs less energy for this deformation. Therefore, with the increase of chain length n the number of interlayer hydrogen bonds for n = even can be more easily increased via a slight chain bending. Therefore, this odd−even difference is weakened with the increase of the chain length, as indicated in Figure 42.

3.5.4. Odd–Even Effect on Exchange Kinetics

The BP_n self-assembled monolayers were immersed into a solution of hexadecane thiol to investigate the exchange of self-assembled molecules with external solution molecules and the influence of this exchange on capacitance and charge-transfer rate.[173] Although the capacitance and charge transfer of the self-assembled monolayers of BP_n (n = 0−6) on Au(111) did not display an odd−even effect, the exchange kinetics of these self-assembled monolayers with external alkanethiol molecules in solution such as hexadecane thiol did exhibit an odd−even effect on the length of the alkyl chain of the self-assembled monolayer.[173]

The stability of the BP_n self-assembled monolayer determines how fast the external hexadecane thiol molecules displace the chemisorbed aromatic thiolates. BP_2 and BP_3 are used as an example to illustrate the odd−even difference. The IRAS spectra revealed a substantial difference in the replacement of the self-assembled BP_n molecules with the hexadecane thiol molecules in solution.[173] For the BP_2 monolayer, characterization of hexadecane thiol in terms of the C−H asymmetric stretching mode in CH_3 at ~2966 cm^{-1} can still be observed after only 10 min immersion. However, this vibrational feature is absent for BP_3 at the same immersion time. In addition, the peak intensity of the C−C ring stretch at ~1500 cm^{-1} is obviously decreased for BP_2, in contrast to BP_3 which remains the same as before immersion. These differences suggest that BP_3 displays a higher stability and slower exchange rate than BP_2.

Figure 44 presents the variation of the capacity of the BP_n self-assembled monolayer as a function of the immersion time in a solution of hexadecane thiol for various self-assembled monolayers BP_n (n = 1−6). The measured capacity change reflects the exchange kinetics of the self-assembled BP_n monolayer with the external thiol molecules in solution. Larger capacity changes means higher exchange rate. Obviously, the even-numbered BP_n monolayers (n = 2, 4, and 6) are more prone to exchange with external thiol molecules than the odd-numbered ones (n = 1, 3, and 5).

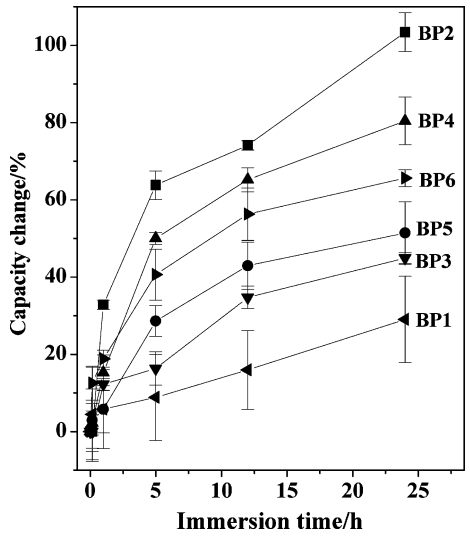

Figure 44. Change of the capacity of the self-assembled BP_n monolayers on Au with time of immersion in a 1 mM solution of hexadecane thiol (MC16). The percentage change of capacity is defined by $[C_{BPn}(t=0)-C_{BPn}(t)]/[C_{BPn}(t=0)-C_{MC16}]$ with $C_{BPn}(t=0)$ as the capacity of the BP_n monolayer after immersion time t and C_{MC16} as the capacity of a pure MC16 monolayer on Au(111). Solid lines are guides to the eye. Reprinted from ref 173, Copyright 2003, with permission from Elsevier.

Clearly, the odd−even effect on the exchange kinetics results from differences in the film structures. The odd and even numbers of CH_2 units of BP_n impact the thiolate−substrate bonding. The odd−even difference in the structure of the self-assembled monolayers BP_n is complex. For BP_n (n = odd) shown in Figure 29c, the sulfur sp^3 bonding configuration forms a favorable bulk-like close packing of the aromatic rings.[69,71] For BP_n (n = even), however, the long axis of the biphenyl rings is closer to the substrate, in contrast to the monolayer with n = odd, resulting in a lower coverage of BP_n with an even number of CH_2 units. To increase the molecular coverage for forming an energetically favorable bulk-like packing of the biphenyl units for BP_n (n = even), the C−S−Au has to deviate from the normal 109° of sulfur sp^3 hybridization. In contrast, the increase of coverage will increase intermolecular repulsion, which is energetically unfavorable. Thus, a competition of the two opposite trends of increasing molecular coverage via distorting C−S−Au bond angle versus increasing intermolecular repulsion gives the monolayer (n = even) with 10−15% lower coverage than the monolayer of molecules with n = odd. Overall, for BP_n (n = even) the less dense packing structure has weaker intermolecular interactions. Therefore, the self-assembled BP_n monolayer with n = even is higher in energy. This is further supported by the desorption behavior and electrochemical stability of these self-assembled BP_n monolayers based on an odd−even alternation of the reduction desorption peak potential.[174] Since the BP_n monolayer with n = even is more energetic, it is understandable that the activation energy for molecular exchange with the external thiol for BP_n (n = even) monolayers is lower than that for BP_n (n = odd) monolayers. This is consistent with the odd−even difference in exchange kinetics of the BP_n monolayer with external hexadecane thiol shown in Figure 44.

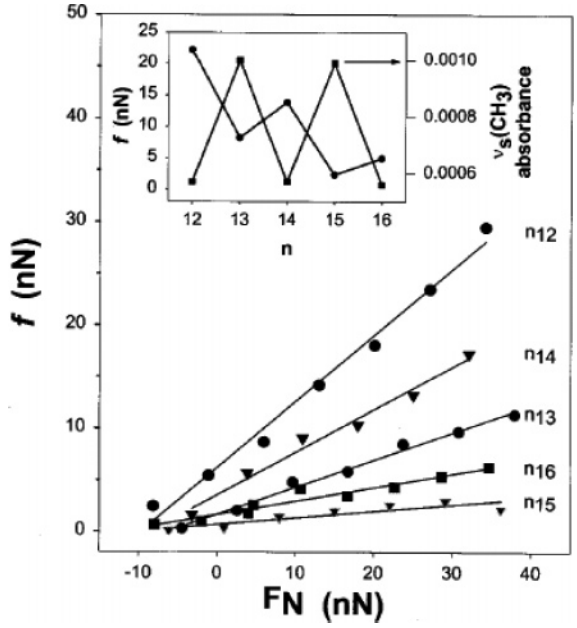

Figure 45. Friction force (f) versus the contact load (F_N) for $CH_3(CH_2)_nS-Au$ ($n = 12-16$) monolayers on Au. The inset plots f versus n at $F_N = \sim 25$ nN and the absorbance of the lower energy symmetric methyl stretching mode $\nu_{sym}(CH_3)$ obtained for each monolayer. Reprinted with permission from ref 99. Copyright 1998 American Chemical Society.

3.5.5. Odd–Even Effect on Tribological Property

The friction of organic self-assembled monolayers on solid surfaces attracts considerable interest because the self-assembled organic layers could be used as lubricants in the development of microelectromechanical machines.[175,176] Friction and related topics have been addressed.[177] The interfacial and surface friction was studied with interfacial force microscopy (IFM) which can provide quantitative and stable force measurements over a wide spectrum of interfacial interactions. It simultaneously measures the normal force (both attractive and repulsive) and lateral friction of the self-assembled monolayer. There are two methods for studies of interfacial force. One is direct measurement with a naked probe tip. Another is carried out using a tip coated with organic molecules such as alkanethiolates on a Au-terminated tip, which explores the friction at the organic/organic interface.

One example of the first method is the study of the tribology between the self-assembled $CH_3(CH_2)_nS-Au$ ($n = 12-16$) monolayers and a bare probe tip using friction force microscopy (FFM).[99] The friction force at a microcontact is a function of the contact load, contact area, and surface free energies of the two contacting materials. Figure 45 presents the microcontact friction force between the self-assembled monolayer and tip as a function of contact load (F_N). The inset of Figure 45 shows an odd−even alternation of $\nu_{sym}(CH_3)$ absorbance intensity, clearly demonstrating the odd−even difference in the orientation of the terminal CH_3 groups in the self-assembled monolayers $CH_3(CH_2)_nS-Au$. More importantly, the inset illustrates a complex dependence of friction at $F_n \approx 25$ nN on molecular chain length. Clearly, there is an odd−even alternation in the friction force depending on the odd or even number of CH_2 units in the molecular chain. This overall decreasing trend of friction force with the increase of chain length implies that there is possibly a mechanical contribution such as adlayer elasticity which is associated with the increase of chain length.[178−180] This mechanical contribution to the friction is superimposed on the contribution of friction force resulting from the odd−even difference in the orientation of the terminal CH_3 of the self-assembled monolayers. It is suggested that the odd−even effect on friction is driven by an odd−even difference in the compressibility of the self-assembled monolayers, which is closely related to the spatial orientation of the terminal group of the self-assembled monolayer.[99]

Another model was proposed for interpreting the odd−even alternation of the friction properties of the self-assembled monolayers of normal alkanethiols on Au(111).[79] In this model the different exposure of the topmost CH_2 group gives rise to an odd−even change of van der Waals interactions between the organic monolayer and the contact AFM tip. Compared to the self-assembled $CH_3(CH_2)_nS-Au$ monolayer with an odd number of CH_2 units, the topmost CH_2 unit of $CH_3(CH_2)_nS-Au$ (n = even) has a larger exposure. Thus, the larger van der Waals interactions between the $CH_3(CH_2)_nS-Au$ monolayer (n = even) and the contacting tip resulting from a larger exposure of the topmost CH_2 unit leads to a larger friction response than that seen for the $CH_3(CH_2)_nS-Au$ monolayer (n = odd).

There is not an obvious odd−even difference in the friction properties for the self-assembled $C_6H_5(CH_2)_nS-Au$ monolayers, though the friction response of this series of phenyl-ring-terminated monolayers generally decreases with increasing chain length.[79] The reason for the absence of an odd−even effect on friction force in this system is not clear. On the basis of the second model it may possibly be attributed to the blocking effect of the large overlying phenyl ring on its underlying CH_2 groups. This blocking effect largely obscures the odd−even difference of the van der Waals interaction between the self-assembled monolayer and the contacting tip.

To resolve the intrinsic driving force for the odd−even effect of friction behavior of these self-assembled monolayers, further study on this issue is necessary. Since the exposure of the topmost CH_2 in the three series of self-assembled monolayers 4′-$CH_3(CH_2)_mOC_6H_4C_6H_4$-4-$CH_2S-Au$, 6-$CH_3(CH_2)_mOC_{10}H_6$-2-$CH_2S-Au$, and 4′-$CH_3(CH_2)_mOC_6H_4C_6H_4$-4-$S-Au$ are larger than that of $C_6H_5(CH_2)_nS-Au$ monolayers, studying the friction behavior of these three series of molecules as a function of chain length will be helpful in resolving the two models discussed above and elucidating the intrinsic driving force for the odd−even effect of tribological properties of the self-assembled monolayers on Au(111) films.

Using the second method of tribology study, one example is the tribological properties of $Au-S-(CH_2)_mCOOH$ self-assembled on Au(111) single-crystal surfaces measured with a $HOOC-(CH_2)_m-S$-coated Au tip or $CH_3(CH_2)_mS$-coated Au tip. For tips coated with $CH_3(CH_2)_{15}SH$, a difference in the friction behavior is observed for the self-assembled monolayers of $HOOC(CH_2)_{15}-S-Au$ and $HOOC(CH_2)_{10}-S-Au$, possibly due to the odd−even difference in the orientation of the ending COOH groups of the two self-assembled monolayers.[181]

3.5.6. Odd–Even Effect on Electron Transfer

Ferrocyanides are well suited for differentiating the conductivity of membrane systems due to the fact that the electron-transfer rate from these ions is quite slow.[182−184]

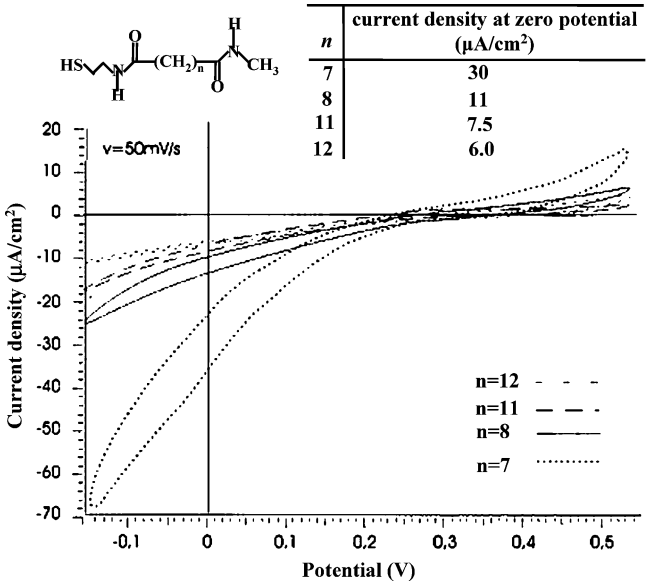

Figure 46. Cyclic voltammetry of the self-assembled monolayers of diamidothiolates having an alkyl chain with an even or odd number ($n = 7, 8, 11, 12$) of CH_2 units on Au(111) films showing the electron-transfer behavior of these monolayers. Reprinted with permission from ref 129. Copyright 2000 American Chemical Society.

Cyclic voltammetry of ferrocyanide ions in bulk water is a common technique for measuring the conductivity of monolayers. It has been used to study electron transfer through the self-assembled monolayers of diamidothiolates on Au(111) films. As shown in Figure 46, the diamidothiolate monolayers with an even number of CH_2 units are better insulators than those with an odd number ($n - 1$) of CH_2 groups.[129] This behavior indicates that the self-assembled monolayers of diamidothiolates with an even number of CH_2 units are much less permeable to ferrocyanide ions than those with an odd number ($n - 1$) of CH_2 groups. This odd−even difference is related to the orientation of terminal CO− and N−H groups which influences formation of the hydrogen bond between the terminal moieties of two adjacent molecules in the self-assembled monolayer as shown in Figure 35b,c.

3.5.7. Odd–Even Effect on Electrochemical Property

The electrochemical properties of both alkanethiolate and BP_n self-assembled monolayers were studied experimentally. For alkanethiolate monolayers, the desorption potential exhibits a continuous negative shift with increasing chain length. There is no odd−even alternation observed.[185] However, a clean odd−even effect on the desorption potential of BP_n self-assembled monolayer was revealed.[174] Figure 47 shows the observed odd−even effect. The average potential difference between monolayers with an odd and even number of CH_2 units is 83 mV.[174] In addition, Figure 47 shows a continuous shift superimposed on the odd−even variation.

This odd−even effect is proposed to be related to the odd−even difference in the intermolecular interaction schematically shown in Figure 29c. The larger coverage of BP_n ($n =$ odd) associated with a strong intermolecular interaction can stabilize these BP_n monolayers to a larger extent, in contrast to BP_n monolayers ($n =$ even). The role of intermolecular interactions in stabilizing the BP_n monolayers is consistent with the stabilization effect of the intermolecular interactions between the CH_2 groups of two adjacent $CH_3(CH_2)_nS-$

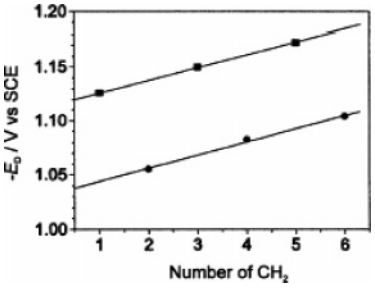

Figure 47. Desorption peak potential (E_D) of BP_n self-assembled monolayers on gold as a function of the length n of the methylene spacer chain. Reprinted from ref 174, Copyright 2002, with permission from Elsevier.

molecules evidenced in the negative shift of the desorption peak with an increase of molecular chain length.[185]

In addition to the odd−even effect on the desorption potential of BP_n, the area of the desorption peak presents an odd−even effect as well.[174] In each series (odd series or even series) the peak area continuously increases with the increase of molecular chain length. The trend of increasing area in each series results from the decrease of capacitance due to the increasing thickness of the self-assembled monolayer. This odd−even change in desorption peak area possibly involves a contribution from both capacitive current and Faradaic charge. It can be simply attributed to the odd−even variation in the capability of ion penetration as the BP_n monolayer ($n =$ even) with a lower coverage has larger channels provided for penetration of ions into this self-assembled monolayer, in contrast to the BP_n monolayer ($n =$ odd).

3.6. Odd–Even Effect on Chemical Reactivity of Organic Self-Assembled Monolayers

3.6.1. Odd–Even Effect on Reactivity Measured by Ion/Surface Collision

Organic functionalization of a solid surface is the most promising strategy to controllably modify surface chemical and physical properties. Ion/surface collisions have been extensively used to probe the physical and chemical properties of surfaces. For organic self-assembled monolayers on metal surfaces, this technique was used to study the chemical reactivity of self-assembled monolayers such as $CH_3(CH_2)_{m-1}SH$ ($m = 11-16$, 18),[186−190] 4′-$CH_3(CH_2)_m$-$OC_6H_4C_6H_4$-4-SH ($m = 14-17$),[190] and $CF_3(CH_2)_nSH$ ($n = 12-15$)[170] on Au(111).

Generally, pyrazine and d_6-benzene molecular ions were used as probe ions because they form product ions with the hydrocarbon-covered monolayer surface.[186] For example, $C_6D_6^{+\bullet}$ + H-SAM surface → $C_6D_6 + C_3H_5^+ \rightarrow C_7D_6H^+ + C_2H_4$. Detection of the product $C_7D_6H^+$ shows addition of H atom of the self-assembled monolayer onto the incident probe ion $C_6D_6^+$. The odd−even effects on the extent of the addition reactions of hydrogen atoms and methyl groups of the $CH_3(CH_2)_{m-1}S-$Au monolayers with probe ions were revealed.[186]

For the self-assembled monolayers of $CH_3(CH_2)_{m-1}S-$Au the probe ions used were $C_4H_4N_2^+$ and $C_6D_6^+$. For both pyrazine and d_6-benzene the ratio of the hydrogen addition fragment ion versus the corresponding surface-induced dissociation daughter ions was taken as the extent of the hydrogen addition reaction. The measured ratios were used to compare a series of self-assembled $CH_3(CH_2)_{m-1}S-$Au

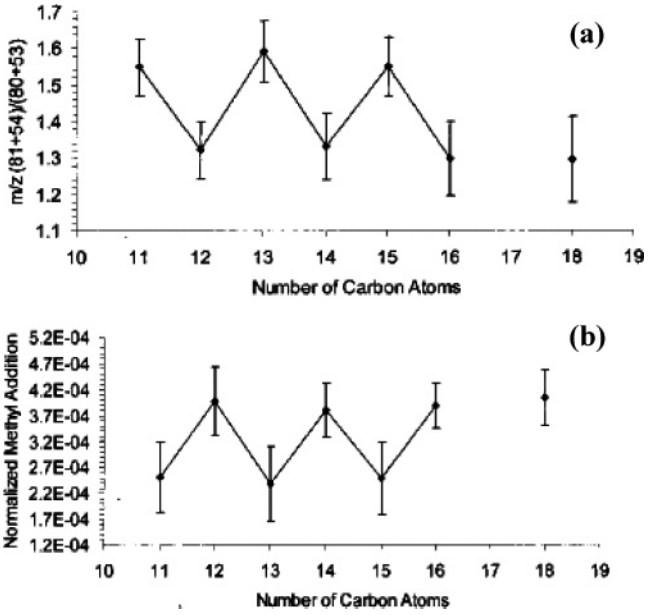

Figure 48. (a) Ratio of $(MpH^+ + (MpH-HCN)^+)/(Mp^{+\bullet} + (Mp-HCN)^+)$ in terms of $(81 + 54)/(80 + 53)$ for 30 eV pyrazine molecular ions versus the number of carbon atoms in a molecule for *n*-alkanethiolate monolayers on Au(111) films. (b) Normalized methyl addition (*m*/*z* 95) of pyrazine molecular ions versus the number of carbon atoms in a molecule for *n*-alkanethiolate monolayers on Au(111) films.

monolayers. Figure 48a shows the extent of reaction for hydrogen addition from the self-assembled monolayer as a function of the number of carbon atoms, *m*. An odd−even effect is revealed. The molecules with an odd number of carbon atoms have larger reactivity for hydrogen addition. The same odd−even effect was observed when d_6-benzene was used as a probe ion. Thus, the odd−even difference in reactivity was attributed to the structural odd−even difference of the self-assembled monolayers.

Figure 48b shows the extent of alkyl addition reaction with the probe ion as a function of molecular length. The reaction between the incident pyrazine molecular ions and the alkanethiolate self-assembled monolayer results in a direct methyl addition to $C_4H_4N_2^+$ and then formation of the $C_5H_7N_2^+$ ion. A clear odd−even alternation of the extent of methyl addition which is independent of the incident probe ion was revealed in Figure 48b. Opposite to the odd−even effect of hydrogen addition, the self-assembled monolayers of $CH_3(CH_2)_{m-1}S-Au$ with m = even have higher reactivity for methyl addition than the monolayers with m = odd.

The two opposite odd−even effects on the hydrogen addition and methyl addition result from the structural odd−even difference of the self-assembled monolayers. For the monolayers $CH_3(CH_2)_nS-Au$ with an even number of CH_2 units in terms of odd number of carbon atoms in a molecule (Figure 38a), one C−H bond of the terminal CH_3 group is aligned approximately perpendicular to the Au substrate. This geometry makes the alkanethiolate monolayer with an even number of CH_2 groups more reactive in hydrogen addition. In addition, the higher reactivity of the hydrogen addition is possibly partially attributed to the exposed hydrogen atoms of the outermost CH_2 group in terms of high exposure of the topmost CH_2 group. For a molecule with an odd number of CH_2 units, however, all three hydrogen atoms of the methyl group are in a plane nearly parallel to the Au substrate and the hydrogen atoms of the topmost CH_2 units point toward the substrate (Figure 38b), resulting in a lower reactivity for hydrogen addition. For the $CH_3(CH_2)_nS-Au$ monolayer with an odd number of CH_2 units in terms of an even number of carbon atoms in the molecule, the terminal CH_3-CH_2- bond is nearly perpendicular to the substrate. This results in methyl addition with the incident probe ions occurring more readily than for the monolayers with an even number of CH_2 groups.

The reactivity for hydrogen addition and methyl addition of the self-assembled 4′-$CH_3(CH_2)_mOC_6H_4C_6H_4$-4-S−Au ($m$ = 14−17) monolayers[190] was also investigated. For hydrogen addition, monolayers with m = odd exhibit higher reactivity than those with m = even. Similarly to the $CH_3(CH_2)_n$-S−Au monolayers, methyl addition of 4′-$CH_3(CH_2)_m$-$OC_6H_4C_6H_4$-4-S−Au monolayers displays an odd−even effect opposite to its hydrogen addition.[190]

As mentioned before, a smaller odd−even difference in the orientation of the terminal CH_3-CH_2- moiety revealed in the studies of wettability and vibrational features of the $CH_3(CH_2)_nS-Au$ monolayers than those of 4′-$CH_3(CH_2)_m$-$OC_6H_4C_6H_4$-4-S−Au monolayers is probably due to the low rotation barrier of the alkyl chain in $CH_3(CH_2)_nS-Au$ compared to the high rotation barrier associated with the head moiety in 4′-$CH_3(CH_2)_mOC_6H_4C_6H_4$-4-S−Au.[100,121−123] However, the small odd−even difference in the orientation of the terminal CH_3 for alkanethiolate monolayers is clearly identified by ion−surface reactions as shown in Figure 48. This shows the high sensitivity of this technique in differentiating surface structure. Thus, the low-energy ion/surface reaction could be developed as an analytical tool for characterizing the structures and properties of organic self-assembled surfaces.

The ion−surface reactions of CF_3-, CF_3CF_2-, and $C_{10}F_{21}$-terminated alkanethiolate self-assembled monolayers on the Au substrate display interesting odd−even effects.[170] Compared to CH_3-terminated alkanethiolate,[186−189] substitution of C_nH_{2n+1} with all-trans C_mF_{2m+1} as a terminal moiety significantly impacts the ion−surface interaction processes including atom/group transfer, electron transfer, and energy transfer. Notably, as the $CF_3(CH_2)_nS-Au$ monolayers exhibit an odd−even effect on the wettability and orientation of the terminal CF_3 group,[103,191] their ion−surface reactivity presents an odd−even effect as well.[170] First, the reactivity for F addition between the incident benzene ion and the surface fluorine atoms for the monolayers with an even number of CH_2 units is greater than that for the monolayers with an odd number of CH_2 groups. This is because the exposed fluorine atoms of $CF_3(CH_2)_nS-Au$ (n = even) are more accessible to abstraction by the incident ion than those of $CF_3(CH_2)_n$-S−Au (n = odd) (see Figure 34). For the H addition reaction of the $CF_3(CH_2)_nS-Au$ monolayer, its odd−even effect is opposite to that of the F and H addition of the CH_3-terminated alkanethiolate monolayers. This is understandable since the topmost CH_2 groups of $CF_3(CH_2)_nS-Au$ monolayers play the same role as CH_3 groups of $CH_3(CH_2)_n$-S−Au monolayers in the H addition reaction. Also, the terminal CF_3CH_2- group of the monolayers with an odd number of CH_2 units has higher reactivity than that for the monolayers with an even number of CH_2 groups because the former has a vertical CF_3CH_2- moiety which is more accessible for the projectile ions (Figure 34), consistent with the odd−even effect for methyl addition by the methyl-terminated alkanethiolate monolayers.

3.6.2. Odd–Even Effect on Degradation of Monolayer upon Electron Irradiation

Using electron-beam patterning of self-assembled monolayers to develop one category of new lithographic resist is a promising strategy to extend lithography down to the nanometer scale.[12,82] One advantage of using the self-assembled monolayer as a resist is that the induced change by electron bombardment can be controlled via different molecular structure of the monolayer.[192−201] For example, 4′-nitro-1,1′-biphenyl-4-thiol self-assembled monolayer on Au was selected as a model to study the electron-beam-induced modification because the resistance of the aromatic self-assembled monolayers toward electron irradiation permitted subsequent selective chemical modification of the terminal functional groups, allowing the design of chemical lithographic patterns and templates.[192,193]

In contrast to the damage and disorder seen for self-assembled monolayers of normal alkanethiolates upon electron-beam irradiation,[199,200,202−208] damage to the self-assembled $CH_3-(C_6H_4)_2-(CH_2)_n-S-Au$ monolayer was found to be reduced.[114] In addition, the orientational order of the self-assembled monolayer and molecular chemical binding to the Au surface were retained upon electron irradiation, though both are slightly reduced. Although the general trend of the modification by electron irradiation is similar for this series of molecules with different $(CH_2)_n$ chain lengths, the extent of the change of the surface structure induced by electron irradiation strongly depends on the original structure of the self-assembled monolayer before irradiation.

Some of this series of self-assembled monolayers such as BP_1, BP_4, and BP_5 display pronounced odd−even differences in their reactions toward electron irradiation and the change in the monolayers upon electron-beam irradiation.[114] The densely packed monolayers with n = odd such as BP_1 and BP_5 are much more stable with respect to electron irradiation than the less densely packed monolayers with n = even such as BP_4, evidenced by their difference in the extent of degradation of monolayer upon electron irradiation. This is likely because the more ordered and densely packed monolayer (n = odd) is better able to delocalize and more rapidly relax the initial electronic excitation.

3.6.3. Odd–Even Effect on Phase Formation of the Polymerized Monolayer upon UV Irradiation

The chromatic phase transitions of polydiacetylenes (PDAs), such as the transition between blue and red phases, have been observed for single crystals and Langmuir−Blodgett (LB) films.[209−214] Notably, in this section blue and red phases refer to polymers with long and short conjugation length, respectively.[209−214] It is well known that the localized chemical environment of the backbone of the polymer may significantly impact its chromatic properties.[209−212] Studies show that sulfurized diacetylenes can self-assemble onto Au(111) films and then be polymerized upon UV irradiation.[215−223] Compared to formation of LB polymer films, the covalent binding between sulfurized monomer and the Au(111) film via molecular self-assembly and subsequent UV-induced polymerization definitely limits the degree of free motion within the monolayer. This limitation possibly may be used to tune the polymerizability of monomer monolayers and even the chromatic property of the polymerized films.

Polymerization of diacetylene monomer monolayer self-assembled on Au(111) is taken as an example for understanding structural factors of polymerization. Studies on how the structural distortion of diacetylenes upon self-assembly on Au influences the polymerization efficiency and chromatic properties of the polymerized self-assembled monolayer is key for potential application of these materials as a chemical sensor.[224−226]

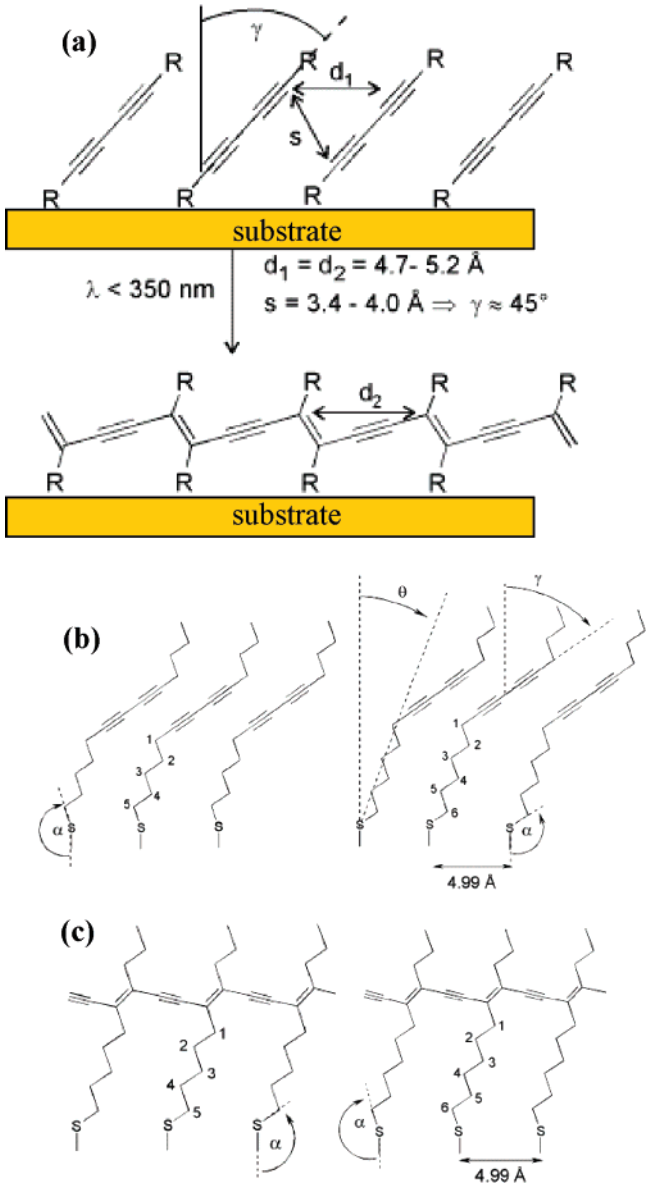

Figure 49. (a) Steric constraints for the diacetylene self-assembled monolayers required for polymerization on a solid substrate. (b) Schematic representation of the structures of unpolymerized diacetylene monolayers for odd (five CH_2 units, left) and even (six CH_2 groups, right) numbered alkyl spacers. (c) Schematic representation of the structure of polymerized diacetylene monolayers for odd (five CH_2 units, left) and even (six CH_2 units, right) numbered alkyl spacers. Notably, for a clearer presentation, a terminal chain $CH_3(CH_2)_3-$ is used to represent the terminal $CH_3-(CH_2)_{15}-$ chain of monomers, $CH_3(CH_2)_{15}-C\equiv C-C\equiv C-(CH_2)_n-S-Au$. Reprinted from ref 228, Copyright 2000, with permission from Elsevier.

Previous studies show that an effective polymerization of diacetylene monolayer requires a tilt angle (γ) of the diacetylene group of ~45° with respect to the surface normal as schematically shown in Figure 49a.[212,213,227] The diacetylene (DA) monomers studied are $CH_3(CH_2)_{15}-C\equiv C-C\equiv C-(CH_2)_n-S-$ including 15,4-DA, 15,5-DA, 15,6-DA, and 15,9-DA corresponding to n = 4, 5, 6, and 9, respectively.

Notably, to constrain the tilt angle of ~45° for the requirement of effective polymerization, significant modification of the Au−S−C bond angle at the interface between the sulfurized diacetylene monomer and the Au substrate is necessary. As shown in the left panel of Figure 49b for the alkyl spacer with an odd number of CH_2 units between the bonded sulfur atom and the diacetylene group, the Au−S−C bond angle of the self-assembled *monomer* monolayer should be distorted into ~180° to maintain a γ angle of ~45° for effective polymerization.[153] However, previous studies have shown that the binding of the head group sulfur via sp^3 hybridization with a Au−S−C bond angle of ~109° is the most energetically stable. To obtain both the sp^3 hybridization in terms of the Au−S−C bond angle of ~109° for stable chemical binding on Au(111) and the diacetylene tilt angle of ~45° for effective polymerization, some gauche defects must occur within the alkyl spacer with an odd number of CH_2 units in the sulfurized diacetylene molecules of the self-assembled *monomer* monolayers.[228] The gauche defects were confirmed by the observed vibrational feature centered at 2928 cm^{-1} of the disordered component in the infrared spectra of the self-assembled monomer monolayers with an odd number of CH_2 units (15,5-DA and 15,9-DA).[228]

For an alkyl chain with an even number of CH_2 units (the right panel of Figure 49b), however, the all-trans alkyl chain without gauche defects can meet the requirements of both ~109° of sp^3 hybridization and ~45° for effective polymerization. Thus, there are no gauche defects in the alkyl spacer with an even number of CH_2 units, supported by the absence of vibrational feature at 2928 cm^{-1} in the infrared spectra of the self-assembled monomer monolayer before UV polymerization.[228]

The structural odd−even difference of the self-assembled monolayer of *monomers* results in an odd−even effect in the phase formation of polymer and polymerization efficiency upon UV excitation. For a highly conjugated system, the C═C and C≡C transitions are significantly shifted in contrast to transitions of C═C at 1620 cm^{-1} and C≡C at 2260 cm^{-1} in the monomer.[229−231] The sharp peaks with high intensity at 1459 cm^{-1} for C═C and 2088 cm^{-1} for C≡C in the Raman spectra of the self-assembled monolayer of the polymer show that the *monomer* monolayer with an alkyl spacer of an odd number of CH_2 units can form appreciable amounts of the long-conjugation-length blue-phase polymer.[228] However, a monolayer of *monomers* with an alkyl spacer of an even number of CH_2 units almost exclusively forms a short-conjugation-length red-phase polymer, evidenced by the absence of vibrational features at ~1459 and 2088 cm^{-1}.[228]

This odd−even difference in the phase formation of polymerization on Au(111) is attributed to the limited extent of freedom within the alkyl spacer. Figure 49c schematically shows the structure of the polymer monolayers formed on Au(111) films in which the polymer backbone (diacetylene units) is constrained at an orientation parallel to the Au surface. For the polymer phase formed from monomers with an alkyl spacer of an odd number of CH_2 units, the C−S−Au bond angle nearly remains at ~109° (left panel of Figure 49c). However, it tends to be ~180° for the polymer phase formed from monomers with an alkyl spacer of an even number of CH_2 groups (right panel of Figure 49c). Definitely, a spacer with an odd number of CH_2 units in the polymerized monolayer is the least strained structure because the Au−S−C bond angle is already close to the 109° required for a stable binding in this self-assembled polymer monolayer and the sp^3-hybridized sulfur can be easily accommodated for this spacer. Thus, the alkyl spacer chain with an odd number of CH_2 groups in the polymerized monolayer is an all-trans chain without gauche defects. Compared to the odd-numbered alkyl chain, however, the alkyl spacer with an even number of CH_2 groups in the polymerized monolayer has significant gauche defects because it needs to accommodate the sp^3-hybridized sulfur atom with a nearly linear C−S−Au bond angle (right panel of Figure 49c). Furthermore, these gauche defects partially transfer strain in the alkyl spacer into the polymer backbone, resulting in formation of shorter-conjugation-length red-phase polymer from *monomers* with an even number of CH_2 units. Formation of high-conjugation-length polymer (blue phase) from monomers with an alkyl spacer having an odd number of CH_2 units and short-conjugation-length polymer (red phase) from monomers with an even-numbered alkyl spacer was confirmed by the observation and absence of downshifted C═C and C≡C transitions at ~1459 and 2088 cm^{-1}.[228]

4. Comparison of the Origin and Features of Odd–Even Effects on Different Substrates

Organic self-assembled monolayers exhibiting odd−even effects can be classified into two types on the basis of the different interactions between the organic molecule and the substrate. In the first category of organic monolayer (category I) the interaction is weak van der Waals interaction. This kind of monolayer includes various organic self-assembled monolayers on HOPG and other layered substrates such as MoS_2. The second type (category II) is the organic self-assembled monolayer chemically bonded to a substrate, such as organosulfur monolayers on Au(111), in which organic molecules self-assemble on a substrate via forming strong chemical bonds between a molecular head group and the surface atoms of the substrate. The difference in the two categories of molecule−substrate interactions partially contributes to the difference in the odd−even effects on structures and properties of the two categories of organic self-assembled monolayers on solid surfaces.

The odd−even effects of the two classes of self-assembled monolayers have different driving forces. The driving force for production of odd−even effects in the first class of self-assembled monolayer is maximization of intermolecular interactions, including interactions between two adjacent molecules within a lamella and interaction between molecules from two adjacent lamellae. Particularly, interactions between functional groups of two adjacent molecules play a major role. The molecule−substrate interactions do not play as important a role as these interactions are similar for self-assembled monolayers of different organic molecules. In fact, previous extensive STM studies of the first type of self-assembled monolayers[11,39] confirmed that all long-chain organic molecules adopt a closest packing pattern on HOPG in which two adjacent molecules maintain a spacing of ~4.2 Å. Molecules with different functional groups do not give rise to a significant difference in the surface coverage of CH_2 units of these self-assembled monolayers. This suggests similar molecule−substrate interactions for different self-assembled monolayers.

As previous studies have shown odd−even effects were not observed in the self-assembled monolayers of *n*-alkanes.[11,39] Compared to *n*-alkanes, substituting its CH_2 or ending CH_3 moiety by another functional group such as

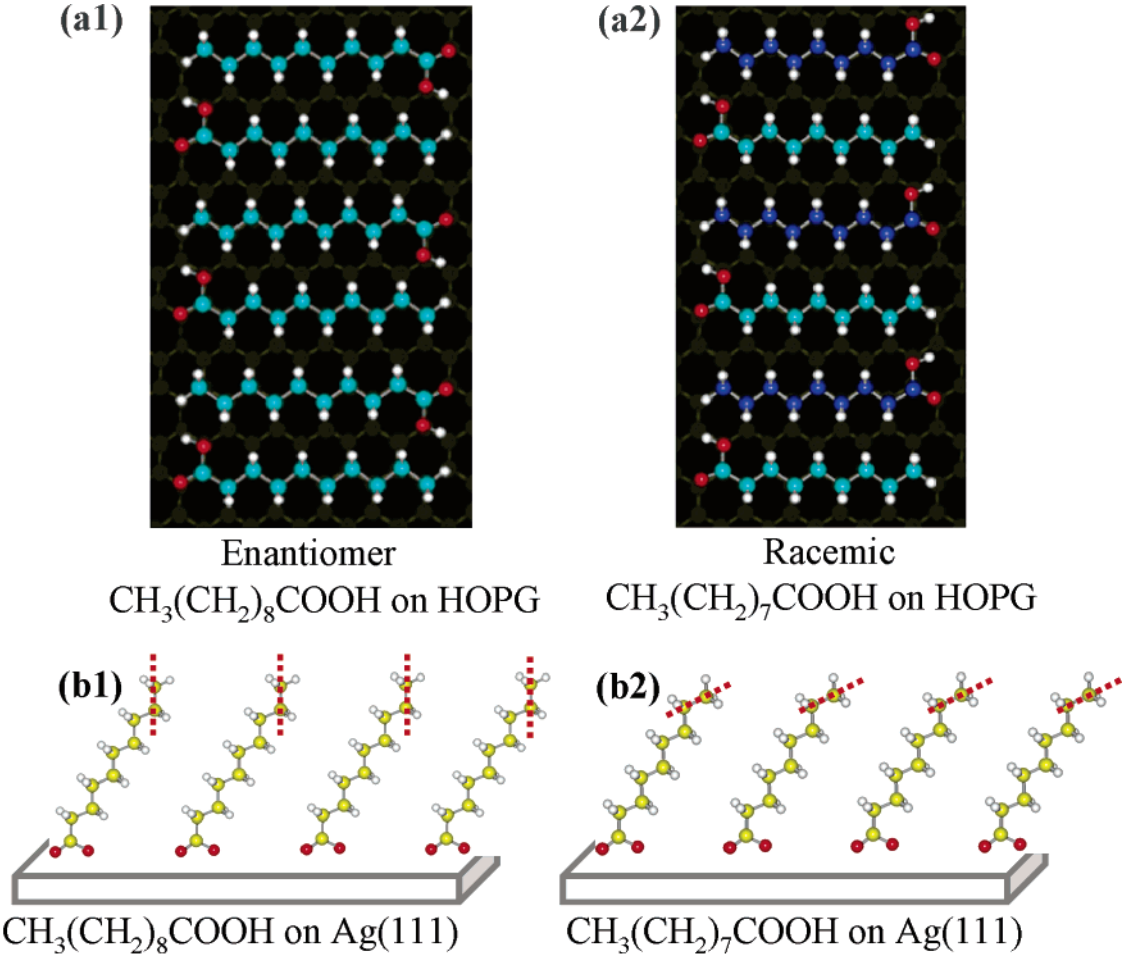

Figure 50. Schematic presentation for the structural difference between two categories of organic self-assembled monolayers which have distinctly different origins and features of odd−even effects. (a1 and a2) Plane of the carbon skeleton is parallel to the HOPG surface. The interaction between the self-assembled molecules and graphite is a weak van der Waals interaction. The odd−even difference is seen in the molecular packing structure and chirality. (b1 and b2) Two oxygen atoms of the carboxylic acid group chemically bind to the metal surface. The molecular alkyl chain is tilted from the surface normal by a certain angle. The offset of one CH_2 unit of the alkyl chain results in odd−even effects in the orientation of the terminal CH_3-CH_2- moiety and interfacial properties of the self-assembled monolayers.

COOH possibly may induce an odd−even effect. Once a functional group is added to the *n*-alkane, the intermolecular interaction must be different. Repulsion between two adjacent molecules, such as the interaction between the terminal CH_3 of one molecule and the COOH of an adjacent molecule, could be different between monolayers of molecules with an odd number of CH_2 units and those with an even number of CH_2 units. In order to maximize intermolecular interactions and form the most stable self-assembled structure, each of the two monolayers could adopt a different molecular packing pattern such as packing with two opposite faces alternatively as in $CH_3(CH_2)_{n-2}COOH$ (n = odd) but the same face as in $CH_3(CH_2)_{n-2}COOH$ (n = even). Thus, compared to molecule−substrate interactions, intermolecular interactions are the major driving force in the production of odd−even effects of the first category of self-assembled monolayer.

The odd−even effects seen in the second type of organic self-assembled monolayer are driven by chemical binding of the molecular head group to the substrate but are not so strongly governed by maximization of intermolecular weak interactions. Thus, the odd−even effects exhibited in the monolayers chemically bonded to solid surfaces are *chemical-bond*-driven odd−even effects, in contrast to the *weak-interaction*-driven odd−even effects in the first kind of organic monolayer. Figure 50 schematically presents the structural difference in the self-assembled monolayers of categories I and II exhibiting odd−even effects.

The difference in the driving force for formation of odd−even effects also results in a difference in the tunability of these odd−even effects. For the first class of organic monolayer the structure and property odd−even effects cannot be modified by simply substituting molecular head or terminal groups because the head or terminal groups play a dominant role in the production of the odd−even effects. For each molecule of a self-assembled monolayer on HOPG it experiences at least three interactions including the interaction with its adjacent molecules in a lamella, the interaction with its neighboring molecules of the adjacent lamellae, and the interaction with its substrate. Each of these interactions is associated with molecular functional groups, shape, and size. The first and second interactions (called intermolecular interactions) determine the molecular packing pattern in the self-assembled monolayer. Replacing one moiety/group of this molecule may significantly change the intermolecular interactions and therefore make new molecules adopt a different packing pattern to reach a new energetic equilibrium. The structure of the new equilibrium system possibly does not exhibit an odd−even effect in the molecular self-assembled structure. For example, $CH_3(CH_2)_{n-2}$-COOH exhibits structural and chiral odd−even effects. Replacing the COOH group with an OH group or CH_3 group

results in disappearance of the original odd−even effect and in a very few cases introduction of new ones.

For the second kind of organic self-assembled monolayer (category II), which is bonded to a substrate via formation of a chemical bond between the head group and the substrate, the originally exhibited odd−even effects still exist if its terminal moiety (see sections 3.2.3, 3.2.4, 3.2.5, 3.2.7, and 3.2.8) or some group of the head moiety (see sections 3.2.2 and 3.2.6) is replaced. It is understandable that there is possibly some modification for the original odd−even effects upon replacement of the head moiety and/or the terminal group by other groups. In fact, modification of odd−even effects via substitution of the functional group is important. It suggests the possibility that the odd−even effects on structure and property can be precisely tuned via introduction of a new functional group without changing the molecular frame. Thus, self-assembled monolayers of a number of other organic molecules of category II could exhibit new odd−even effects.

For each type of self-assembled monolayer exhibiting an odd−even effect the weak van der Waals interaction between molecules and substrate for category I (or the strong chemical bond for category II) should be equivalent for every molecule of the self-assembled monolayer. This requires that the substrates should have microscopic equivalence in geometry, chemical affinity for molecule, and macroscopic ordering of the 2D lattice. This understanding is consistent with the absence of an odd−even effect for organic monolayers on rough substrate surfaces without lattice ordering such as the natural SiO_x layer of a silicon single-crystal wafer. The inhomogeneous binding sites in structure and chemistry at a microscopic scale will definitely not produce a macroscopic structural ordering and chemical homogeneity of the organic monolayer. Because the main analytical techniques used to examine the odd−even effects, such as XPS, FTIR, and contact angle measurements, take average macroscopic information over a large detection area of a photo or electron beam (0.1−5 mm), an odd−even difference in structure and property cannot be observed in this kind of self-assembled monolayer, even though odd−even effects on structure and property could possibly exist at a microscopic scale. In addition, obtaining a homogeneous chemical binding in the second category of self-assembled monolayer also requires that the reactivity of the self-assembled molecules with the substrate should be specific. Otherwise, an odd−even effect will not be observed, though the substrate has homogeneous reaction sites. For example, an odd−even effect will possibly be absent if both ending groups A and B of molecule $A-(CH_2)_n-B$ have a similar reactivity with the surface of the substrate.

Due to the above requirements of the geometrical and chemical homogeneity for the substrates, the odd−even effect was not observed in organic self-assembled monolayers on substrates except HOPG, MoS_2, Au(111), and Ag(111) under ambient conditions. This is because these clean substrates with homogeneous structure and evenly distributed reactive sites can be prepared well under ambient conditions.

5. Summary and Future Work

The molecular chain length odd−even effect is an important phenomenon in physical chemistry and materials science and closely related to surface structures and functions of these materials. A wide spectrum of molecular self-assembled monolayers exhibit numerous odd−even effects in structure and property. All the odd−even effects revealed in the self-assembled monolayers on solid surfaces have a common structural feature of self-assembled molecules: the odd−even number of CH_2 units. This review has mainly discussed odd−even effects on structure and property revealed in organic self-assembled monolayers on solid substrates. Two categories of organic self-assembled monolayers bound to substrates via weak van der Waals interactions and strong chemical bonds, respectively, were reviewed.

In general, the scope of self-assembled monolayers exhibiting odd−even effects could be extended by replacing the molecular moiety/group/atom and using a different spacer unit. A simple approach is replacement of the terminal moiety/group, some portion of the head moiety, or the tethered group of the head moiety. Notably, simple replacement of the molecular functional group does not produce an odd−even effect for the first class of self-assembled monolayers of organic molecules. However, it is an effective way for introduction of an odd−even effect for the second category of self-assembled monolayer.

For the second class of self-assembled monolayer, a number of new substrates including various metal and semiconductor single-crystal surfaces which have 2D lattice ordering, homogeneous structure, and evenly distributed reactive sites can be prepared easily under vacuum conditions. For example, Si(100)-2 × 1,[232−234] Si(111)-7 × 7,[235] Ge(100),[236] and metal surfaces[237] have a homogeneous surface structure and reactive sites as well as high chemical reactivity for various organic molecules. Thus, future study using these substrates will possibly significantly extend the scope of odd−even effects of organic self-assembled monolayers on solid surfaces. To develop the self-assembled monolayer formed by weak van der Waals interactions between organic molecules and the substrate surface, Au(111) is definitely a good substrate since the adsorption energy of each CH_2 unit on this surface is ∼6.0 kJ/mol.[207] Although for Au(111) there is not the same lattice match as that between the carbon skeleton of the all-trans alkyl chain and the zigzag surface lattice of HOPG, formation of self-assembled monolayers via weak van der Waals interactions could be possible. Whether these proposed monolayers can exhibit an odd−even effect on packing structure and even chirality on the Au(111) surface or not is an interesting topic to study.

On the other hand, observation of an odd−even effect for a molecular self-assembled monolayer on some substrate may provide an analytical method for examining the structural and chemical homogeneities of the solid surface since the homogeneity is a main factor determining whether the odd−even effect in the structure and property of the organic self-assembled monolayers can be observed or not.

6. Acknowledgments

This work was partially supported by the National Science Foundation. F.T. acknowledges the support of the Harold W. Dodds Honorific Fellowship from Princeton University.

7. References

(1) Wade, L. J. *Organic Chemistry*, 5th ed.; Prentice Hall: New Jersey, 2002.
(2) Naher, U.; Bjornholm, S.; Frauendorf, S.; Garcias, F.; Guet, C. *Phys. Rep.-Rev. Sect. Phys. Lett.* **1997**, *285*, 245.
(3) Torres, M. B.; Fernandez, E. M.; Balbas, L. C. *Phys. Rev. B* **2005**, *71*, 155412.
(4) Largo, A.; Redondo, P.; Barrientos, C. *J. Phys. Chem. A* **2004**, *108*, 6421.

(5) Pellarin, M.; Cottancin, E.; Lerme, J.; Vialle, J. L.; Broyer, M.; Tournus, F.; Masenelli, B.; Melinon, P. *Eur. Phys. J. D* **2003**, *25*, 31.
(6) Zhao, J.; Yang, J. L.; Hou, J. G. *Phys. Rev. B* **2003**, *67*, 085404.
(7) Hakkinen, H.; Landman, U. *Phys. Rev. B* **2000**, *62*, R2287.
(8) Brechignac, C.; Busch, H.; Cahuzac, P.; Leygnier, J. *J. Chem. Phys.* **1994**, *101*, 6992.
(9) Love, J. C.; Estroff, L. A.; Kriebel, J. K.; Nuzzo, R. G.; Whitesides, G. M. *Chem. Rev.* **2005**, *105*, 1103.
(10) Ma, Z.; Zaera, F. *Surf. Sci. Rep.* **2006**, *61*, 229.
(11) Giancarlo, L. C.; Flynn, G. W. *Annu. Rev. Phys. Chem.* **1998**, *49*, 297.
(12) Ulman, A. *Chem. Rev.* **1996**, *96*, 1533.
(13) Kramer, S.; Fuierer, R. R.; Gorman, C. B. *Chem. Rev.* **2003**, *103*, 4367.
(14) Tirrell, M. V.; Katz, A. *MRS Bull.* **2005**, *30*, 700.
(15) Bein, T. *MRS Bull.* **2005**, *30*, 713.
(16) Boncheva, M.; Whitewsides, G. M. *MRS Bull.* **2005**, *30*, 736.
(17) Pflaum, J.; Bracco, G.; Schreiber, F.; Colorado, R.; Shmakova, O. E.; Lee, T. R.; Scoles, G.; Kahn, A. *Surf. Sci.* **2002**, *498*, 89.
(18) Venables, J. A. *Introduction to Surface and Thin Film Processes*; Cambridge University Press: Cambridge, U.K., 2000.
(19) Kern, W.; Vossen, J. L. *Thin Film Processes II*; Academic Press: San Diego, CA, 1991.
(20) Schlesinger, M. P.; Paunovic, M. P. *Modern Electroplating*; John Wiley & Sons: New York, 2000.
(21) Baudrand, D. *Plat. Surf. Finish* **2000**, *87*, 42.
(22) Hou, Z. Z.; Abbott, N. L.; Stroeve, P. *Langmuir* **1998**, *14*, 3287.
(23) Dubrovsky, T. B.; Hou, Z. Z.; Stroeve, P.; Abbott, N. L. *Anal. Chem.* **1999**, *71*, 327.
(24) Pham, T.; Jackson, J. B.; Halas, N. J.; Lee, T. R. *Langmuir* **2002**, *18*, 4915.
(25) Poirier, G. E. *Chem. Rev.* **1997**, 97, 1117.
(26) Liu, G. Y.; Xu, S.; Qian, Y. L. *Acc. Chem. Res.* **2000**, *33*, 457.
(27) Houston, J. E.; Kim, H. I. *Acc. Chem. Res.* **2002**, *35*, 547.
(28) Schreiber, F. *Prog. Surf. Sci.* **2000**, *65*, 151.
(29) Laibinis, P. E.; Whitesides, G. M.; Allara, D. L.; Tao, Y. T.; Parikh, A. N.; Nuzzo, R. G. *J. Am. Chem. Soc.* **1991**, *113*, 7152.
(30) Tao, Y. T. *J. Am. Chem. Soc.* **1993**, *115*, 4350.
(31) Allara, D. L.; Nuzzo, R. G. *Langmuir* **1985**, *1*, 45.
(32) Allara, D. L.; Nuzzo, R. G. *Langmuir* **1985**, *1*, 52.
(33) Ocko, B. M.; Kraack, H.; Pershan, P. S.; Sloutskin, E.; Tamam, L.; Deutsch, M. *Phys. Rev. Lett.* **2005**, *94*, 017802.
(34) Magnussen, O. M.; Ocko, B. M.; Deutsch, M.; Regan, M. J.; Pershan, P. S.; Abernathy, D.; Grubel, G.; Legrand, J. F. *Nature* **1996**, *384*, 250.
(35) Gun, J.; Iscovici, R.; Sagiv, J. *J. Colloid Interface Sci.* **1984**, *101*, 201.
(36) Gun, J.; Sagiv, J. *J. Colloid Interface Sci.* **1986**, *112*, 457.
(37) Shalamov, V. T. *Graphite*; Norton: New York, 1981.
(38) Rowntree, P. A.; Ph.D. Thesis, Princeton University, 1990.
(39) Cyr, D. M.; Venkataraman, B.; Flynn, G. W. *Chem. Mater.* **1996**, *8*, 1600.
(40) Tao, F.; Cai, Y. G.; Bernasek, S. L. *Langmuir* **2005**, *21*, 1269.
(41) Tao, F.; Bernasek, S. L. *J. Phys. Chem. B* **2005**, *109*, 6233.
(42) Cai, Y. G.; Bernasek, S. L. *J. Am. Chem. Soc.* **2003**, *125*, 1655.
(43) Cai, Y. G.; Bernasek, S. L. *J. Am. Chem. Soc.* **2004**, *126*, 14234.
(44) Cai, Y. G.; Bernasek, S. L. *J. Phys. Chem. B* **2005**, *109*, 4514.
(45) Hibino, M.; Sumi, A.; Tsuchiya, H.; Hatta, I. *J. Phys. Chem. B* **1998**, *102*, 4544.
(46) Hibino, M.; Sumi, A.; Hatta, I. *Jpn. J. Appl. Phys. Part 1* **1995**, *34*, 610.
(47) Hibino, M.; Sumi, A.; Hatta, I. *Jpn. J. Appl. Phys. Part 1* **1995**, *34*, 3354.
(48) Kishi, E.; Matsuda, H.; Kuroda, R.; Takimoto, K.; Yamano, A.; Eguchi, K.; Hatanaka, K.; Nakagiri, T. *Ultramicroscopy* **1992**, *42*, 1067.
(49) Kuroda, R.; Kishi, E.; Yamano, A.; Hatanaka, K.; Matsuda, H.; Eguchi, K.; Nakagiri, T. *J. Vac. Sci. Technol. B* **1991**, *9*, 1180.
(50) Cai, Y. G.; Ph.D. Thesis, Princeton University, 2003.
(51) Tao, F.; Goswami, J.; Bernasek, S. L. *J. Phys. Chem. B* **2006**, *110*, 4199.
(52) Fang, H. B.; Giancarlo, L. C.; Flynn, G. W. *J. Phys. Chem. B* **1998**, *102*, 7421.
(53) Fang, H. B.; Giancarlo, L. C.; Flynn, G. W. *J. Phys. Chem. B* **1998**, *102*, 7311.
(54) Yablon, D. G.; Giancarlo, L. C.; Flynn, G. W. *J. Phys. Chem. B* **2000**, *104*, 7627.
(55) Yablon, D. G.; Wintgens, D.; Flynn, G. W. *J. Phys. Chem. B* **2002**, *106*, 5470.
(56) Boese, R.; Weiss, H. C.; Blaser, D. *Angew. Chem., Int. Ed.* **1999**, *38*, 988.
(57) Thalladi, V. R.; Boese, R.; Weiss, H. C. *Angew. Chem., Int. Ed.* **2000**, *39*, 918.
(58) Thalladi, V. R.; Boese, R.; Weiss, H. C. *J. Am. Chem. Soc.* **2000**, *122*, 1186.
(59) Thalladi, V. R.; Nusse, M.; Boese, R. *J. Am. Chem. Soc.***2000**, *122*, 9227.
(60) Tsai, C. J.; Chen, Y. *J. Polym. Sci., Polym. Chem.* **2002**, *40*, 293.
(61) Mizuno, M.; Hirai, A.; Matsuzawa, H.; Endo, K.; Suhara, M.; Kenmotsu, M.; Han, C. D. *Macromolecules* **2002**, *35*, 2595.
(62) Hirano, H.; Watase, S.; Tanaka, M. *J. Appl. Polym. Sci.* **2004**, *91*, 1865.
(63) Fey, T.; Holscher, M.; Keul, H.; Hocker, H. *Polym. Inst.* **2003**, *52*, 1625.
(64) Alimova, L. L.; Atovmyan, E. G.; Filipenko, O. S. *Kristallografiya* **1987**, *32*, 97.
(65) Kim, K.; Plass, K. E.; Matzger, A. J. *J. Am. Chem. Soc.* **2005**, *127*, 4879.
(66) De Feyter, S.; Grim, P. C. M.; van Esch, J.; Kellogg, R. M.; Feringa, B. L.; De Schryver, F. C. *J. Phys. Chem. B* **1998**, *102*, 8981.
(67) Wei, Y.; Kannappan, K.; Flynn, G. W.; Zimmt, M. B. *J. Am. Chem. Soc.* **2004**, *126*, 5318.
(68) Kadotani, T.; Taski, S.; Okabe, H.; Kai, S. *Jpn. J. Appl. Phys.* **1996**, *35*, L1345.
(69) Kadotani, T.; Taki, S.; Kai, S. *Jpn. J. Appl. Phys., Part 1* **1997**, *36*, 4440.
(70) Taki, S.; Sagara, K.; Kadotani, T.; Kai, S. *Jpn. J. Appl. Phys.* **1999**, *68*, 709.
(71) Taki, S.; Kadotani, T.; Kai, S. *J Jpn. J. Appl. Phys.* **1999**, *68*, 1286.
(72) Taki, S.; Kai, S. *Jpn. J. Appl. Phys., Part 1* **2001**, *40*, 4187.
(73) Taki, S.; Okabe, H.; Kai, S. *Jpn. J. Appl. Phys., Part 1* **2003**, *42*, 7053.
(74) Ooishi, M.; Okabe, H.; Taki, S.; Takeuchi, M.; Kamiya, N.; Kai, S. *Tech. Rep. Kyushu Univ.* **1999**, *72*, 147.
(75) Wintgens, D.; Yablon, D. G.; Flynn, G. W. *J. Phys. Chem. B* **2003**, *107*, 173.
(76) Tao, F.; Bernasek, S. L. *Langmuir* **2007**, *23*, 3513.
(77) Taub, H. In *NATO Advanced Study of Institute, Series C: Mathematical and Physical Sciences*; Lang, G. L. G., F., Ed.; Kluwer: Dordrecht, 1988, Vol. 228.
(78) Morishige, K.; Kato, T. *J. Chem. Phys.* **1999**, *111*, 7095.
(79) Lee, S.; Puck, A.; Graupe, M.; Colorado, R.; Shon, Y. S.; Lee, T. R.; Perry, S. S. *Langmuir* **2001**, *17*, 7364.
(80) Hansen, F. Y.; Newton, J. C.; Taub, H. *J. Chem. Phys.* **1993**, *98*, 4128.
(81) Herwig, K. W.; Wu, Z.; Dai, P.; Taub, H.; Hansen, F. Y. *J. Chem. Phys.* **1997**, *107*, 5186.
(82) Ulman, A. *An introduction to ultrathin organic films: from Langmuir-Blodgett to self-assembly*; Academic Press: Boston, 1991.
(83) Whitesides, G. M. *Sci. Am.* **1995**, *9*, 146.
(84) Ulman, A. *Thin films: self-assembled monolayer of thiols*; Academic Press: San Diego, 1998.
(85) Bowden, F. P. *The Frication and Lubrication of Solids*; Oxford University Press: London, 1968.
(86) Kaelble, D. H. *Physical Chemistry of Adhesions*; Wiley-Interscience: New York, 1971.
(87) Fendler, J. H. *Chem. Mater.* **2001**, *13*, 3196.
(88) Kakkar, A. K. *Chem. Rev.* **2002**, *102*, 3579.
(89) Flink, S.; van Veggel, F. C. J. M.; Reinhoudt, D. N. *Adv. Mater.* **2000**, *12*, 1315.
(90) Chaki, N. K.; Vijayamohanan, K. *Biosens. Bioelectron.* **2002**, *17*, 1.
(91) Mirsky, V. M. *Trends Anal. Chem.* **2002**, *21*, 439.
(92) Nuzzo, R. G.; Zegarski, B. R.; Dubois, L. H. *J. Am. Chem. Soc.* **1987**, *109*, 733.
(93) Dubois, L. H.; Nuzzo, R. G. *Annu. Rev. Phys. Chem.* **1992**, *43*, 437.
(94) Porter, M. D.; Bright, T. B.; Allara, D. L.; Chidsey, C. E. D. *J. Am. Chem. Soc.* **1987**, *109*, 3559.
(95) Nuzzo, R. G.; Dubois, L. H.; Allara, D. L. *J. Am. Chem. Soc.* **1990**, *112*, 558.
(96) Alloway, D. M.; Hofmann, M.; Smith, D. L.; Gruhn, N. E.; Graham, A. L.; Colorado, R.; Wysocki, V. H.; Lee, T. R.; Lee, P. A.; Armstrong, N. R. *J. Phys. Chem. B* **2003**, *107*, 11690.
(97) Nishi, N.; Hobara, D.; Yamamoto, M.; Kakiuchi, T. *J. Chem. Phys.* **2003**, *118*, 1904.
(98) Kato, H. S.; Noh, J.; Hara, M.; Kawai, M. *J. Phys. Chem. B* **2002**, *106*, 9655.
(99) Wong, S. S.; Takano, H.; Porter, M. D. *Anal. Chem.* **1998**, *70*, 5209.
(100) Chang, S. C.; Chao, I.; Tao, Y. T. *J. Am. Chem. Soc.* **1994**, *116*, 6792.
(101) Colorado, R.; Villazana, R. J.; Lee, T. R. *Langmuir* **1998**, *14*, 6337.
(102) Nuzzo, R. G.; Fusco, F. A.; Allara, D. L. *J. Am. Chem. Soc.* **1987**, *109*, 2358.
(103) Graupe, M.; Takenaga, M.; Koini, T.; Colorado, R.; Lee, T. R. *J. Am. Chem. Soc.* **1999**, *121*, 3222.

(104) Shon, Y. S.; Lee, S.; Colorado, R.; Perry, S. S.; Lee, T. R. *J. Am. Chem. Soc.* **2000**, *122*, 7556.
(105) Tamada, K.; Nagasawa, J.; Nakanishi, F.; Abe, K.; Ishida, T.; Hara, M.; Knoll, W. *Langmuir* **1998**, *14*, 3264.
(106) Shaporenko, A.; Brunnbauer, M.; Terfort, A.; Grunze, M.; Zharnikov, M. *J. Phys. Chem. B* **2004**, *108*, 14462.
(107) Ishida, T.; Mizutani, W.; Aya, Y.; Ogiso, H.; Sasaki, S.; Tokumoto, H. *J. Phys. Chem. B* **2002**, *106*, 5886.
(108) Fuxen, C.; Azzam, W.; Arnold, R.; Witte, G.; Terfort, A.; Woll, C. *Langmuir* **2001**, *17*, 3689.
(109) Ishida, T.; Choi, N.; Mizutani, W.; Tokumoto, H.; Kojima, I.; Azehara, H.; Hokari, H.; Akiba, U.; Fujihira, M. *Langmuir* **1999**, *15*, 6799.
(110) Ishida, T.; Mizutani, W.; Akiba, U.; Umemura, K.; Inoue, A.; Choi, N.; Fujihira, M.; Tokumoto, H. *J. Phys. Chem. B* **1999**, *103*, 1686.
(111) Ishida, T.; Mizutani, W.; Choi, N.; Akiba, U.; Fujihira, M.; Tokumoto, H. *J. Phys. Chem. B* **2000**, *104*, 11680.
(112) Ishida, T.; Mizutani, W.; Tokumoto, H.; Choi, N.; Akiba, U.; Fujihira, M. *J. Vac. Sci. Technol. A* **2000**, *18*, 1437.
(113) Heister, K.; Rong, H. T.; Buck, M.; Zharnikov, M.; Grunze, M.; Johansson, L. S. O. *J. Phys. Chem. B* **2001**, *105*, 6888.
(114) Frey, S.; Rong, H. T.; Heister, K.; Yang, Y. J.; Buck, M.; Zharnikov, M. *Langmuir* **2002**, *18*, 3142.
(115) Rong, H. T.; Frey, S.; Yang, Y. J.; Zharnikov, M.; Buck, M.; Wuhn, M.; Woll, C.; Helmchen, G. *Langmuir* **2001**, *17*, 1582.
(116) Azzam, W.; Cyganik, P.; Witte, G.; Buck, M.; Woll, C. *Langmuir* **2003**, *19*, 8262.
(117) Beardmore, K. M.; Kress, J. D.; Gronbech-Jensen, N.; Bishop, A. R. *Chem. Phys. Lett.* **1998**, *286*, 40.
(118) Yourdshahyan, Y.; Zhang, H. K.; Rappe, A. M. *Phys. Rev. B* **2001**, *63*, 081405.
(119) Gottschalck, J.; Hammer, B. *J. Chem. Phys.* **2002**, *116*, 784.
(120) Seki, K.; Ito, E.; Oji, H.; Yoshimura, D.; Hayashi, N.; Sakurai, Y.; Hosoi, Y.; Yokoyama, T.; Imai, T.; Ouchi, Y.; Ishii, H. *Synth. Met.* **2001**, *119*, 19.
(121) Li, T. W.; Chao, I.; Tao, Y. T. *J. Phys. Chem. B* **1998**, *102*, 2935.
(122) Allen, G. F. *Internal Rotation in Molecules*; Wiley: New York, 1974.
(123) Spellmeyer, D. C.; Grootenhuis, P. D. J.; Miller, M. D.; Kuyper, L. F.; Kollman, P. A. *J. Phys. Chem.* **1990**, *94*, 4483.
(124) Colorado, R.; Lee, T. R. *J. Phys. Org. Chem.* **2000**, *13*, 796.
(125) Breitung, E. M.; Vaughan, W. E.; McMahon, R. J. *Rev. Sci. Instrum.* **2000**, *71*, 224.
(126) Dhull, J. S.; Sharma, D. R. *J. Phys. D: Appl. Phys.* **1982**, *15*, 2307.
(127) Coulson, C. A.; Eisenber. D. *Proc. R. Soc. London A* **1966**, *291*, 454.
(128) Chabinyc, M. L.; Chen, X. X.; Holmlin, R. E.; Jacobs, H.; Skulason, H.; Frisbie, S. D.; Mujica, V.; Ratner, M. A.; Rampi, M. A.; Whitesides, G. M. *J. Am. Chem. Soc.* **2002**, *124*, 11730.
(129) Schneider, J.; Messerschmidt, C.; Schulz, A.; Gnade, M.; Schade, B.; Luger, P.; Bombicz, P.; Hubert, V.; Fuhrhop, J. H. *Langmuir* **2000**, *16*, 8575.
(130) Whitesides, G. M.; Laibinis, P. E. *Langmuir* **1990**, *6*, 87.
(131) Bain, C. D.; Troughton, E. B.; Tao, Y. T.; Evall, J.; Whitesides, G. M.; Nuzzo, R. G. *J. Am. Chem. Soc.* **1989**, *111*, 321.
(132) Hatchett, D. W.; Stevenson, K. J.; Lacy, W. B.; Harris, J. M.; White, H. S. *J. Am. Chem. Soc.* **1997**, *119*, 6596.
(133) Azzaroni, O.; Vela, M. E.; Andreasen, G.; Carro, P.; Salvarezza, R. C. *J. Phys. Chem. B* **2002**, *106*, 12267.
(134) Wang, M. C.; Liao, J. D.; Weng, C. C.; Klauser, R.; Shaporenko, A.; Grunze, M.; Zharnikov, M. *Langmuir* **2003**, *19*, 9774.
(135) Liao, J. D.; Wang, M. C.; Weng, C. C.; Klauser, R.; Frey, S.; Zharnikov, M.; Grunze, M. *J. Phys. Chem. B* **2002**, *106*, 77.
(136) Azzaroni, O.; Vela, M. E.; Fonticelli, M.; Benitez, G.; Carro, P.; Blum, B.; Salvarezza, R. C. *J. Phys. Chem. B* **2003**, *107*, 13446.
(137) Brewer, N. J.; Foster, T. T.; Leggett, G. J.; Alexander, M. R.; McAlpine, E. *J. Phys. Chem. B* **2004**, *108*, 4723.
(138) Alkire, R. C.; Gerischer, H.; Kolb, D. M.; Tobias, C. W. *Advances in Electrochemistry and Electrochemical Engineering*; Wiley-Interscience: New York, 1978.
(139) Adzic, R.; Gerischer, H.; Tobias, C. W. *Advances in Electrochemistry and Electrochemical Engineering*; Wiley-Interscience: New York, 1984.
(140) Trasatti, S. *The Work Function in Electrochemistry*; Wiley-Interscience: New York, 1977.
(141) Herrero, E.; Buller, L. J.; Abruna, H. D. *Chem. Rev.* **2001**, *101*, 1897.
(142) Li, J.; Abruña, H. D. *J. Phys. Chem. B* **1997**, *101*, 244.
(143) Jennings, G. K.; Laibinis, P. E. *J. Am. Chem. Soc.* **1997**, *119*, 5208.
(144) Zamborini, F. P.; Campbell, J. K.; Crooks, R. M. *Langmuir* **1998**, *14*, 640.
(145) Lin, S. Y.; Tsai, T. K.; Lin, C. M.; Chen, C. H.; Chan, Y. C.; Chen, H. W. *Langmuir* **2002**, *18*, 5473.
(146) Liu, Y. C. *Langmuir* **2003**, *19*, 6888.
(147) Liu, Y. C.; Chuang, T. C. *J. Phys. Chem. B* **2003**, *107*, 9802.
(148) Chen, I. W. P.; Chen, C. C.; Lin, S. Y.; Chen, C. H. *J. Phys. Chem. B* **2004**, *108*, 17497.
(149) Walczak, M. M.; Chung, C. K.; Stole, S. M.; Widrig, C. A.; Porter, M. D. *J. Am. Chem. Soc.* **1991**, *113*, 2370.
(150) Weast, R. C. *Handbook of Chemistry and Physics*; Chemical Rubber Co.: Boca Raton, FL, 1981.
(151) Mortimer, C. E. *Chemistry: A Conceptual Approach*, 4th ed.; Van Nostrand: New York, 1979.
(152) Kevan, S. D.; Gaylord, R. H. *Phys. Rev. B* **1987**, *36*, 5809.
(153) Sellers, H.; Ulman, A.; Shnidman, Y.; Eilers, J. E. *J. Am. Chem. Soc.* **1993**, *115*, 9389.
(154) Bao, S.; Mcconville, C. F.; Woodruff, D. P. *Surf. Sci.* **1987**, *187*, 133.
(155) Prince, N. P.; Seymour, D. L.; Woodruff, D. P.; Jones, R. G.; Walter, W. *Surf. Sci.* **1989**, *215*, 566.
(156) Miura, Y. F.; Takenaga, M.; Koini, T.; Graupe, M.; Garg, N.; Graham, R. L.; Lee, T. R. *Langmuir* **1998**, *14*, 5821.
(157) Colorado, R., Jr.; Graupe, M.; Takenaga, M.; Koini, T.; Lee, T. R. *Mater. Res. Soc. Symp. Proc.* **1999**, *546*, 237.
(158) Colorado, R., Jr.; Graupe, M.; Kim, H. I.; Takenaga, M.; Oloba, O.; Lee, S.; Perry, S. S.; Lee, T. R. *ACS Symp.* **2001**, *781*, 58.
(159) Colorado, R., Jr.; Lee, T. R. *Langmuir* **2003**, *19*, 3288.
(160) Evans, S. D.; Ulman, A. *Chem. Phys. Lett.* **1990**, *170*, 462.
(161) Campbell, I. H.; Kress, J. D.; Martin, R. L.; Smith, D. L.; Barashkov, N. N.; Ferraris, J. P. *Appl. Phys. Lett.* **1997**, *71*, 3528.
(162) Campbell, I. H.; Rubin, S.; Zawodzinski, T. A.; Kress, J. D.; Martin, R. L.; Smith, D. L.; Barashkov, N. N.; Ferraris, J. P. *Phys. Rev. B* **1996**, *54*, 14321.
(163) Zehner, R. W.; Parsons, B. F.; Hsung, R. P.; Sita, L. R. *Langmuir* **1999**, *15*, 1121.
(164) Bastide, S.; Butruille, R.; Cahen, D.; Dutta, A.; Libman, J.; Shanzer, A.; Sun, L. M.; Vilan, A. *J. Phys. Chem. B* **1997**, *101*, 2678.
(165) Vilan, A.; Shanzer, A.; Cahen, D. *Nature* **2000**, *404*, 166.
(166) Ashkenasy, G.; Cahen, D.; Cohen, R.; Shanzer, A.; Vilan, A. *Acc. Chem. Soc.* **2002**, *35*, 121.
(167) Bruening, M.; Cohen, R.; Guillemoles, J. F.; Moav, T.; Libman, J.; Shanzer, A.; Cahen, D. *J. Am. Chem. Soc.* **1997**, *119*, 5720.
(168) Crispin, X.; Geskin, V.; Crispin, A.; Cornil, J.; Lazzaroni, R.; Salaneck, W. R.; Bredas, J. L. *J. Am. Chem. Soc.* **2002**, *124*, 8131.
(169) Peisert, H.; Knupfer, M.; Fink, J. *Appl. Phys. Lett.* **2002**, *81*, 2400.
(170) Smith, D. L.; Wysocki, V. H.; Colorado, R.; Shmakova, O. E.; Graupe, M.; Lee, T. R. *Langmuir* **2002**, *18*, 3895.
(171) Park, B.; Chandross, M.; Stevens, M. J.; Grest, G. S. *Langmuir* **2003**, *19*, 9239.
(172) Sun, H. *J. Phys. Chem. B* **1998**, *102*, 7338.
(173) Felgenhauer, T.; Rong, H. T.; Buck, M. *J. Electroanal. Chem.* **2003**, *550*, 309.
(174) Long, Y. T.; Rong, H. T.; Buck, M.; Grunze, M. *J. Electroanal. Chem.* **2002**, *524*, 62.
(175) Maboudian, R. *Surf. Sci. Rep.* **1998**, *30*, 209.
(176) Houston, J. E.; Kim, H. I. *Acc. Chem. Soc.* **2002**, *35*, 547.
(177) Persson, B. N. J. *Sliding Friction*; Springer-Verlag: Berlin, 1998.
(178) Thomas, R. C.; Houston, J. E.; Crooks, R. M.; Kim, T.; Michalske, T. A. *J. Am. Chem. Soc.* **1995**, *117*, 3830.
(179) Finot, M. O.; McDermott, M. T. *J. Am. Chem. Soc.* **1997**, *119*, 8564.
(180) Joyce, S. A.; Thomas, R. C.; Houston, J. E.; Michalske, T. A.; Crooks, R. M. *Phys. Rev. Lett.* **1992**, *68*, 2790.
(181) Kim, H. I.; Houston, J. E. *J. Am. Chem. Soc.* **2000**, *122*, 12045.
(182) Rouse, T. O.; Weininge, J. L. *J. Electrochem. Soc.* **1966**, *113*, C77.
(183) Conway, B. E.; Currie, J. C. *J. Electrochem. Soc.* **1978**, *125*, 257.
(184) Fuhrhop, J. H.; Bedurke, T.; Gnade, M.; Schneider, J.; Doblhofer, K. *Langmuir* **1997**, *13*, 455.
(185) Widrig, C. A.; Chung, C.; Porter, M. D. *J. Electroanal. Chem.* **1991**, *310*, 335.
(186) Wolf, K. V.; Cole, D. A.; Bernasek, S. L. *Langmuir* **2001**, *17*, 8254.
(187) Wolf, K. V.; Cole, D. A.; Bernasek, S. L. *J. Phys. Chem. B* **2002**, *106*, 10382.
(188) Wolf, K. V.; Cole, D. A.; Bernasek, S. L. *Anal. Chem.* **2002**, *74*, 5009.
(189) Evans, C.; Pradeep, T.; Shen, J. W.; Cooks, R. G. *Rapid Commun. Mass Spectrom.* **1999**, *13*, 172.
(190) Angelico, V. J.; Mitchell, S. A.; Wysocki, V. H. *Anal. Chem.* **2000**, *72*, 2603.
(191) Colorado, R. L., T. R. *J. Phys. Org. Chem.* **2000**, *13*, 796.
(192) Eck, W.; Stadler, V.; Geyer, W.; Zharnikov, M.; Golzhauser, A.; Grunze, M. *Adv. Mater.* **2000**, *12*, 805.
(193) Golzhauser, A.; Eck, W.; Geyer, W.; Stadler, V.; Weimann, T.; Hinze, P.; Grunze, M. *Adv. Mater.* **2001**, *13*, 806.
(194) Lercel, M. J.; Redinbo, G. F.; Pardo, F. D.; Rooks, M.; Tiberio, R. C.; Simpson, P.; Craighead, H. G.; Sheen, C. W.; Parikh, A. N.; Allara, D. L. *J. Vac. Sci. Technol. B* **1994**, *12*, 3663.
(195) Baer, D. R.; Engelhard, M. H.; Schulte, D. W.; Guenther, D. E.; Wang, L. Q.; Rieke, P. C. *J. Vac. Sci. Technol. A* **1994**, *12*, 2478.

(196) Seshadri, K.; Froyd, K.; Parikh, A. N.; Allara, D. L.; Lercel, M. J.; Craighead, H. G. *J. Phys. Chem.* **1996**, *100*, 15900.
(197) Hild, R.; David, C.; Muller, H. U.; Volkel, B.; Kayser, D. R.; Grunze, M. *Langmuir* **1998**, *14*, 342.
(198) Maoz, R.; Cohen, S. R.; Sagiv, J. *Adv. Mater.* **1999**, *11*, 55.
(199) Heister, K.; Frey, S.; Golzhauser, A.; Ulman, A.; Zharnikov, M. *J. Phys. Chem. B* **1999**, *103*, 11098.
(200) Zharnikov, M.; Frey, S.; Heister, K.; Grunze, M. *Langmuir* **2000**, *16*, 2697.
(201) Frey, S.; Heister, K.; Zharnikov, M.; Grunze, M. *Phys. Chem. Chem. Phys.* **2000**, *2*, 1979.
(202) Olsen, C.; Rowntree, P. A. *J. Chem. Phys.* **1998**, *108*, 3750.
(203) Rowntree, P.; Dugal, P. C.; Hunting, D.; Sanche, L. *J. Phys. Chem.* **1996**, *100*, 4546.
(204) Jager, B.; Schurmann, H.; Muller, H. U.; Himmel, H. J.; Neumann, M.; Grunze, M.; Woll, C. *Z. Phys. Chem.-Int. J. Res. Phys. Chem. Chem. Phys.* **1997**, *202*, 263.
(205) Muller, H. U.; Zharnikov, M.; Volkel, B.; Schertel, A.; Harder, P.; Grunze, M. *J. Phys. Chem. B* **1998**, *102*, 7949.
(206) Zharnikov, M.; Geyer, W.; Golzhauser, A.; Frey, S.; Grunze, M. *Phys. Chem. Chem. Phys.* **1999**, *1*, 3163.
(207) Volkel, B.; Golzhauser, A.; Muller, H. U.; David, C.; Grunze, M. *J. Vac. Sci. Technol. B* **1997**, *15*, 2877.
(208) Kondoh, H.; Nozoye, H. *J. Phys. Chem. B* **1998**, *102*, 2367.
(209) Kuriyama, K.; Kikuchi, H.; Kajiyama, T. *Langmuir* **1996**, *12*, 2283.
(210) Day, D.; Lando, J. B. *Macromolecules* **1980**, *13*, 1478.
(211) Tieke, B. *Adv. Polym. Sci.* **1985**, *71*, 79.
(212) Lando, J. B. In *Polydiacetylenes*; Bloor, D. C., R. R., Ed.; Dordrecht: Nijhoff, 1985.
(213) Enkelmann, V. *Adv. Polym. Sci.* **1984**, *63*, 91.
(214) Schott, M.; Wegner, G. In *Nonlinear Optical Properties of Organic Moleucles and Crystals*; Chemla, D. S., Zyss, J., Eds.; Academic Press: Orlando, 1987.
(215) Batchelder, D. N.; Evans, S. D.; Freeman, T. L.; Haussling, L.; Ringsdorf, H.; Wolf, H. *J. Am. Chem. Soc.* **1994**, *116*, 1050.
(216) Kim, T.; Ye, Q.; Sun, L.; Chan, K. C.; Crooks, R. M. *Langmuir* **1996**, *12*, 6065.
(217) Chan, K. C.; Kim, T.; Schoer, J. K.; Crooks, R. M. *J. Am. Chem. Soc.* **1995**, *117*, 5875.
(218) Mowery, M. D.; Evans, C. E. *J. Phys. Chem. B* **1997**, *101*, 8513.
(219) Menzel, H.; Mowery, M. D.; Cai, M.; Evans, C. E. *J. Phys. Chem. B* **1998**, *102*, 9550.
(220) Menzel, H.; Mowery, M. D.; Cai, M.; Evans, C. E. *Adv. Mater.* **1999**, *11*, 131.
(221) Menzel, H.; Mowery, M. D.; Cai, M.; Evans, C. E. *Macromolecules* **1999**, *32*, 4343.
(222) Mowery, M. D.; Menzel, H.; Cai, M.; Evans, C. E. *Langmuir* **1998**, *14*, 5594.
(223) Kim, T.; Chan, K. C.; Crooks, R. M. *J. Am. Chem. Soc.* **1997**, *119*, 189.
(224) Mino, N.; Tamura, H.; Ogawa, K. *Langmuir* **1991**, *7*, 2336.
(225) Charych, D. H.; Nagy, J. O.; Spevak, W.; Bednarski, M. D. *Science* **1993**, *261*, 585.
(226) Cheng, Q.; Stevens, R. C. *Adv. Mater.* **1997**, *9*, 481.
(227) Cao, G.; Mallouk, T. E. *J. Solid State Chem.* **1991**, *94*, 59.
(228) Menzel, H.; Horstmann, S.; Mowery, M. D.; Cai, M.; Evans, C. E. *Polym.* **2000**, *41*, 8113.
(229) Lieser, G.; Tieke, B.; Wegner, G. *Thin Solid Films* **1980**, *68*, 77.
(230) Mino, N.; Tamura, H.; Ogawa, K. *Langmuir* **1992**, *8*, 594.
(231) Bower, D. I.; Maddams, W. F. *The Vibrational Spectroscopy of Polymers*; Cambridge University Press: Cambridge, 1989.
(232) Hamers, R. J.; Coulter, S. K.; Ellison, M. D.; Hovis, J. S.; Padowitz, D. F.; Schwartz, M. P.; Greenlief, C. M.; Russell, J. N. *Acc. Chem. Res.* **2000**, *33*, 617.
(233) Filler, M. A.; Bent, S. F. *Prog. Surf. Sci.* **2003**, *73*, 1.
(234) Wolkow, R. A. *Annu. Rev. Phys. Chem.* **1999**, *50*, 413.
(235) Tao, F.; Xu, G. Q. *Acc. Chem. Res.* **2004**, *37*, 882.
(236) Loscutoff, P. W.; Bent, S. F. *Annu. Rev. Phys. Chem.* **2006**, *57*, 467.
(237) Ma, Z.; Zaera, F. *Surf. Sci. Rep.* **2006**, *61*, 229.

CR050258D